UNITED NATIONS EDUCATIONAL, SCIENTIFIC AND CULTURAL ORGANIZATION
INTERNATIONAL ATOMIC ENERGY AGENCY
INTERNATIONAL CENTRE FOR THEORETICAL PHYSICS
I.C.T.P., P.O. BOX 586, 34100 TRIESTE, ITALY, CABLE: CENTRATOM TRIESTE

H4.SMR/1011 - 15

Fourth Workshop on Non-Linear Dynamics and Earthquake Prediction

6 - 24 October 1997

Self-exciting Homopolar Dynamos and Polarity Reversals of the Geomagnetic Field

R. HIDE

Oxford University
Dept. of Atmospheric, Oceanic and Planetary Physics
Clarendon Laboratory
Oxford, UNITED KINGDOM

A study of two novel self-exciting single-disk homopolar dynamos: theory

By Raymond Hide[1], Anne C. Skeldon[2]† and David J. Acheson[3]

[1]*Department of Physics (Atmospheric, Oceanic and Planetary Physics), Oxford University, Clarendon Laboratory, Parks Road, Oxford OX1 3PU, UK*

[2]*Department of Theoretical Mechanics, University of Nottingham, University Park, Nottingham NG7 2RD, UK*

[3]*Jesus College, Oxford OX1 3DW, UK*

We investigate the novel set of nonlinear ordinary differential equations

$$\dot{x} = x(y-1) - \beta z, \quad \dot{y} = \alpha(1-x^2) - \kappa y \quad \text{and} \quad \dot{z} = x - \lambda z, \quad \text{where} \quad \dot{x} \equiv \mathrm{d}x/\mathrm{d}\tau, \quad \text{etc.}$$

They govern the behaviour of two (mathematically equivalent) self-exciting homopolar dynamo systems, each comprising a Faraday disk and coil arrangement, the first with a capacitor and the second with a motor connected in series with the coil, where in each case the applied couple G that drives the disk (of moment of inertia A) into rotation with angular speed $\Omega(t)$ is assumed steady. The independent variable τ denotes time t measured in units of L/R s, where L is the self-inductance of the system and R the total series resistance. The dependent variable $x(\tau)$ is the electric current $I(t)$ generated in the system measured in units of $(G/M)^{1/2}$ A, where $2\pi M$ is the mutual inductance between the disk and coil, and $y(\tau)$ corresponds to $\Omega(t)$ measured in units R/M rad s^{-1}. In the case of the series capacitor (of capacitance C), the third independent variable $z(\tau)$ is the charge $Q(t)$ on the capacitor measured in units $(G/M)^{1/2}(L/R)$ C; in the case of the series motor, $z(\tau)$ is the angular speed $\omega(t)$ with which the armature of the motor is driven into rotation by the torque $HI(t)$ due to the current $I(t)$ passing through it, measured in units $(L/R)(M/G)^{1/2}(H/B)$ rad s^{-1}, where B is the moment of inertia of the armature. Common to both systems are the dimensionless parameters $\alpha \equiv GLM/R^2A$ and $\kappa \equiv KL/RA$, where K is the coefficient of (linear) mechanical friction in the disk. In the case of the capacitor, $\beta \equiv L/CR^2$ and $\lambda \equiv L/RrC$ where r is the leakage resistance of the capacitor; in the case of the motor, $\beta \equiv H^2L/R^2B$ and $\lambda \equiv DL/RB$ where D is the coefficient of (linear) mechanical friction in the motor.

The behaviour of the system, including its sensitivity to initial conditions, depends on the four parameters $(\alpha, \beta, \kappa, \lambda)$, the least interesting case being when the system fails to function as a self-exciting dynamo capable of amplifying a small adventitious electric current because α/κ is not large enough for motional induction to overcome ohmic dissipation. Otherwise, i.e. where α/κ exceeds a critical value dependent on β and λ, dynamo action occurs in which the detailed time dependence of the current $x(\tau)$ and of the other variables $y(\tau)$ and $z(\tau)$ depends critically on the exact values of $(\alpha, \beta, \kappa, \lambda)$, and in some cases also on the initial conditions. In the simplest cases, $x(\tau)$ tends to solutions which (apart from the sign of $x(\tau)$, which depends of the sign of the

† Present address: Department of Mathematics, City University, Northampton Square, London EC1V 0HB, UK.

Proc. R. Soc. Lond. A (1996) **452**, 1369–1395
Printed in Great Britain

initial disturbance) are either independent of τ or vary harmonically with τ. At other values of $(\alpha, \beta, \kappa, \lambda)$, multiple solutions are found, some of which are periodic (but non-harmonic), including square $x(\tau)$ and saw-tooth $y(\tau)$ and $z(\tau)$ waveforms, and others chaotic. A full elucidation of this behaviour will require extensive numerical studies over wide ranges of all these parameters, but bifurcation theory applied to the stability or otherwise of the equilibrium solutions $(x_0, y_0, z_0) = (0, \alpha/\kappa, 0)$ and $(\pm[1 - (\kappa/\alpha)(1 + \beta/\lambda)]^{1/2}, 1 + \beta/\lambda, x_0/\lambda)$ provides theoretical guidance. It shows in particular the usefulness of a regime diagram in parameter space of the first quadrant of the $(\beta, \alpha/\kappa)$ plane where there is one line $\alpha/\kappa = 1 + \beta/\lambda$ where symmetry breaking bifurcations occur and parts of two lines $\alpha/\kappa = 1 + \lambda$ and

$$\alpha/\kappa = [(2\beta - \kappa\lambda - \lambda^2)/2(\kappa - \beta/\lambda) + 3\beta/2\lambda + 1]$$

upon which Hopf bifurcations occur, all meeting at the point $(\beta, \alpha/\kappa) = (\lambda^2, 1 + \lambda)$ of the Takens–Bogdanov 'double-zero eigenvalue' type, with reflectional symmetry.

The equations governing self-exciting homopolar dynamos can be used as the basis of nonlinear low-dimensional analogues in the study of the temporal behaviour of certain phenomena of interest in geophysical fluid dynamics. These include the main geomagnetic field produced by self-exciting magnetohydrodynamic (MHD) dynamo action in the Earth's liquid metallic core and the 'El Niño–Southern Oscillation' of the Earth's atmosphere–ocean system (considerations of which prompted the present study), which has certain characteristics resembling those found in nonlinear relaxation oscillators and is produced by complex global-scale interactions between the atmosphere and oceans. Geophysical implications of the findings of the present study of simple (but not over-simplified) physically realistic dynamos will be discussed elsewhere, in the context of the further computational investigations needed to elucidate more fully the rich and complex behaviour indicated by the results obtained to date.

1. Introduction

Geophysicists accept that the main magnetic fields of the Earth and other planets are generated by the self-exciting magnetohydrodynamic (MHD) dynamo mechanism in the electrically conducting fluid regions of their interiors, as first proposed by Larmor (for references see, for example, Moffatt 1978; Melchior 1986; Jacobs 1987–91). However, the task of investigating such dynamos in detail by solving the highly nonlinear MHD equations under appropriate boundary conditions is not yet feasible. Current theoretical research comprises mathematical studies of systems of varying degrees of complexity, all of them very much simpler than the prototype.

The most striking property of the geomagnetic field, as revealed by the study of fossilized field directions in igneous and sedimentary rocks, is that the geomagnetic dipole has reversed its polarity many times over geological history (for references see Jacobs 1994). The duration of a reversal event is no more than about 10^4 years, which is much shorter than the average interval between reversals, about 10^6 years. However, the time series of reversals is highly irregular and exhibits some intervals as long as 30×10^6 years with no reversals. This irregularity may reflect the effects on the core motions that are produced by *changing* boundary conditions at the core–mantle boundary associated *inter alia* with very slow convection in the mantle (Hide 1967), but it is possible that it also includes manifestations in core motions of 'deterministic

chaos', now known to be typical of many nonlinear systems operating under *fixed* boundary conditions (see, for example, Lorenz 1993: Thompson & Stewart 1986).

The investigation of such issues is well beyond the present capability of models based on the partial differential equations of MHD. so it is necessary to proceed by studying suitable 'low-dimensional' analogues governed by ordinary, albeit nonlinear, differential equations. The first such analogue was proposed by Bullard (1955), who analysed the behaviour of the simplest imaginable system consisting of a single Faraday disk and coil arrangement driven by a constant applied couple G. In the Bullard dynamo (where mechanical friction is neglected), the direction of the electric current $I(t)$ generated by the dynamo remains unidirectional and the system exhibits periodic relaxation oscillations with properties that depend critically on the starting conditions (see equation (B 2)). The magnetic field is related to the current by Ampère's law, so the Bullard system gives periodic relaxation oscillations of the magnetic field, but no reversals of its direction. In subsequent work, it was shown that by coupling two such Bullard dynamo systems together (Rikitake 1958, 1966; see also Moffatt 1978; Moreau 1990; Turcotte 1993; Jacobs 1994; Marzocchi *et al.* 1995; cf. Hide 1995), or by introducing a resistive shunt (Malkus 1972; Robbins 1977; see also Ghil & Childress 1987), it is possible to produce chaotic reversals in the direction of the current $I(t)$ generated by the dynamo. These and related electromechanical systems have been studied by mathematicians interested in their nonlinear behaviour and also by theoretical geophysicists concerned with the interpretation of the observed time series of geomagnetic polarity reversals (Jacobs 1994; Turcotte 1993).

The present study was started by one of us (R.H.) for reasons in the first instance unconnected with the geodynamo problem. It was prompted by a remark made by Dr David L. T. Anderson of Oxford University, when during a seminar he emphasized that nonlinear systems capable of chaotic multiperiod relaxation oscillations were of interest to theoretical oceanographers and meteorologists concerned with modelling the so-called 'El Niño–Southern Oscillation' (ENSO), on interannual time scales, of the atmosphere–ocean system (see, for example, Philander 1990; Neelin *et al.* 1994; Willebrandt & Anderson 1993). Heat storage in the oceans is considered to be important in the dynamical processes underlying the ENSO, so it was decided out of curiosity to study the effect on the behaviour of a single-disk dynamo of introducing a suitable storage element, namely a series capacitor. Multiple oscillations were indeed found in this new system (see § 4), and when these results were mentioned to Dr F. J. Lowes of the University of Newcastle-upon-Tyne, he drew attention to a paper by Paynter (1982) in which it is pointed out that a capacitor can be equivalent to a motor as a circuit element. So, fortuitously, the investigation turns out to be more relevant to the geodynamo problem than was originally anticipated, for an electric motor can be seen as the rough analogue of hydrodynamical eddies driven largely by Lorentz forces in the core.

2. Two single-disk systems

Figures 1 and 2 illustrate two single-disk dynamo systems and their circuit diagrams, one with a capacitor and the other with a motor in series with the coil. In each system there is an electrically conducting Faraday disk driven into rotation with angular speed $\Omega(t)$ (where t denotes time) by a steady couple G. The disk is surrounded by a stationary coil of inductance L which is connected by brushes (slid-

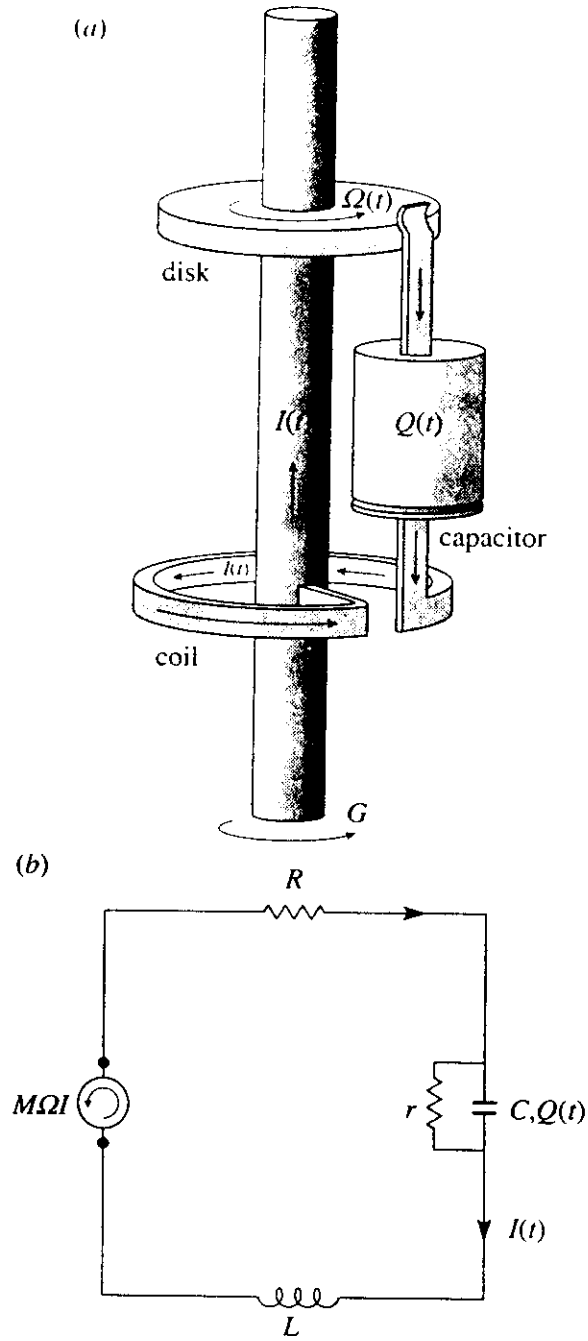

Figure 1. (*a*) Single disk dynamo with a capacitor in series with the coil, and (*b*) equivalent circuit diagram (see equations (2.3) and (2.15).

ing contacts) to the axle and to the rim of the disk. If a magnetic field is present, then a radial electromotive force (e.m.f.) is produced in the rotating disk, sending an electric current $I(t)$ through the stationary elements (coil and capacitor or motor) *via* the brushes.

If Q is the charge on the capacitor then

$$\dot{Q} = I - Q/rC, \tag{2.1}$$

where the dot denotes differentiation with respect to time t and C and r the capacitance and leakage resistance of the capacitor, respectively (see figure 1). If ω is the speed of rotation of the motor, B is the moment of inertia of the armature, HI the torque on the armature produced by the current I and $D\omega$ is the decelerating torque

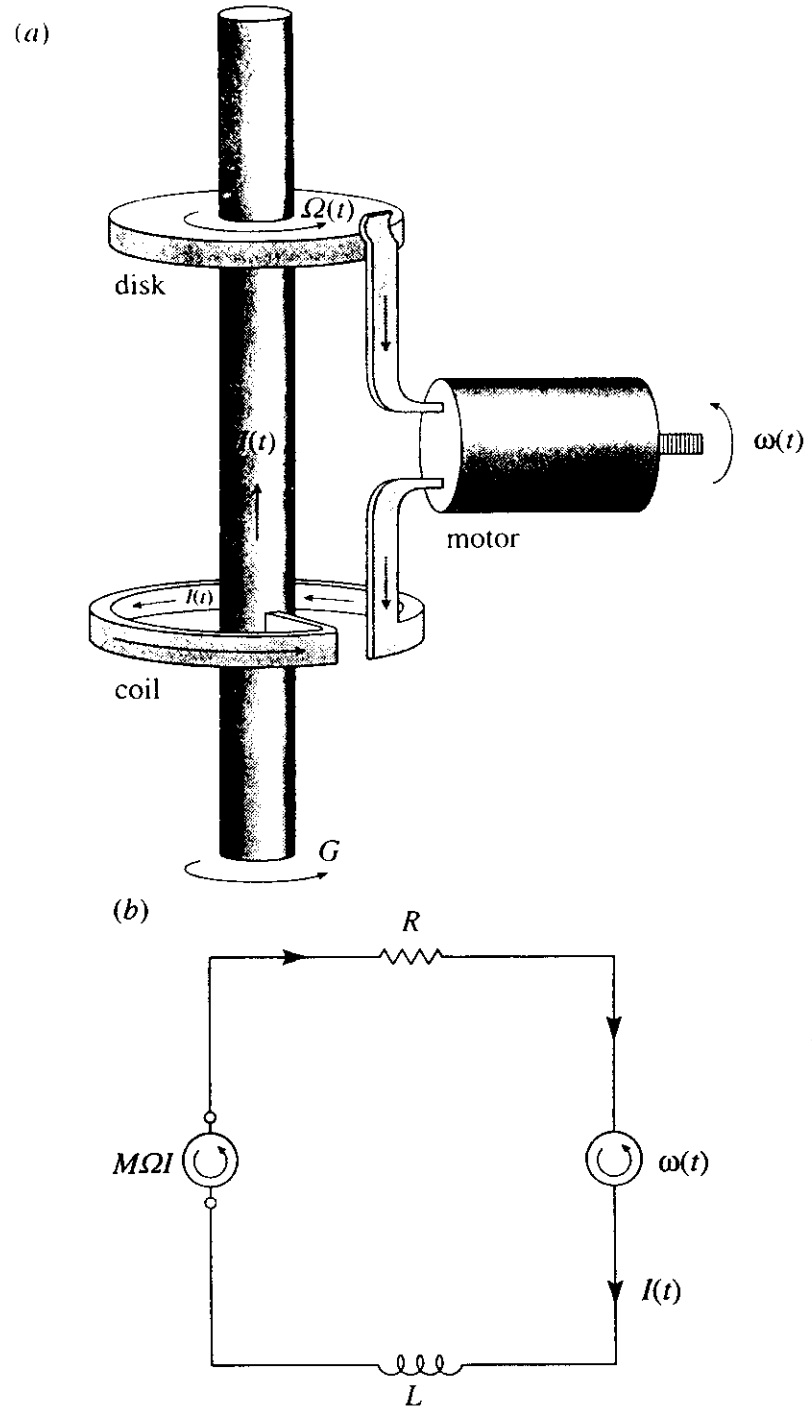

Figure 2. (*a*) Single disk dynamo with a motor in series with the coil, and (*b*) equivalent circuit diagram (see equations (2.4) and (2.15).

due to mechanical friction in the motor, then

$$B\dot{\omega} = HI - D\omega. \tag{2.2}$$

Denote by $2\pi M$ the mutual inductance between the coil and the rim of the disk. Assume that the coil is wound in the sense shown in figure 1, that Ω is positive when in the same sense as that of the applied couple, and that the magnetic field acting on the disk is produced by the current I in the system, so that the e.m.f. generated by the motion of the disk is $MI\Omega$ (but see Moffatt 1979). This e.m.f is balanced by the sum of the voltage drops RI, $L\dot{I}$, and *either* Q/C in the case of the capacitor *or* $H\omega$ in the case of the motor, where R is the total electrical resistance in the system.

Thus,

$$L\dot{I} + RI + Q/C = MI\Omega, \tag{2.3}$$

or

$$L\dot{I} + RI + H\omega = MI\Omega. \tag{2.4}$$

A third equation is needed to complete the set governing the three dependent variables, $I(t)$, $\Omega(t)$ and either $Q(t)$ or $\omega(t)$. This comes from mechanical considerations of torque balance in the disk (cf. equation (2.2)). If A is the moment of inertia of the disk and K the coefficient of linear mechanical friction, then

$$A\dot{\Omega} = G - MI^2 - K\Omega. \tag{2.5}$$

It is instructive to consider the energetics of the two systems. By equation (2.5), the rate of change of kinetic energy of the disk $\frac{1}{2}A\Omega^2$ satisfies

$$\frac{\mathrm{d}}{\mathrm{d}t}(\tfrac{1}{2}A\Omega^2) = G\Omega - M\Omega I^2 - K\Omega^2. \tag{2.6}$$

By equations (2.3) and (2.4) the rate of change of the magnetic energy of the coil $\frac{1}{2}LI^2$ satisfies

$$\frac{\mathrm{d}}{\mathrm{d}t}(\tfrac{1}{2}LI^2) = M\Omega I^2 - RI^2 - \frac{QI}{C}, \tag{2.7}$$

or

$$\frac{\mathrm{d}}{\mathrm{d}t}(\tfrac{1}{2}LI^2) = M\Omega I^2 - RI^2 - HI\omega. \tag{2.8}$$

By equation (2.1), the rate of change of the electrostatic energy of the capacitor $\frac{1}{2}Q^2C$ satisfies

$$\frac{\mathrm{d}}{\mathrm{d}t}\left(\frac{1}{2}\frac{Q^2}{C}\right) = \frac{QI}{C} - \frac{Q^2}{rC^2}. \tag{2.9}$$

By equation (2.2), the rate of change of the kinetic energy of the armature of the motor $\frac{1}{2}B\omega^2$ satisfies

$$\frac{\mathrm{d}}{\mathrm{d}t}(\tfrac{1}{2}B\omega^2) = HI\omega - D\omega^2. \tag{2.10}$$

The interactions expressed by equations (2.6)–(2.10) are illustrated in figures 3 and 4, from which it is readily seen that the rate of change of the total energy, $\frac{1}{2}(LI^2 + A\Omega^2 + Q^2/C)$ or $\frac{1}{2}(LI^2 + A\Omega^2 + B\omega^2)$, satisfies

$$\frac{1}{2}\frac{\mathrm{d}}{\mathrm{d}t}\left(LI^2 + A\Omega^2 + \frac{Q^2}{C}\right) = G\Omega - RI^2 - K\Omega^2 - \frac{Q^2}{rC^2}, \tag{2.11}$$

or

$$\frac{1}{2}\frac{\mathrm{d}}{\mathrm{d}t}\left(LI^2 + A\Omega^2 + B\omega^2\right) = G\Omega - RI^2 - K\Omega^2 - D\omega^2, \tag{2.12}$$

which do not involve the coupling terms $M\Omega I^2$ and QI/C or $HI\omega$. These show that the rate of change of total energy is equal to the rate at which energy is supplied to the system by the action of the driving couple G, less the rate at which energy is degraded into heat by ohmic heating and mechanical friction.

Self-exciting dynamo action involves the amplification through motional induction of a tiny adventitious electric current in the system until a new state is attained in which (I, Ω, Q or ω) are either steady with non-zero values given by equation (3.2) or

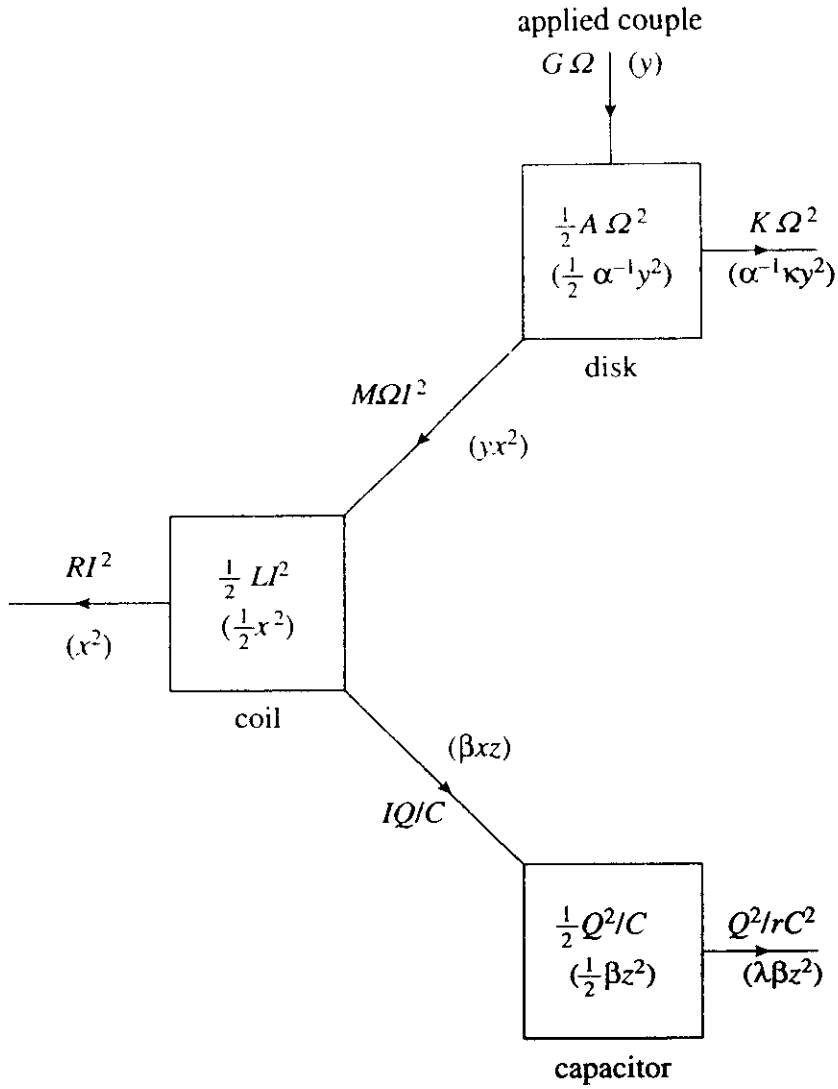

Figure 3. Illustrating energetics of single-disk dynamo with a capacitor in series with the coil (see equations (2.6), (2.7), (2.9), (2.11) and (2.19)–(2.22)).

fluctuate with time. In that state the rate $G\Omega$ at which work is done on the system by the applied couple is instantaneously (in the steady case), or on average over a suitable interval (in the fluctuating case), balanced by dissipation due to ohmic heating and mechanical friction ($RI^2+K\Omega^2$ plus Q^2/rC^2 or $D\omega^2$, see equations (2.11) and (2.12) and figures 3 and 4). Dynamo action is impossible, however, unless Ω is large enough, notably greater than R/M, for motional induction to overcome ohmic dissipation. Otherwise, i.e when $\Omega < R/M$, the system settles down to a steady and stable equilibrium state $(I, \Omega, Q \text{ or } \omega) = (0, G/K, 0)$ (see equation (3.1)) characterized by an energy balance between $G\Omega$ and $K\Omega^2$.

In certain circumstances the dynamo equilibrates in a steady state given by equation (3.2), where the sign of I and of Q or ω depends on the sign of the initial disturbance, but $(I, \Omega, Q \text{ or } \omega)$ are otherwise independent of the properties of the initial disturbances. But for a large range of parameter values, that state is itself unstable to small disturbances, which are amplified into fluctuations in $(I, \Omega, Q \text{ or } \omega)$ of varying degrees of complexity, ranging in character from purely sinusoidal through non-harmonic but periodic behaviour to highly chaotic. Bifurcation theory (see later) provides some guidance in the elucidation of the various regimes of dynamo action

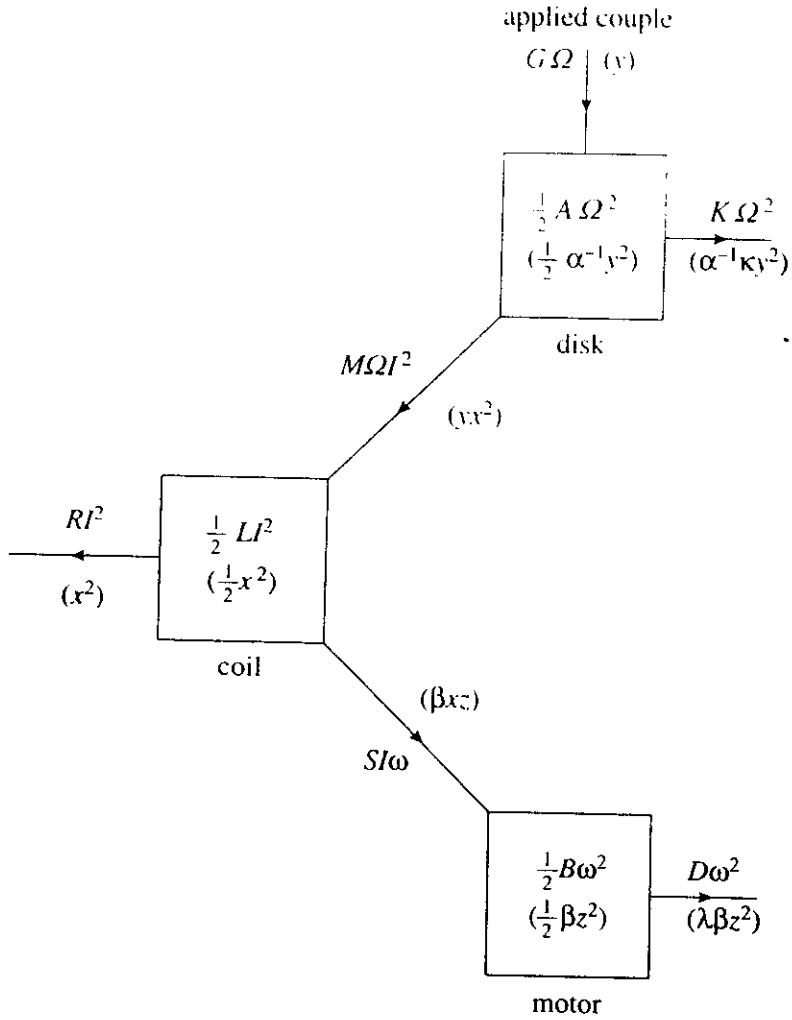

Figure 4. Illustrating energetics of single-disk dynamo with a motor in series with the coil (see equations (2.6), (2.8), (2.10), (2.12) and (2.19)–(2.22)).

in the systems, but the rich behaviour of the systems will only be fully revealed by extensive computational studies, which lie beyond the scope of the present paper.

It is convenient at this stage to replace the dimensional dependent variables $(I(t), \Omega(t), Q(t))$ or $(I(t), \Omega(t), \omega(t))$ and independent variable t by dimensionless variables $(x(\tau), y(\tau), z(\tau))$ and τ. Thus, we choose

$$\tau \equiv \frac{R}{L}t, \quad x \equiv \left(\frac{M}{G}\right)^{1/2} I, \quad y \equiv \frac{M}{R}\Omega, \tag{2.13}$$

(cf. equations (2.3) and (2.4)) and

$$z \equiv \frac{R}{L}\left(\frac{M}{G}\right)^{1/2} Q \quad \text{or} \quad z \equiv \frac{R}{L}\frac{B}{H}\left(\frac{M}{G}\right)^{1/2} \omega. \tag{2.14}$$

In their dimensionless forms, the set of equations (2.1), (2.3) and (2.5) or of equations (2.2), (2.4) and (2.5) give

$$\left.\begin{aligned} \dot{x} &= x(y-1) - \beta z, \\ \dot{y} &= \alpha(1-x^2) - \kappa y, \\ \dot{z} &= x - \lambda z, \end{aligned}\right\} \tag{2.15}$$

where the dot now denotes differentiation with respect to τ. Here

$$\alpha \equiv \frac{GLM}{R^2A}, \quad \kappa \equiv \frac{KL}{RA}. \tag{2.16}$$

and

$$\beta \equiv \frac{L}{CR^2} \quad \text{or} \quad \beta \equiv \frac{H^2L}{R^2B} \tag{2.17}$$

$$\lambda \equiv \frac{L}{RrC} \quad \text{or} \quad \lambda \equiv \frac{DL}{RB}. \tag{2.18}$$

The corresponding energy equations (2.6)–(2.12) give

$$\frac{1}{2}\frac{\mathrm{d}}{\mathrm{d}\tau}x^2 = x^2(y-1) - \beta xz, \tag{2.19}$$

$$\frac{1}{2\alpha}\frac{\mathrm{d}}{\mathrm{d}\tau}y^2 = y(1-x^2) - \frac{\kappa}{\alpha}y^2, \tag{2.20}$$

$$\frac{\beta}{2}\frac{\mathrm{d}}{\mathrm{d}\tau}z^2 = \beta xz - \lambda\beta z^2. \tag{2.21}$$

and

$$\frac{1}{2}\frac{\mathrm{d}}{\mathrm{d}\tau}\left\{x^2 + \frac{1}{\alpha}y^2 + \beta z^2\right\} = y - x^2 - \frac{\kappa}{\alpha}y^2 - \lambda\beta z^2. \tag{2.22}$$

The quantity α can be regarded as a dimensionless measure of the magnitude of the applied couple (G) and κ as a measure of the mechanical friction (coefficient K) in the disk. In the case of the series capacitor β^{-1} and λ measure, respectively, the capacitance (C) and the leakage resistance (r), in suitable units, whereas in the case of a series motor, β^{-1} and λ measure the moment of inertia B of the armature and the mechanical friction (coefficient D) in the motor. But from this point we can treat the problem on its mathematical merits, remembering however that although cases when κ and/or $\lambda = 0$ might be mathematically interesting and even useful, only those cases with $\kappa \neq 0$ and $\lambda \neq 0$ are physically realistic (see Appendix B).

Also worthy of note is that the choice we have made for the units in which the independent variable τ and dependent variables (x, y, z), though physically reasonable and mathematically convenient, is not unique. The expression of α, β, κ and λ in terms of the intrinsic 'time constants' of the system (see Appendix A) provides insight into the nature of these dimensionless parameters.

3. Stability of equilibrium states

Equations (2.15) have a reflection symmetry: they are unchanged if

$$x \to -x, \quad y \to y, \quad z \to -z.$$

The full MHD equations have a similar symmetry, since for every solution $(\boldsymbol{B}(\boldsymbol{r}, t), \boldsymbol{u}(\boldsymbol{u}, t))$ of the dynamo equations (where $\boldsymbol{B}$ denotes the magnetic field at a general point P with position $\boldsymbol{r}$ at time t and $\boldsymbol{u}$ is the Eulerian flow velocity at P), $(-\boldsymbol{B}(\boldsymbol{r}, t), \boldsymbol{u}(\boldsymbol{r}, t))$ is also a solution (but $(-\boldsymbol{B}(\boldsymbol{r}, t), -\boldsymbol{u}(\boldsymbol{r}, t))$ is not!). In the simple dynamo system the current, $x(\tau)$ in the non-dimensionalized coordinates, is analogous to the magnetic field $\boldsymbol{B}$, and y, the non-dimensionalized angular velocity, is analogous to $\boldsymbol{u}$.

Steady solutions to equations (2.15) occur when $\dot{x} = \dot{y} = \dot{z} = 0$. That is, when either

$$x = 0, \quad y = \alpha/\kappa, \quad z = 0, \tag{3.1}$$

or

$$x = \pm\sqrt{1 - \frac{\kappa}{\alpha}\left(1 + \frac{\beta}{\lambda}\right)}, \quad y = 1 + \frac{\beta}{\lambda}, \quad z = \frac{1}{\lambda}x. \tag{3.2}$$

In the first solution, there is no current flowing in the system ($x = 0$), and, in consequence, the motor is stationary or there is no charge on the capacitor ($z = 0$): the disk rotates at a speed, y, such that the mechanical friction produces a decelerating torque sufficient to balance the applied couple.

It is instructive to consider the stability of this solution. A small perturbation to solution (3.1) is considered, that is $x = \epsilon x'$, $y = \alpha/\kappa + \epsilon y'$ and $z = \epsilon z'$. Substituting these values of x, y and z into equations (2.15) and neglecting all terms which are second or higher order in ϵ results in the linear equations

$$\begin{pmatrix} \dot{x}' \\ \dot{y}' \\ \dot{z}' \end{pmatrix} = \boldsymbol{A} \begin{pmatrix} x' \\ y' \\ z' \end{pmatrix}, \tag{3.3}$$

where

$$\boldsymbol{A} = \begin{pmatrix} (\alpha/\kappa) - 1 & 0 & -\beta \\ 0 & -\kappa & 0 \\ 1 & 0 & -\lambda \end{pmatrix}.$$

These equations have a unique solution (see, for example, Perko 1991, p. 17). Furthermore, whether the perturbation (x', y', z') grows or decays is governed by the eigenvalues of $\boldsymbol{A}$, namely

$$-\kappa, \quad \frac{1}{2}\left\{\frac{\alpha}{\kappa} - 1 - \lambda \pm \sqrt{\left(\frac{\alpha}{\kappa} - 1 + \lambda\right)^2 - 4\beta}\right\}. \tag{3.4}$$

If all three eigenvalues have negative real part, then the perturbations decay and the solution is stable. Changes in stability occur when the real part of at least one of the eigenvalues changes sign. This can occur either by one or more eigenvalues passing through zero, or by a complex conjugate pair of eigenvalues crossing the imaginary axis. In the former case a steady bifurcation occurs, while in the latter there is a Hopf bifurcation. The planes of bifurcation points divide the $\alpha, \beta, \kappa, \lambda$-parameter space into different regions of behaviour and, for that reason, they can be particularly useful in classifying the solutions of the set of equations.

For α/κ sufficiently small, all the eigenvalues are negative and solution (3.1) is stable. There is a zero eigenvalue along the curve

$$\frac{\alpha}{\kappa} = \frac{\beta}{\lambda} + 1. \tag{3.5}$$

This is a curve of symmetry-breaking bifurcation points: at this point the pair of steady solutions (3.2) branch from solution (3.1). The curve of bifurcation points is shown in figure 5, and is labelled as s. As $\lambda \to 0$, the slope of this curve in the $(\beta, \alpha/\kappa)$ plane becomes greater and greater until, in the limit $\lambda = 0$, this line is coincident with the axis, where $\beta = 0$.

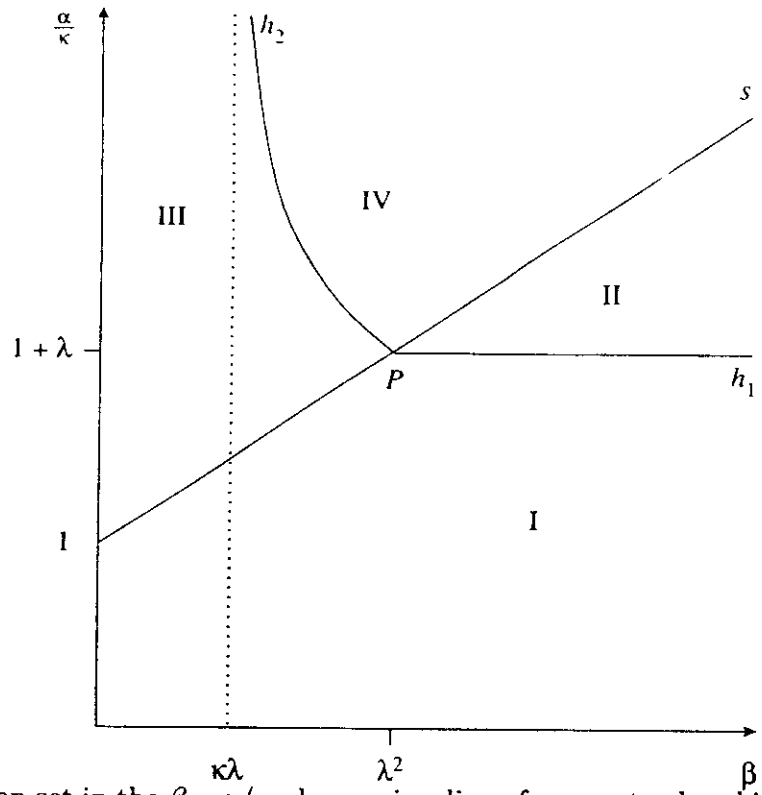

Figure 5. Bifurcation set in the $\beta - \alpha/\kappa$ plane. s is a line of symmetry-breaking bifurcations (see equation (3.5)). h_1 and h_2 are lines of Hopf bifurcation points (see equations (3.6) and (3.9)). P is a double zero eigenvalue point (a Takens–Bogdanov point with symmetry).

When

$$\alpha/\kappa = 1 + \lambda, \quad \text{and} \quad \lambda^2 < \beta \tag{3.6}$$

there is an imaginary pair of eigenvalues and a line of Hopf bifurcations occurs. This line is drawn in figure 5 and labelled h_1. Along the line of Hopf bifurcations the solution to the perturbation equations (3.3) is

$$\begin{aligned} x' &= \frac{\lambda x_0 - \beta z_0}{\sqrt{(\beta - \lambda^2)}} \sin\sqrt{(\beta - \lambda^2)}\tau + x_0 \cos\sqrt{(\beta - \lambda^2)}\tau, \\ y' &= y_0 \mathrm{e}^{-\kappa\tau}, \\ z' &= \frac{x_0 - \lambda z_0}{\sqrt{(\beta - \lambda^2)}} \sin\sqrt{(\beta - \lambda^2)}\tau + z_0 \cos\sqrt{(\beta - \lambda^2)}\tau, \end{aligned} \tag{3.7}$$

where at $\tau = 0$, $(x', y' z') \equiv (x_0, y_0, z_0)$. Note that y' decays with time while x' and z' oscillate harmonically: local to the Hopf bifurcation line and after a sufficiently long time the dynamics will be constrained to the $y \approx \alpha/\kappa$ plane and x and z will execute harmonic oscillations with frequency $\sqrt{(\beta - \lambda^2)}$. Hence, periodic solutions of arbitrarily long period can be produced by changing $(\beta - \lambda^2)$: the smaller $(\beta - \lambda^2)$ the longer the period.

The Hopf bifurcation line stops where it meets the steady bifurcation curve at $(\beta, \alpha/\kappa) = (\lambda^2, 1 + \lambda)$. Labelled P in figure 5, this point is a double zero-eigenvalue point. Hence, solution (3.1), corresponding to no dynamo action, is stable for parameter values within region I of figure 5. If the torque is increased (increasing α) then this state becomes unstable. If the characteristics of the capacitor or motor are such that $\beta < \lambda^2$, then this becomes unstable to a steady solution corresponding to constant current flow given by (3.2). Note that this solution only exists if the

exists if the capacitor has a finite leakage resistance or if the motor has some mechanical friction ($\lambda \neq 0$). If $\beta > \lambda^2$, then the zero-current solution loses stability to a solution in which the current oscillates, but the mean current flow is still zero. When λ is small, these oscillations have angular frequency of approximately $(LC)^{-1/2}$ and $HB^{-1/2}$ for the capacitor and motor cases, respectively. At onset, these oscillations are driven by the rotation of the disk, but only weakly feedback to affect the motion of the disk, i.e. close to onset the oscillations in y are much smaller in amplitude than the oscillations in x and z.

A stability analysis for solution (3.2) shows that the eigenvalues, σ, indicating the stability or otherwise satisfy the cubic equation

$$\sigma^3 + \left(\kappa + \lambda - \frac{\beta}{\lambda}\right)\sigma^2 + \left(2(\alpha - \kappa) + \kappa\lambda - \frac{3\beta\kappa}{\lambda}\right)\sigma + 2(\alpha\lambda - \kappa\lambda - \beta\kappa) = 0. \quad (3.8)$$

Consistent with the analysis for solution (3.1) there is a single zero eigenvalue if $\alpha/\kappa = 1 + \beta/\lambda$ and two zero eigenvalues at the point P.

At a Hopf bifurcation of solutions (3.2), the three eigenvalues must be of the form, $\sigma_1, \mathrm{i}\omega, -\mathrm{i}\omega$. Rather than solve the cubic equation (3.8) explicitly, it is simpler to derive necessary and sufficient conditions that must be satisfied for this to hold. If the cubic equation is written as

$$\sigma^3 + a\sigma^2 + b\sigma + c = 0,$$

then the eigenvalues are of the required form if, and only if,

$$ab = c \quad \text{and} \quad b > 0.$$

Substituting for a, b and c from equation (3.8) gives

$$\frac{\alpha}{\kappa} = \frac{2\beta - \kappa\lambda - \lambda^2}{2(\kappa - (\beta/\lambda))} + \frac{3}{2}\frac{\beta}{\lambda} + 1, \quad \text{if} \quad 1 + \frac{3}{2}\frac{\beta}{\lambda} < \frac{\alpha}{\kappa} + \frac{1}{2}\lambda, \quad (3.9)$$

when $\kappa \neq \beta/\lambda$, and

$$\lambda = \sqrt{\beta} \quad \text{for} \quad \alpha/\kappa > 1 + \sqrt{\beta} \quad (3.10)$$

when $\kappa = \beta/\lambda$.

Along the Hopf bifurcation line (3.9) each of the two solution branches given by (3.2) lose their stability; two different periodic solutions are produced simultaneously in different parts of the phase space. These correspond to solutions in which the current oscillates about a non-zero mean, but as discussed later, both of these solutions are unstable and not physically realizable. The Hopf bifurcation line is drawn in figure 5 as curve h_2. Note that this line of Hopf bifurcations also ends at the point P. Furthermore, although the curves s and h_1 are only dependent on the ratio α/κ, this is not true for h_2. The frequency of the Hopf bifurcations, ω_2, is given by

$$\omega_2^2 = 2(\alpha - \kappa) + \kappa\lambda - 3\beta\kappa/\lambda, \quad (3.11)$$

which tends to zero as the point P is approached. The line h_2 asymptotes to the line $\beta = \kappa\lambda$. Since $\beta = \lambda^2$ at P, h_2 lies to the right or left of P, according as $\kappa > \lambda$ or $\kappa < \lambda$: figure 5 shows the latter case.

The three lines s, h_1 and h_2 all meet at the double zero-eigenvalue point P. This type of zero-eigenvalue point is a Takens–Bogdanov point with reflection symmetry: it has been well studied (for example, see § 7.3 of Guckenheimer & Holmes 1986). It is straightforward to show, using centre manifold reduction and normal form analysis,

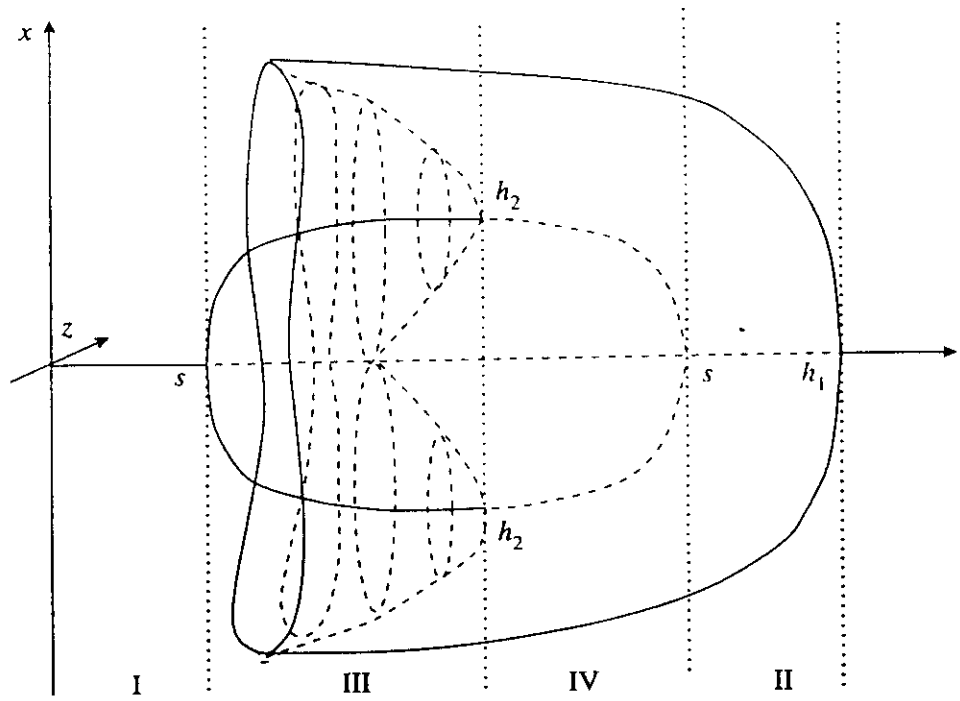

Figure 6. Bifurcation diagram showing a representation of the solution as a clockwise path around P in the parameter plane is traversed, starting in region I. The two points at which the symmetry-breaking line is crossed are marked s (see equation (3.5)). Similarly, the points where the two Hopf bifurcation lines are crossed are marked h_1 and h_2 (see equations (3.6) and (3.9)).

that local to P, the behaviour may be described by equation 7.3.22 (p. 371) in Guckenheimer & Holmes (1986) for $a_3 = -1$ and with $b_3 = -1$ if $\lambda < 1.5\kappa$ and $b_3 = +1$ if $\lambda > 1.5$. The analysis culminating in figure 7.3.9 on p. 376 is relevant. In both cases, in addition to the bifurcation lines shown in figure 5, there is a line of homoclinic connections which emerges from P. In order to explain how this occurs, a schematic bifurcation diagram is shown in figure 6. In this diagram we imagine taking a path clockwise around P and plot a measure of the solution against the distance travelled around P. The convention that stable solutions are shown with solid lines and unstable solutions with dashed lines, is used.

The left of figure 6 starts at a point in region I where the steady solution (3.1) is stable. Travelling clockwise around P, the line s is traversed. At this point, solution (3.1) becomes unstable and two stable solutions (3.2) bifurcate. Continuing further, h_2 is reached, and the steady solutions (3.2) are themselves destabilized at Hopf bifurcations. Two periodic solutions are produced, related to each other by the reflection symmetry of the original equations. These bifurcate subcritically so the periodic solutions produced are unstable. Since there are now no stable solutions local to solution (3.2), as region IV is entered there will be a jump to a large stable periodic solution. On continuing around P this large stable periodic solution shrinks until it disappears in the Hopf bifurcation at h_1. We have now returned to region I where solution (3.1) is stable. There is hysteresis in the point at which the stable solution jumps from the steady-state solution to the large periodic solution at h_2 and so we now consider circling P in an anti-clockwise direction, again starting from region I. As we cross from region I into region II, the steady solution (3.1) loses stability and is replaced by a stable periodic solution. Stepping back across regions II and IV this solution grows until at some point in region III it coalesces with a large unstable periodic orbit and disappears. The system will jump down to one of the two stable steady solutions (3.2) present in region III. To understand how this large stable pe-

riodic solution is destroyed we need to return to the two unstable periodic solutions produced at h_2. On travelling anti-clockwise away from h_2, these two solutions grow until they hit the unstable steady solution (3.1). This is the homoclinic connection mentioned earlier. It is a global solution: it takes an infinite time to traverse the resulting orbit and it is structurally unstable, but its presence can have a profound effect on the dynamical behaviour of the equations, a point we shall return to later. Continuing further, the homoclinic connection destroys the periodic cycles produced on solutions (3.2) and leaves one large unstable periodic solution in their place. It is this solution which grows until it coalesces with the large stable periodic solution and both are removed from the solution set.

For chaos to occur, the solution has to be stretched and folded in phase space in a particular way. This process is often associated with the presence of global solutions, with the tendency for the orbit to approach a steady solution playing a key role. Local to global solutions, period doubling cascades and chaos are found in many systems, with global bifurcations often acting as organizing centres. The homoclinic connection that emerges from P is suggestive of the presence of chaos.

At the point P in parameter space, two of the eigenvalues are zero and one is equal to $-\kappa$. This means that in a small neighbourhood of P, the dynamics are essentially planar: the negative eigenvalue contracts the dynamics down on to the centre manifold. It is well known that there can be no chaos in two-dimensional phase space, and for this reason, no chaos is expected local to P. However, this restriction is lifted for parameter values away from P. One region where chaos is likely to occur in this problem is close to the line h_2 but away from the point P. A similar scenario, where a Takens–Bogdanov point provides a mechanism for the occurrence of a homoclinic bifurcation, which in turn provides a mechanism for chaos away from the Takens–Bogdanov point, has been observed before in an electronic oscillator by Healey *et al.* (1991). In the limit of $\lambda = 0$, the region where this occurs is squashed to nothing and no chaos can be produced by this mechanism.

4. Numerical integrations

The foregoing analysis, though revealing and instructive, gives only a hint of the full behaviour of the system. Numerical integrations show vastly more complicated behaviour, which is impossible to classify in simple terms. Here we present a few results for a limited number of parameter values. Much further numerical work will be needed to elucidate the behaviour of the system more fully.

The case when $\lambda = 0$ is physically unrealistic (for it corresponds to a capacitor with no leakage resistance or a motor with no mechanical friction), see § 2, but its treatment is instructive as a starting point. As λ is decreased the slope of the line s in figure 5 increases, squashing regions III and IV, until in the limit $\lambda = 0$ the symmetry-breaking bifurcation line s is coincident with the abscissa and regions III and IV do not exist. The equations were integrated using a fourth-order Runge–Kutta method with adaptive time stepping. The solutions were integrated over many cycles to ensure that a stable final state had been reached. For values of the parameters in region I, the numerical integrations always converged to the steady solution given by (3.1). For α just greater than 0.1 and $\kappa = 0.1$, a periodic solution was found. This is shown in figure 7*a* for $\alpha = 0.15$. As predicted by the analysis, close to the bifurcation point, this periodic orbit lies approximately in the $y = \alpha/\kappa = 1$ plane. Figure 7*a* shows six representations of this solution: all the following numerical solutions are

presented in the same format. Figure 7*a*(i) shows the phase space, plotting x against y against z. In order to aid the interpretation of this picture, we have plotted in 7*a*(ii) the projection of this phase space solution on the x–z-plane and in 7*a*(iii) the projection on the x–y-plane. The remaining three figures, 7*a*(iv)–(vi) show the time series of the x, y and z coordinates, respectively. The almost planar nature of this particular example is seen in both the projection on the x–y-plane and the time series for the y coordinate. In terms of the physical system, the current oscillates about zero with corresponding oscillations of the charge on the capacitor or in the speed of the motor, while the speed of rotation of the disk remains at an almost constant level.

As α is increased this periodic orbit grows in size and bends out of the $y = 1$ plane. Further periodic solutions arise at saddle-node bifurcations so that multiple solutions states are possible: which solution is found depends on the initial conditions. One example is shown in figure 7*b*: this can be characterized as having two distinct 'humps' in the x time series (the current). Whereas the solution 7*a* appears to wind once round the line $x = 1, y = 1$ and once round the line $x = -1, y = 1$, the solution 7*b* winds around each line twice. In this example, the disk periodically switches from rotating in one direction to rotating in the opposite direction (7*b*(v)).

As α is increased, more and more periodic solutions are found for the same parameter values. As an example, figures 8*a*–*d* show four different periodic solutions, all of which exist for $\alpha = 50$, $\beta = 1$, $\kappa = 0.1$, $\lambda = 0$. Each of these solutions has a different number of 'humps' in the x time series corresponding to a different number of windings. The examples 8*a*–*d* have 6, 9 and 14 windings, respectively. Solutions for all the intermediate integers have also been found. All exist in the same region of phase space: they are nested such that the solutions with most humps are on the inside. The innermost solution is almost a square wave with sharp spikes at the switching point. Each of the solutions has a slightly different period. For the innermost solution the current remains almost constant for most of the time (figure 8*d*(iv)), while the speed of rotation of the disk and either the charge on the capacitor or the speed of the motor gradually increase (figure 8*e*(iv)). At a critical level the speed of rotation of the disk drops rapidly (in an oscillatory manner) and the sign of the current reverses.

These results facilitate the discussion of the physically realistic case of $\lambda \neq 0$. Then, similar nested solutions are found again in region II and also to the right of region IV. However, chaotic solutions are also found as a result of the homoclinic bifurcation discussed in § 3. These solutions take the form of flipping between the two unstable periodic cycles which appear simultaneously along the line h_2. Two examples are shown. In the first, shown in figure 9*a*, the orbit passes only a few times around the unstable periodic orbit before flipping to the other orientation. The second, shown in figure 9*b*, is for parameter values very close to the Hopf bifurcation line h_2 in the $(\beta, \alpha/\kappa)$ plane. In the second case, the current spends a long time oscillating about a positive non-zero mean before rapidly flipping and oscillating about a negative non-zero mean. We have only observed this second type of chaotic behaviour in a small region of parameter space. It bears some resemblance to the observed time series for geomagnetic dipole reverses in two senses, firstly that the timescale in which the solution flips from one unstable periodic orbit to the other is much shorter than the time for which the solution remains in either orientation. Secondly, the time for which the x-coordinate remains positive (or negative) varies—in the example piece of time series shown here, the time between flips varies by a factor of six.

An attractive feature of the systems we have investigated is that they are physi-

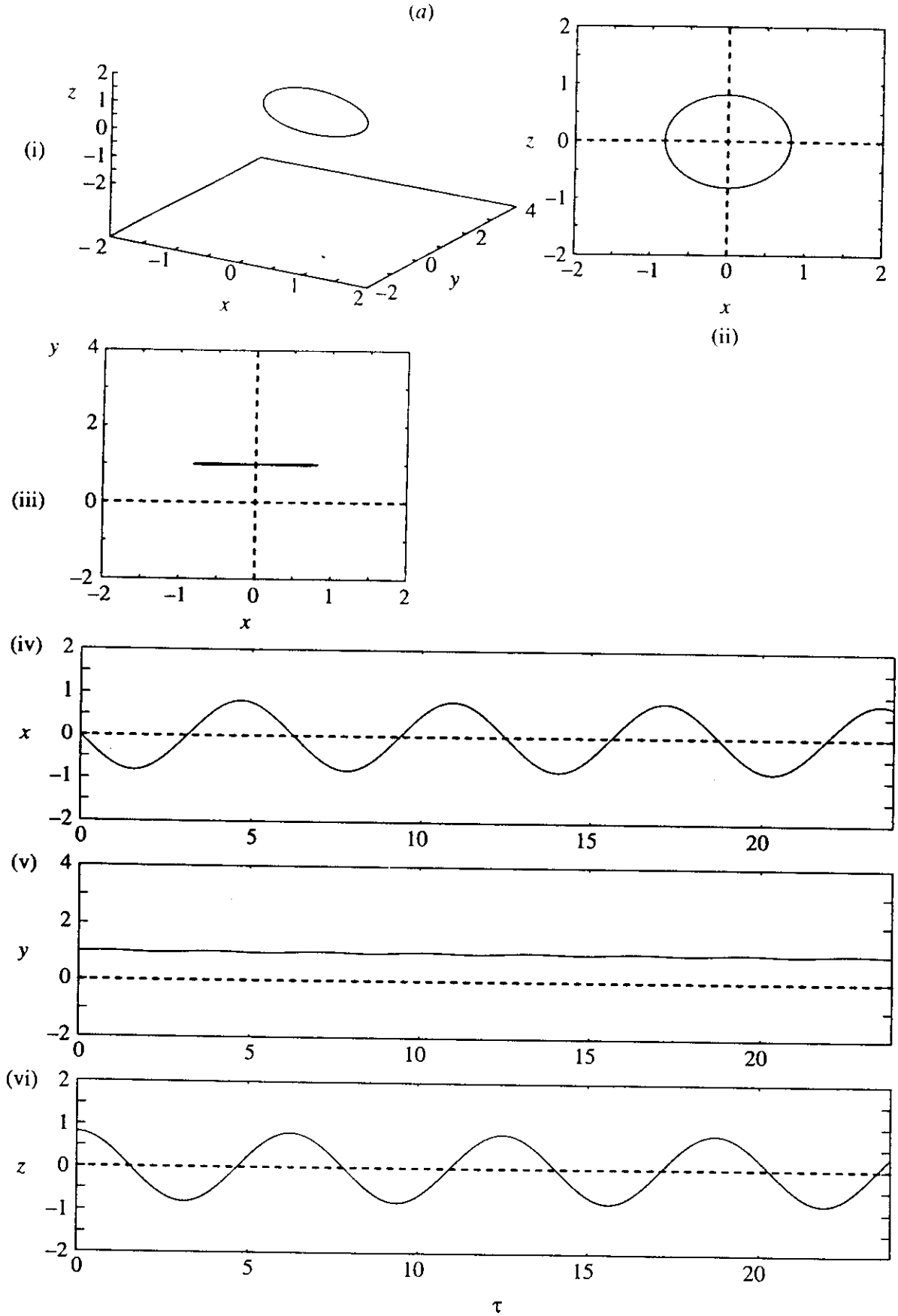

Figure 7. Numerical integrations, $\kappa = 0.1, \lambda = 0$: (*a*) $\alpha = 0.15$, $\beta = 1.0$.; (*b*) $\alpha = 5.0$, $\beta = 1.0$. In each case, (i) is a phase space plot, the axes are x, y and z; (ii) is the projection of the phase space in the x–z-plane; (iii) is the projection of the phase space in the x–y-plane; (iv) is the time-series of the x-coordinate and similarly (v) and (vi) are the time-series of the y and z-coordinates, respectively (see equations (2.15)).

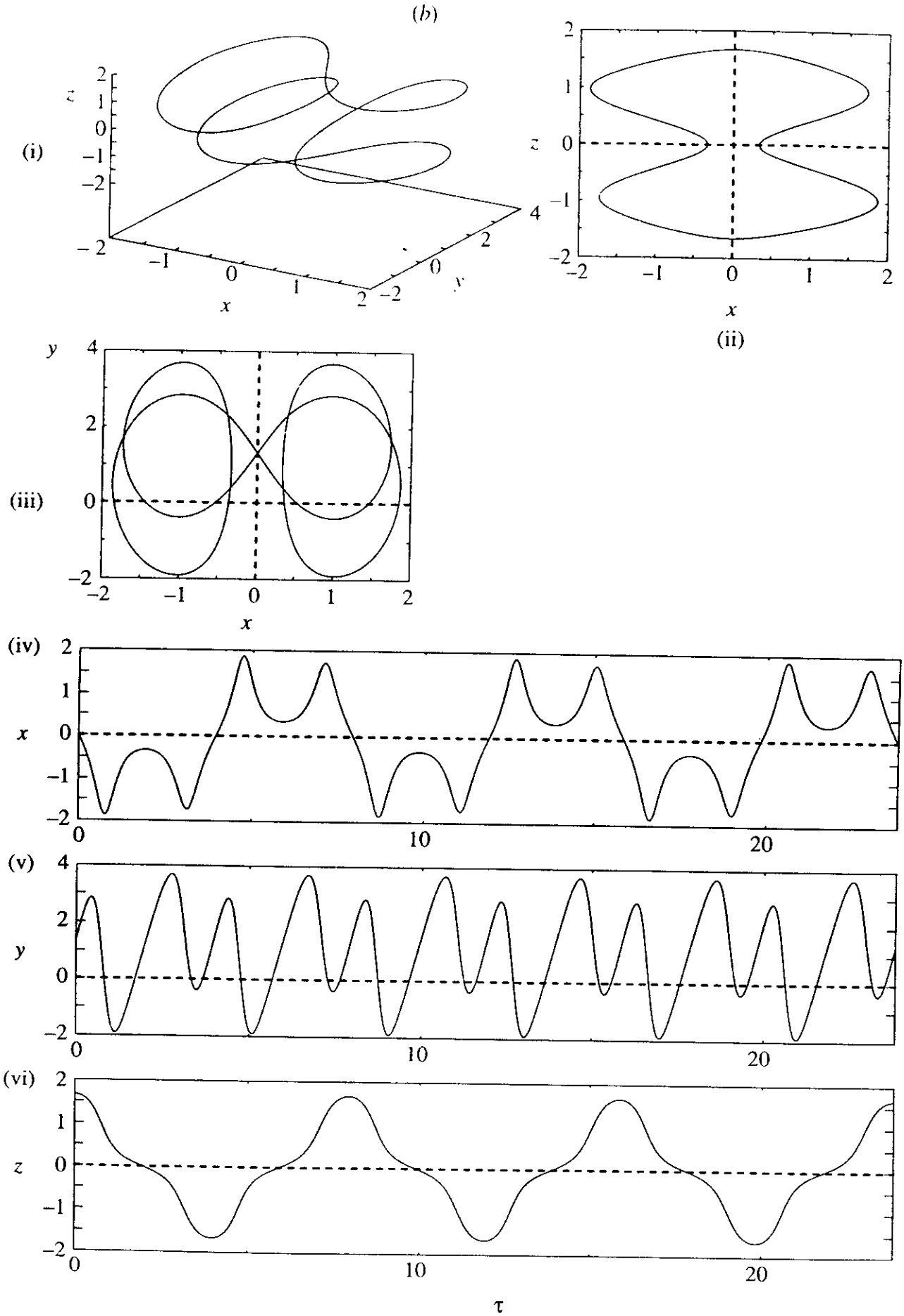

Figure 7. (*Cont.*)

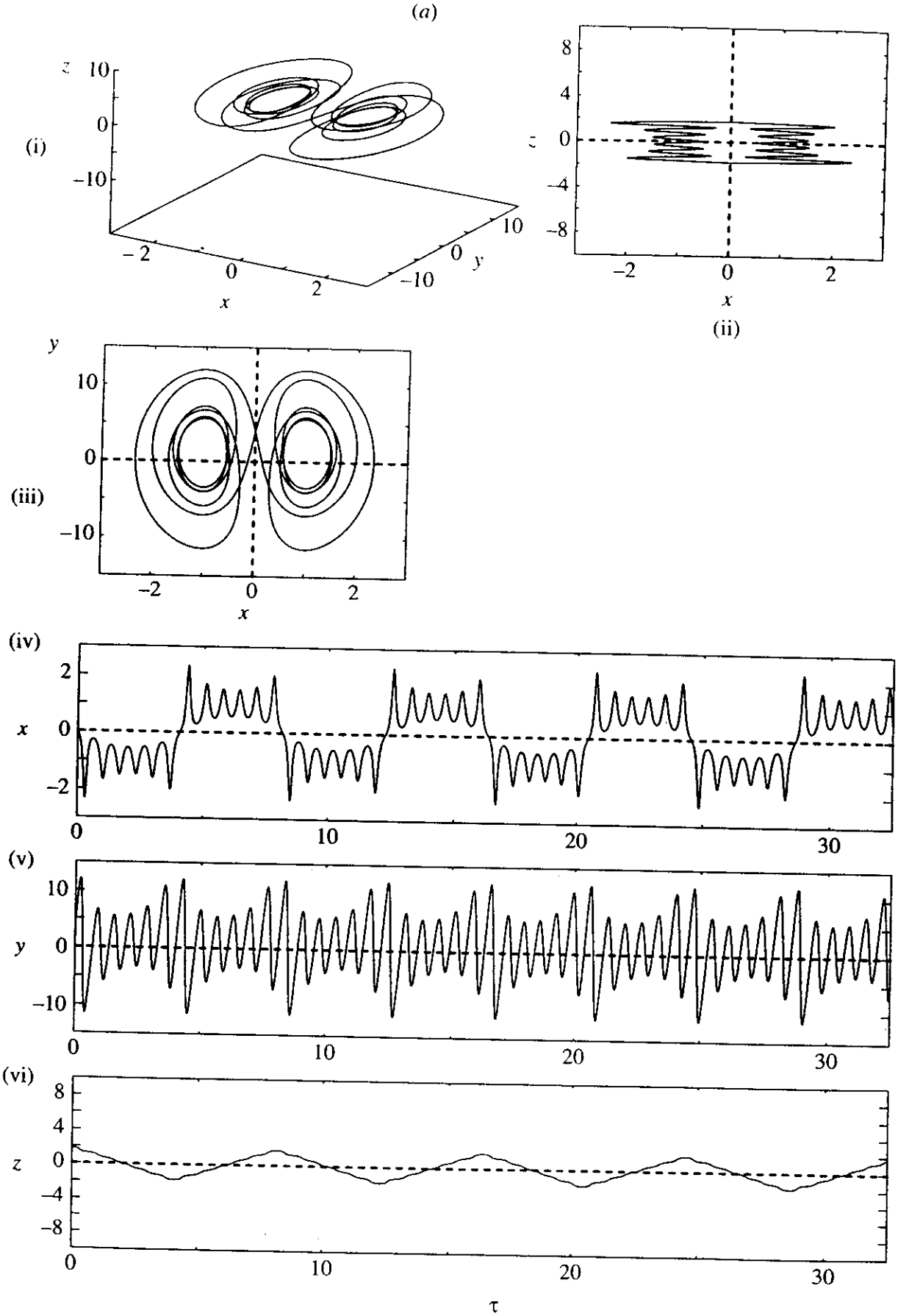

Figure 8. Examples of four different solutions which all occur for the same values of the parameters, that is $\alpha = 50.0$, $\beta = 1.0$, $\kappa = 0.1$, $\lambda = 0.0$. All are stable solutions; which is observed depends on the initial conditions for x, y and z.

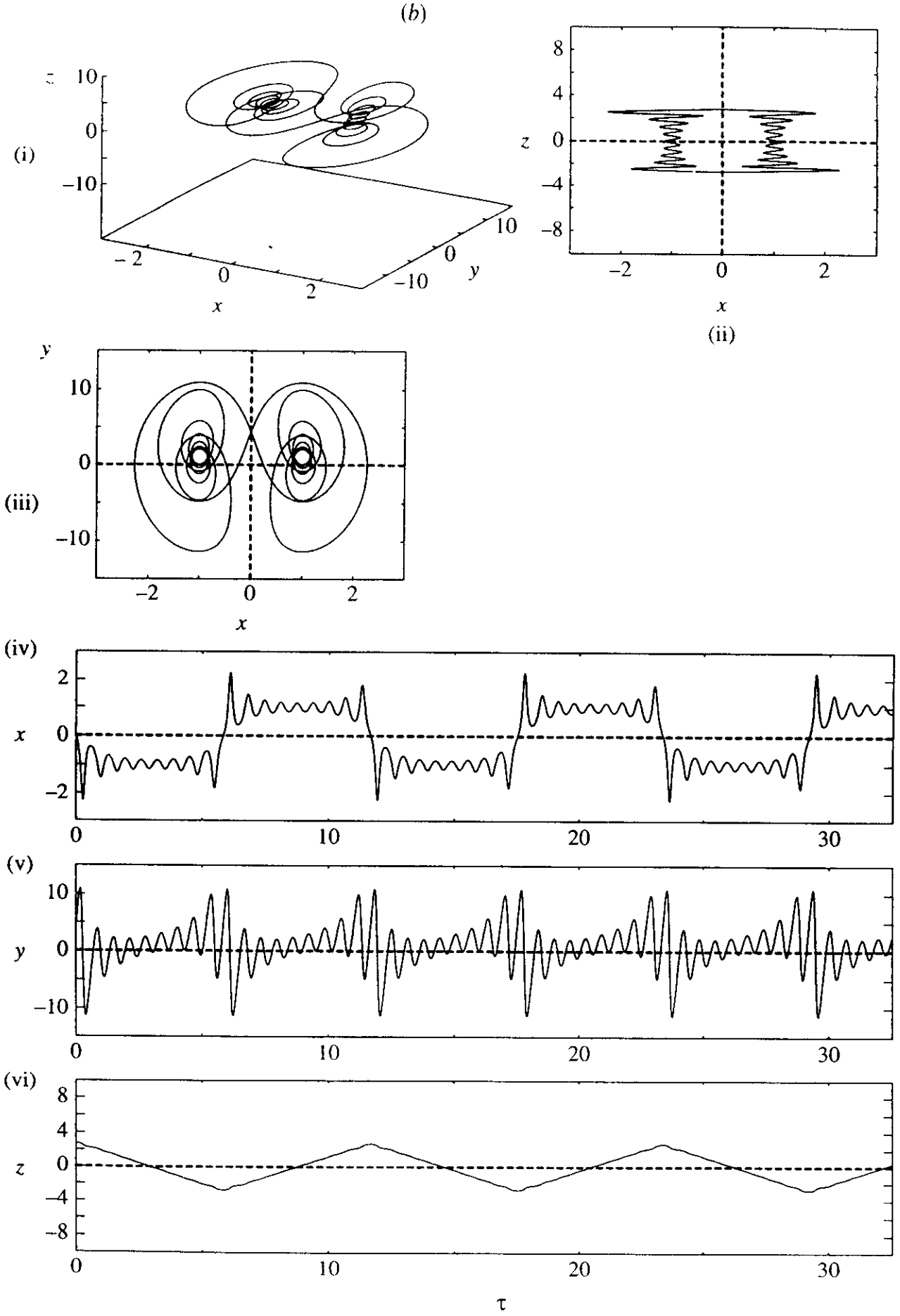

Figure 8. (*Cont.*)

(c)

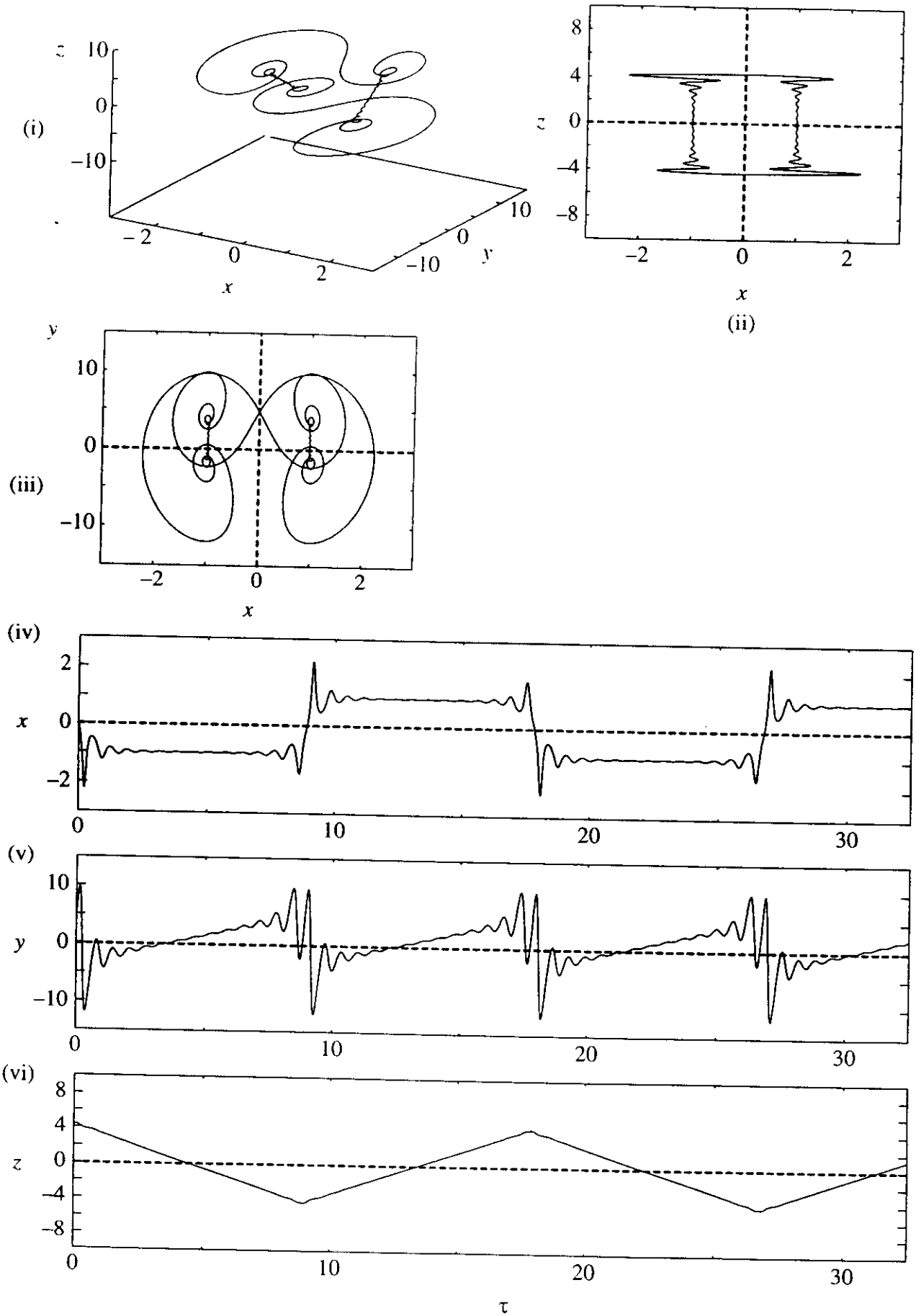

Figure 8. (*Cont.*)

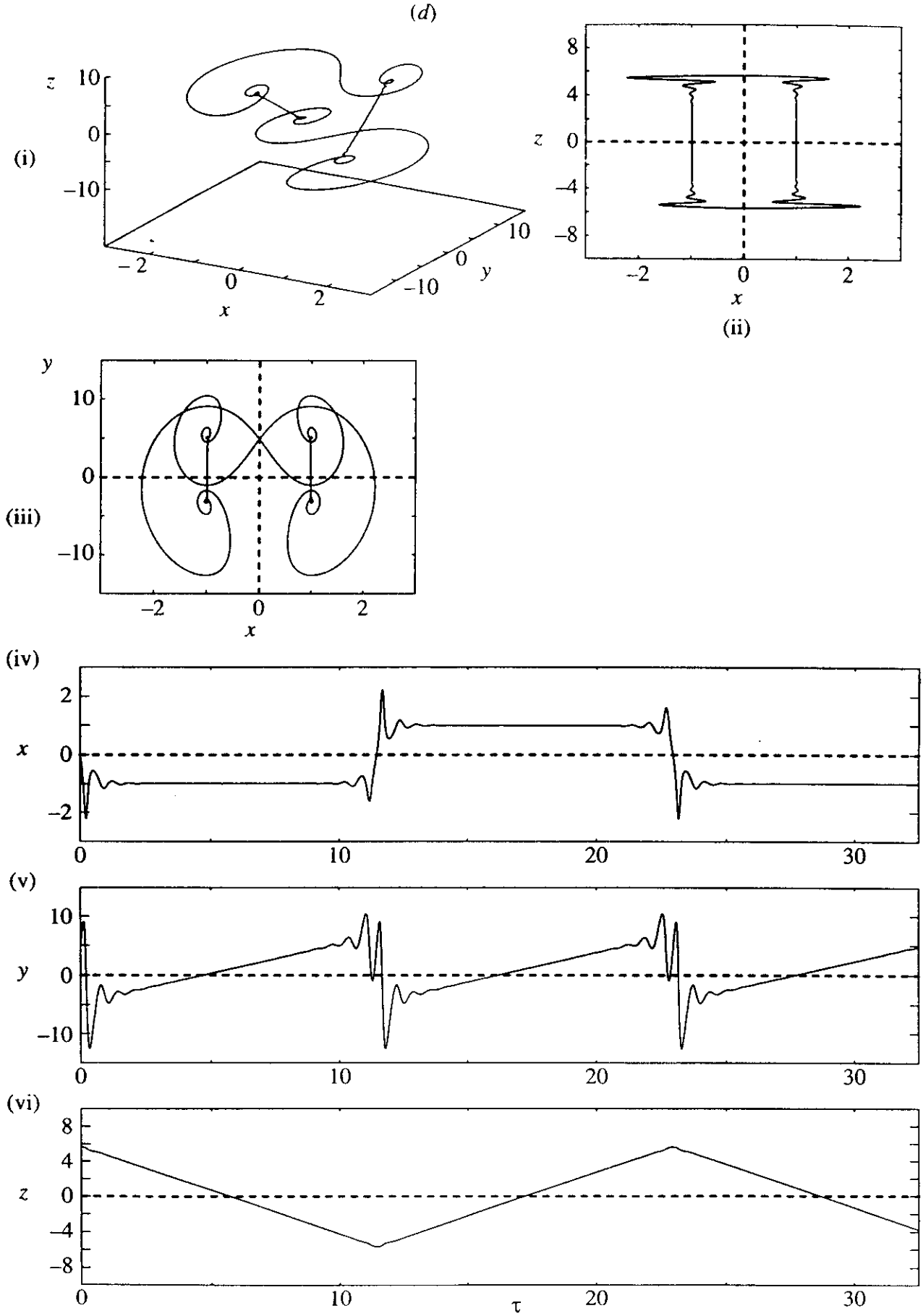

Figure 8. (*Cont.*)

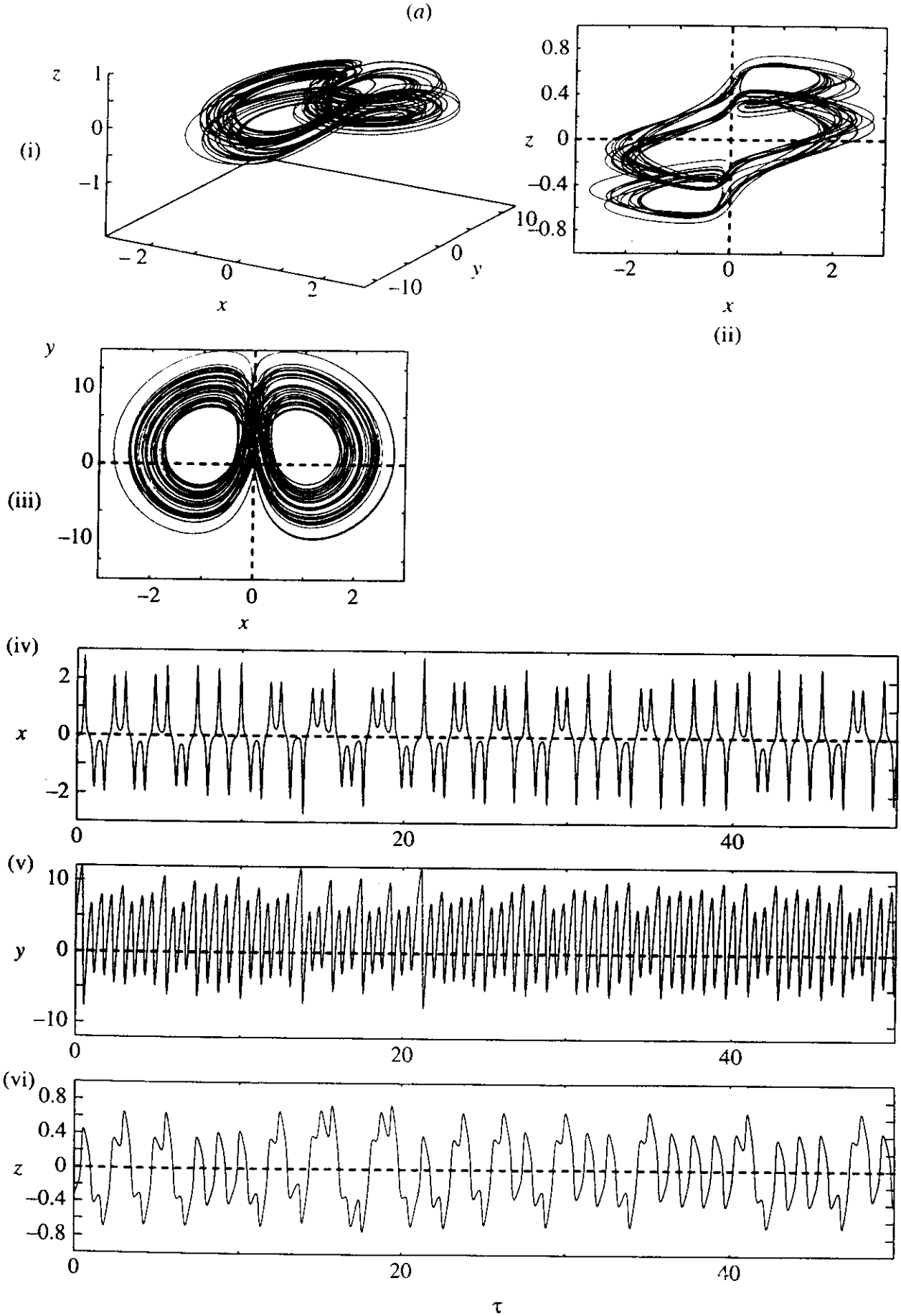

Figure 9. Numerical integrations for (*a*) $\alpha = 20.0$, $\beta = 2.0$, $\kappa = 1.0$, $\lambda = 1.2$; (*b*) $\alpha = 100.0$, $\beta = 1.01$, $\kappa = 1.0$, $\lambda = 1.0$.

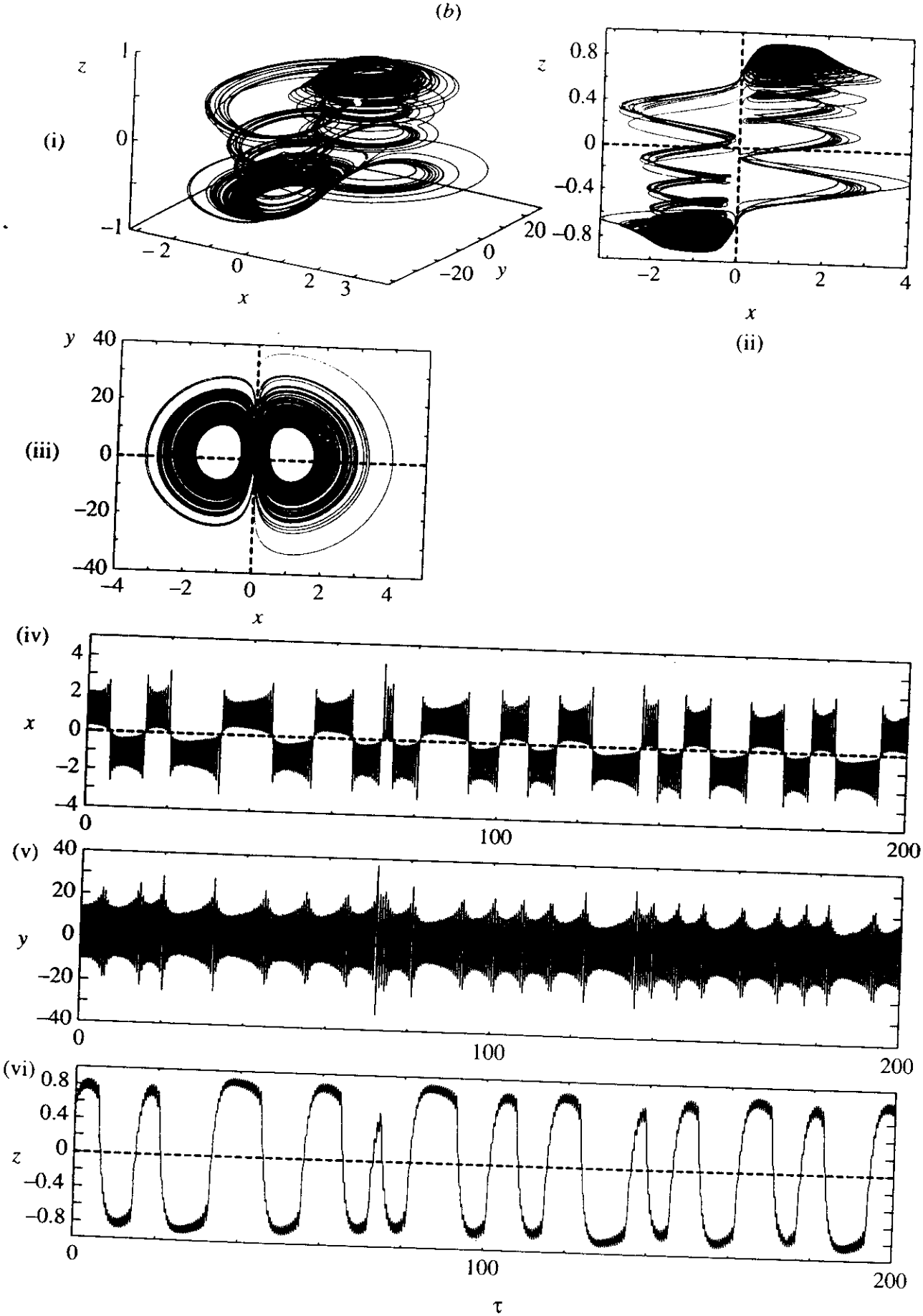

Figure 9. (*Cont.*)

cally realistic and could in principle be constructed in the laboratory. But the range of parameters attainable there would be limited by practical considerations, so mathematical and computational analysis provides the best approach.

The systems are rich in their behaviour, detailed studies of which in future work should prove rewarding. The recognition of λ as a key parameter in the production of chaos in these nonlinear systems is one of the main findings of the present work, but further studies including statistical calculations will be needed to elucidate the underlying processes fully. As noted in § 1, the addition of a shunt promotes chaotic behaviour when $\beta = 0$ and it should do likewise when $\beta \neq 0$; this is another matter deserving future study. It is easy to extend the theory to include a shunt in the systems studied in this paper. The dependence on β of oscillation periods and waveforms is also particularly noteworthy, and this also deserves further attention in future work.

Appendix A. Dimensionless variables and parameters and intrinsic time-constants

The electromechanical systems discussed in this paper are worthy of study because they are physically realistic, but they would not be efficient engineering devices. Their main interest stems from their potential use in providing insight and guidance in the study of various phenomena in geophysical and astrophysical fluid dynamics (see, for example, Hide 1994).

It is instructive to consider the four dimensionless parameters $(\alpha, \beta, \kappa, \lambda)$ (see equations (2.16)–(2.18)) in terms of intrinsic 'time constants' of the systems, namely

$$\frac{L}{R}, \quad \frac{M}{R}, \quad \left(\frac{A}{G}\right)^{1/2}, \quad \frac{A}{K}, \quad \frac{K}{G}, \quad rC \quad \text{or} \quad \frac{B}{D}, \quad \text{and} \quad (LC)^{1/2} \text{ or } \left(\frac{BL}{H^2}\right)^{1/2}, \tag{A 1}$$

in seconds. In § 2 we choose the 'ohmic decay time' L/R as the unit in terms of which τ is measured, but any of the other quantities (or combinations thereof) given in (A 1) could be used. (The ohmic decay time for the Earth's liquid metallic core, where the main geomagnetic field is produced by self-exciting MHD dynamo action, is tens of thousands of years!) In terms of these time constants, the dimensionless parameters $(\alpha, \beta, \kappa, \lambda)$ can be expressed as follows:

$$\alpha \equiv \frac{GLM}{R^2 A} = \left[\frac{L}{R}\right]\left[\frac{M}{R}\right]\left[\left(\frac{A}{G}\right)^{1/2}\right]^{-2}, \tag{A 2}$$

$$\kappa \equiv \frac{KL}{RA} = \left[\frac{L}{R}\right]\left[\frac{A}{K}\right]^{-1}, \tag{A 3}$$

$$\beta \equiv \frac{L}{CR^2} = \left[(LC)^{1/2}\right]^{-2}\left[\frac{L}{R}\right]^2, \tag{A 4}$$

$$\text{or} \quad \beta \equiv \frac{H^2 L}{R^2 B} = \left[\frac{L}{R}\right]^2\left[\left(\frac{BL}{H^2}\right)^{1/2}\right]^{-2}, \tag{A 5}$$

$$\text{and} \quad \lambda \equiv \frac{L}{RrC} = \left[\frac{L}{R}\right][rC]^{-1}, \tag{A 6}$$

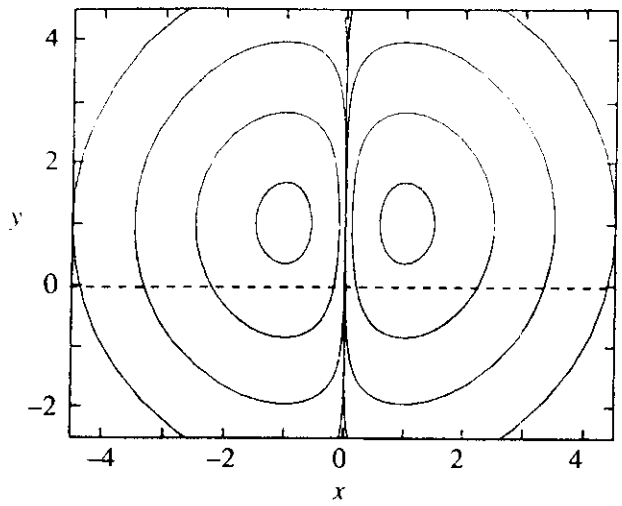

Figure 10. Phase plane for the Bullard system. The trajectories show typical solution paths for a number of different starting conditions (see equations (B 1)).

$$\text{or} \quad \lambda \equiv \frac{DL}{RB} = \left[\frac{L}{R}\right]\left[\frac{B}{D}\right]^{-1}. \tag{A 7}$$

The theoretically significant parameter α/κ (see, for example, figure 5) satisfies

$$\frac{\alpha}{\kappa} \equiv \frac{GM}{RK} = \left[\frac{M}{R}\right]\left[\frac{A}{K}\right]\left[\left(\frac{A}{G}\right)^{1/2}\right]^{-2} = \left[\frac{M}{R}\right]\left[\frac{K}{G}\right]^{-1}. \tag{A 8}$$

Self-exciting homopolar dynamo action requires *inter alia* high values of G and M and low values of R and K, conditions which would be hard to achieve in the laboratory.

Appendix B. Structural instability of the Bullard system

In this case, namely $\kappa = 0$ and $\beta = \lambda = 0$ in our notation, equations (2.15) reduce to

$$\begin{aligned} \dot{x} &= x(y-1), \\ \dot{y} &= \alpha(1-x^2). \end{aligned} \tag{B 1}$$

Bullard showed that these equations have an analytic solution given by

$$(y-1)^2 - \alpha(2\ln x - x^2) = (y_0-1)^2 - \alpha(2\ln x_0 - x_0^2), \tag{B 2}$$

where $(x(0), y(0)) = (x_0, y_0)$. Steady solutions ($\dot{x} = \dot{y} = 0$) arise when $x_0 = \pm 1$, $y_0 = 1$. Otherwise the solutions vary periodically (but non-harmonically) with time, with a period and trajectory dependent on the initial conditions. They may be represented in the phase plane (i.e. a plot of y against x) by two sets of closed curves centred on $y = 1$ and $x = \pm 1$ (see figure 10). These closed curves are trajectories of possible solutions, each characterized by the initial conditions. Since Bullard's system of equations are unchanged if $x \mapsto -x$, the phase space is symmetric about the y-axis. The y-axis itself is invariant under the flow: if x is zero at $\tau = 0$ it will remain zero for all time.

When mechanical friction is added to the system, which is equivalent to the first two of equations (2.15) with β set to zero, this modified Bullard system satisfies

$$\dot{x} = x(y-1), \qquad \dot{y} = \alpha(1-x^2) - \kappa y, \tag{B 3}$$

for which there are three steady solutions: namely either

$$x = 0, \quad y = \alpha/\kappa \tag{B 4}$$

or

$$x = \pm\sqrt{1 - \frac{\kappa}{\alpha}}, \quad y = 1. \tag{B 5}$$

If the mechanical friction is great enough, i.e. $\kappa > \alpha$, then only the first of these solutions can exist. A linear stability analysis like that carried out in §3 shows that this solution is linearly stable if $\kappa > \alpha$. That is, a small perturbation to this solution will decay in time. Furthermore, this solution must be globally stable, i.e. any perturbation will ultimately decay: there can be no closed orbits representing periodic oscillations as found by Bullard. This follows from the fact that in a planar dynamical system there can only be two types of solution bounded for all time, either steady solutions represented by fixed points or periodic solutions represented by closed curves. Any closed curve in the plane must surround a fixed point (see, for example, Perko 1991, p. 231, theorems 3 and 4.) Since the only steady solution lies on the y-axis, any trajectory surrounding this point would have to cross the y-axis. This cannot occur since, as for Bullard's system, the y-axis is invariant under the flow.

There is a bifurcation of solution (B 4) at $\kappa = \alpha$, where (B 4) becomes unstable and the two solutions given by equation (B 5) bifurcate. A linear stability analysis shows that these solutions are stable to small perturbations for all $\alpha > \kappa$ (κ non-zero). We have been unable to show that this solution is globally stable, i.e. that no periodic solutions exist in this case. However, numerical integrations strongly suggest that this is also true.

These results show that the system introduced and analysed by Bullard (1955) is structurally unstable and therefore physically unrealistic (as is the much studied Rikitake dynamo system based on the Bullard system (see Hide 1995)). He evidently considered that the most important finding of his analysis was his demonstration of the possibility of self-maintained oscillations even in the presence of ohmic dissipation. The claim (see Rikitake 1966, p. 61) that this conclusion remains unchanged even if mechanical friction is added to the disk dynamo is refuted by the foregoing analysis.

A.C.S. thanks the EPSRC for support under grant (GR/K41311)

References

Bullard, E. C. 1955 The stability of a homopolar dynamo. *Proc. Camb. Phil. Soc.* **51**, 744–760.

Ghil, M. & Childress, S. 1987 *Topics in geophysical fluid dynamics: atmospheric dynamics, dynamo theory and climate dynamics*. New York: Springer.

Guckenheimer, J. & Holmes, P. 1986 *Nonlinear oscillations, dynamical systems, and bifurcations of vector fields* (Applied Mathematical Science 42). New York: Springer.

Healey, J. J., Broomhead, D. S., Cliffe, K. A., Jones, R. & Mullin, T. 1991 The origins of chaos in a modified Van der Pol oscillator. *Physica* **48D**, 322–339.

Hide, R. 1967 Motions of the Earth's core and mantle, and variations of the main geomagnetic field. *Science* **157**, 55–56.

Hide, R. 1994 Chaos in geophysical fluids. *Phil. Trans. R. Soc. Lond.* A **348**, 431-443.

Hide, R. 1995 Structural instability of the Rikitake disk dynamo. *Geophys. Res. Lett.* **22**, 1057–1059.

Jacobs, J. A. (ed.) 1987–91 *Geomagnetism* (4 volumes). New York: Academic.

Jacobs, J. A. 1994 *Reversals of the Earth's magnetic field*. Cambridge University Press.

Lorenz, E. N. 1993 *The essence of chaos*. London: UCL Press Limited.

Malkus, W. V. R. 1972 Reversing Bullard's dynamo. *Eos* **53**, 617.

Marzocchi, W., Gonzato, G. & Mulargia, F. 1995 Rikitake's geodynamo analysed in terms of classical time series statistics. *Phys. Earth Planet. Inter.* **88**, 83–88.

Melchior, P. 1986 *Physics of the Earth's core*. Oxford: Pergamon.

Moffatt, H. K. 1978 *Magnetic field generation in electrically-conducting fluids*. Cambridge University Press.

Moffatt, H. K. 1979 A self-consistent treatment of simple dynamo systems. *Geophys. Astrophys. Fluid Dyn.* **14**, 147–166.

Moreau, R. 1990 *Magnetohydrodynamics*. Dordrecht: Kluver.

Neelin, J. D., Latif, M. & Jin, F.-F. 1994 Dynamics of coupled ocean-atmosphere models: the tropical problem. *A. Rev. Fluid Mech.* **26**, 617–659.

Paynter, H. M. 1982 The Janet/Busch oscillator: A multivibratory dissipation structure relevant to dynamo theories of geomagnetic flux reversals. In *Proc. 1982 Am. Auto. Control Council*, pp. 34–39.

Perko, L. 1991 *Differential equations and dynamical systems* (Texts in Applied Mathematics 7). Berlin: Springer.

Philander, G. 1990 *El Niño, la Niña and Southern Oscillation*. New York: Academic.

Rikitake, T. 1958 Oscillations of a system of disk dynamos. *Proc. Camb. Phil. Soc.* **54**, 89–105.

Rikitake, T. 1966 *Electromagnetism and the Earth's interior*. New York: Elsevier.

Robbins, K. A. 1977 A new approach to sub-critical instability and turbulent transitions in a simple dynamo. *Math. Proc. Camb. Phil. Soc.* **82**, 309–325.

Thompson, J. M. T. & Stewart, H. B. 1986 *Nonlinear dynamics and chaos*. Chichester: Wiley.

Turcotte, D. L. 1993 *Fractals and chaos in geology and geophysics*. Cambridge University Press.

Willebrandt, J. & Anderson, D. L. T. (eds) 1993 *Modelling ocean climate interactions*. New York: Springer.

Received 12 May 1995; revised 14 August 1995; accepted 2 October 1995

Geophys. J. Int. 1996, 125, F1-F3

FAST-TRACK PAPER

Potential magnetic field and potential vorticity in magnetohydrodynamics

Raymond Hide

Department of Physics (Atmospheric, Oceanic and Planetary Physics), Clarendon Laboratory, University of Oxford, Parks Road, Oxford OX1 3PU, *UK*

Accepted 1996 February 13. Received 1996 February 13; in original form 1996 January 29

SUMMARY

New general expressions are given which extend theorems governing the behaviour of the *potential vorticity* (Ertel) pseudoscalar in continuum mechanics and the *potential magnetic field* (Hide) in electrodynamics. The laws of thermodynamics (involving entropy and *potential temperature*) are readily incorporated into the expressions, the application of which should facilitate both prognostic and diagnostic studies of basic magnetohydrodynamic processes, including those underlying the magnetic fields of stars and planets and other phenomena encountered in astrophysics and geophysics.

Key words: geomagnetism, magnetohydrodynamics, potential magnetic field, potential vorticity.

Consider a continuous medium in which the mass density is $\rho(\mathbf{r}, t)$ and the Eulerian velocity relative to an inertial frame is $\mathbf{u}(\mathbf{r}, t)$ at a general point P with position vector $\mathbf{r}$ at time t. Conservation of mass requires that

$$\frac{D\rho}{Dt} + \rho\nabla\cdot\mathbf{u} = 0 \tag{1}$$

(where $D/Dt \equiv \partial/\partial t + \mathbf{u}\cdot\nabla$), which reduces to $\nabla\cdot\mathbf{u} = 0$ when the medium is incompressible.

If by $\boldsymbol{\xi} \equiv \nabla\times\mathbf{u}$ we denote the (absolute) vorticity, and by

$$\rho^{-1}\boldsymbol{\xi}\cdot\nabla H^* \tag{2}$$

the so-called 'potential vorticity', where $H^* = H^*(\mathbf{r}, t)$ is *any* continuous and differentiable function, then by a very slight extension of Ertel's theorem based on the laws of mechanics (see Ertel 1942; also Pedlosky 1987, Gill 1982), we have

$$\frac{D}{Dt}\left(\frac{\boldsymbol{\xi}\cdot\nabla H^*}{\rho}\right) = \frac{\boldsymbol{\xi}}{\rho}\cdot\nabla\frac{DH^*}{Dt} + \nabla H^*\cdot\boldsymbol{\Psi}, \tag{3}$$

where

$$\boldsymbol{\Psi} \equiv \rho^{-3}\nabla\rho\times\nabla p + \rho^{-1}\nabla\times(\rho^{-1}\mathbf{j}\times\mathbf{B}) + \rho^{-1}\nabla\times(\rho^{-1}\mathbf{F}). \tag{4}$$

Here $p = p(\mathbf{r}, t)$ denotes pressure and $\mathbf{j}\times\mathbf{B}$ the Lorentz ponderomotive force if $\mathbf{j}(\mathbf{r}, t)$ is the electric current density at P and $\mathbf{B}(\mathbf{r}, t)$ is the magnetic field, which satisfies

$$\nabla\cdot\mathbf{B} = 0. \tag{5}$$

When, as in many cases of interest, the acceleration term $D\mathbf{u}/Dt$ in the equation of motion is much smaller in magnitude than the acceleration due to gravity, $\mathbf{g}$, the term $\rho^{-3}\nabla\rho\times\nabla p$ in eq. (4) can be replaced by $\rho^{-2}\nabla\rho\times\mathbf{g}$ without fear of serious error. The term $\mathbf{F}$ in eq. (4) represents the visco-elastic force acting on an element of material of unit volume which at time t is situated at P, reducing in the case of a fluid to the usual term representing the viscous force. Potential vorticity considerations based on eq. (3) [with $\mathbf{B} = 0$, see eq. (4)] play a central role in modern theoretical research in dynamical meteorology and oceanography.

Analogous to the derivation of (3) from the equations of mechanics is the derivation from the equations of electrodynamics of an expression governing the behaviour of the 'potential magnetic field', defined as

$$\rho^{-1}\mathbf{B}\cdot\nabla G^* \tag{6}$$

(where G^*, like H^*, is any continuous and differentiable function of $\mathbf{r}$ and t), namely

$$\frac{D}{Dt}\left(\frac{\mathbf{B}\cdot\nabla G^*}{\rho}\right) = \frac{\mathbf{B}}{\rho}\cdot\nabla\frac{DG^*}{Dt} + \nabla G^*\cdot\boldsymbol{\Phi} \tag{7}$$

(Hide 1983, 1986). Here $\boldsymbol{\Phi}$ comprises several terms, all of which vanish when the medium is a perfect conductor of electricity and thermoelectric effects are negligible. [Consistent with the neglect of relativistic effects, no account is taken of Maxwell displacement currents, and electrostatic forces can be ignored in $\mathbf{F}$, see eq. (4).]

Now make the successive substitutions $H^* = H$ and $H^* = q'H$ in the potential vorticity equation (3), and combine the resulting two equations to obtain

$$\boxed{\frac{D}{Dt}\left[\frac{H}{\rho}\boldsymbol{\xi}\cdot\nabla q'\right] = \left(\frac{\boldsymbol{\xi}\cdot\nabla q'}{\rho}\right)\frac{DH}{Dt} + \frac{H}{\rho}\left(\boldsymbol{\xi}\cdot\nabla\frac{Dq'}{Dt}\right) + H\boldsymbol{\Psi}\cdot\nabla q'.} \tag{8}$$

In the same way, substitute $G^* = G$ and then $G^* = qG$ in the potential magnetic field equation (7), whence

$$\boxed{\frac{D}{Dt}\left[\frac{G}{\rho}\mathbf{B}\cdot\nabla q\right] = \left(\frac{\mathbf{B}\cdot\nabla q}{\rho}\right)\frac{DG}{Dt} + \frac{G}{\rho}\left(\mathbf{B}\cdot\nabla\frac{Dq}{Dt}\right) + G\Phi\cdot\nabla q.} \tag{9}$$

(The functions H, G, q and q' are also arbitrary.) These are useful extensions of the general results expressed by eqs (3) and (7) respectively (to which they reduce when $H = G = 1$), for each contains two arbitrary scalars, rather than just one. For example, eq. (8) with $H = \mathbf{u}\cdot\nabla q'$ leads directly to the relationship between the helicity $(\mathbf{u}\cdot\boldsymbol{\zeta})$ and superhelicity $(\boldsymbol{\xi}\cdot\nabla\times\boldsymbol{\xi})$ pseudoscalars. The electrodynamic counterpart relating magnetic helicity $(\mathbf{A}\cdot\mathbf{B})$ (where $\nabla\times\mathbf{A} = \mathbf{B}$) and magnetic superhelicity $(\mathbf{B}\cdot\nabla\times\mathbf{B})$ follows directly from eq. (9) with $G = \mathbf{A}\cdot\nabla q$ (Hide 1989).

As an application of (8) and (9), we set $H = \mathbf{B}\cdot\nabla q$ in the former and $G = \boldsymbol{\xi}\cdot\nabla q'$ in the latter and then subtract the resulting equations, thereby obtaining a new general expression satisfied by the combined equations of mechanics and electrodynamics needed in theoretical magnetohydrodynamics. Thus

$$\boxed{\begin{aligned}\frac{D}{Dt}\left[\log\frac{\mathbf{B}\cdot\nabla q}{\boldsymbol{\xi}\cdot\nabla q'}\right] &= (\mathbf{B}\cdot\nabla q)^{-1}\left[\mathbf{B}\cdot\nabla\frac{Dq}{Dt} + \rho\Phi\cdot\nabla q\right]\\ &\quad -(\boldsymbol{\xi}\cdot\nabla q')^{-1}\left[\boldsymbol{\xi}\cdot\nabla\frac{Dq'}{Dt} + \rho\Psi\cdot\nabla q'\right].\end{aligned}} \tag{10}$$

Eq. (10) is particularly useful when q and q' are simply related to the coordinates of the general point P. Consider, for example, the case when spherical polar coordinates (r, θ, ϕ) are used and $q = q' = r$. Eq. (10) then reduces to

$$\frac{D}{Dt}\left[\log\left(\frac{B_r}{\xi_r}\right)\right] = \frac{1}{B_r}(\hat{\mathbf{B}}\cdot\hat{\nabla}u_r + \rho\Phi_r) - \frac{1}{\xi_r}[\hat{\boldsymbol{\xi}}\cdot\hat{\nabla}u_r + \rho\Psi_r], \tag{11}$$

where the subscript r denotes the r-component of the corresponding vector, and the operators are

$$\hat{\mathbf{B}}\cdot\hat{\nabla} \equiv \mathbf{B}\cdot\nabla - B_r\partial/\partial r \quad \text{and} \quad \hat{\boldsymbol{\xi}}\cdot\hat{\nabla} \equiv \boldsymbol{\xi}\cdot\nabla - \xi_r\partial/\partial r. \tag{12}$$

Comparable relationships can be found by setting q and q' equal to θ and ϕ.

In geophysical and astrophysical fluid dynamics we are often interested in fluids for which thermoelectric effects are negligible and the electrical conductivity is so high that Alfvén's 'frozen magnetic flux' theorem holds. Then the vector $\Phi = 0$ in eq. (7) [see also (9), (10) and (11)], which when $G^* = r$ and the fluid is incompressible [so that $D\rho/Dt = 0$, see eq. (1)] gives

$$\frac{D}{Dt}B_r = \mathbf{B}\cdot\nabla u_r. \tag{13}$$

This equation has been put to good use by geophysicists in work on the determination of the flow just below the Earth's core–mantle interface from observations of the geomagnetic secular variation [see Roberts & Scott 1965; Backus 1968; see also Bloxham & Jackson 1991 and eq. (16) below].

Also of interest are studies of flows in rapidly rotating systems, where it is convenient to work in a frame of reference that rotates relative to an inertial frame with angular velocity $\boldsymbol{\Omega} = (\Omega\cos\theta, -\Omega\sin\theta, 0)$ about the polar axis. Eqs (1) to (11) hold in the new frame if we re-define $\boldsymbol{\xi}$ as being equal to $\nabla\times\mathbf{u} + 2\boldsymbol{\Omega}$, and add centripetal effects to $\mathbf{g}$ and $\rho\mathbf{r}\times d\boldsymbol{\Omega}/dt$ to $\mathbf{F}$ [see (4)]. Such flows include those where to a first approximation gravity and the total pressure gradient act in the radial direction, viscous forces are negligible, and other forces and torques acting on individual fluid elements are in *magnetostrophic* balance which, when Lorentz forces are also negligible, reduces to *geostrophic* balance. Magnetostrophic balance is characterized here by setting

$$\xi_r = 2\Omega\cos\theta \quad \text{and} \quad \Psi_r = \rho^{-1}[\nabla\times(\rho^{-1}\mathbf{j}\times\mathbf{B})]_r, \tag{14}$$

with $\Psi_r = 0$ in the geostrophic case. When combined with (14), eq. (11) gives

$$\frac{D}{Dt}\log\left(\frac{B_r}{\cos\theta}\right) = \left(\frac{\hat{\mathbf{B}}\cdot\hat{\nabla}}{B_r} - \frac{\hat{\boldsymbol{\xi}}\cdot\hat{\nabla}}{2\Omega\cos\theta}\right)u_r - \frac{[\nabla\times(\rho^{-1}\mathbf{j}\times\mathbf{B})]_r}{2\Omega\cos\theta}. \tag{15}$$

In the case of geostrophic flow over any spherical surface where r is constant and upon which u_r is negligibly small in magnitude in comparison with u_θ and u_ϕ, it follows immediately from (15) that

$$\frac{D}{Dt}(B_r\sec\theta) = 0, \tag{16}$$

implying the conservation of the quantity $B_r\sec\theta$ on moving fluid elements. This result is a familiar one in work on the determination of motions just below the Earth's core–mantle boundary from geomagnetic secular variation data (for references see for example Backus & LeMouël 1986; Bloxham & Jackson 1991), where near-uniqueness can be secured by combining the assumption of geostrophy with Alfvén's frozen magnetic flux theorem [see (13)]. The conditions under which the result can be expected to apply are clearly exposed by its novel derivation here from the powerful general theorems governing the behaviour of potential vorticity and potential magnetic field in magnetohydrodynamic flows, as expressed by eqs (8) and (9).

The full equations of magnetohydrodynamics express not only the laws of mechanics [the basis of (3) and (8)] and of electrodynamics [the basis of (7) and (9)] but also the laws of thermodynamics governing, *inter alia*, the behaviour of specific entropy $\Theta = \Theta(\mathbf{r}, t)$. This quantity satisfies

$$\frac{D\Theta}{Dt} = Q, \tag{17}$$

where $Q = Q(\mathbf{r}, t)$ represents thermal conduction, radiation and other diabatic effects, including ohmic heating. We conclude this short note by observing that eq. (10) with $q = q' = \Theta$ shows that isentropic flows, for which $Q = 0$ by definition, satisfy

$$\frac{D}{Dt}\left(\frac{\mathbf{B}\cdot\nabla\Theta}{\boldsymbol{\xi}\cdot\nabla\Theta}\right) = 0 \tag{18}$$

in regions where Ψ and Φ are also negligibly small. According to (18), within such flows the ratio of the components of $\mathbf{B}$ and $\boldsymbol{\xi}$ in the direction of $\nabla\Theta$, the gradient of specific entropy, is (like Θ itself) conserved on moving fluid elements. A further result of geophysical and astrophysical interest is that eq. (18) reduces to eq. (16) in cases when approximate geostrophic balance obtains and the non-radial components of $\nabla\Theta$ are much weaker than its radial component.

REFERENCES

Backus, G.E., 1968. Kinematics of geomagnetic secular variation in a perfectly-conducting core, *Phil. Trans. R. Soc. Lond.*, A, **263**, 239–266.

Backus, G.E. & LeMouël, J.-L., 1986. The region of the core–mantle boundary where a geostrophic velocity field can be determined from frozen-flux magnetic data, *Geophys. J. R. astr. Soc.*, **85**, 617–628.

Bloxham, J. & Jackson, A., 1991. Fluid flow near the surface of the Earth's outer core, *Rev. Geophys.*, **29**, 97–120.

Ertel, H., 1942. Ein neuer hydrodynamischer Wirbelsatz, *Meteorol. Zeit.*, **59**, 271–281.

Gill, A.E., 1982. *Atmosphere–Ocean Dynamics*, Academic Press, New York, NY.

Hide, R., 1983. The magnetic analogue of Ertel's potential vorticity theorem, *Ann. Geophys.*, **1**, 59–60.

Hide, R., 1986. Frozen vector fields and the inverse problem of inferring motions in the electrically-conducting fluid core of a planet from observations of secular changes in its main magnetic field, *Q. J. R. astr. Soc.*, **27**, 14–20.

Hide, R., 1989. Superhelicity, helicity and potential vorticity, *Geophys. astrophys. Fluid Dyn.*, **48**, 69–79.

Pedlosky, J., 1987. *Geophysical Fluid Dynamics*, 2nd edn, Springer-Verlag, New York, NY.

Roberts, P.H. & Scott, S., 1965. On analysis of the secular variation, I. A hydromagnetic constraint: theory, *J. Geomag. Geoelectr.*, **17**, 137–151.

Topographic Core-Mantle Coupling and Fluctuations in the Earth's Rotation

R. HIDE

Robert Hooke Institute, The Observatory
Clarendon Laboratory, Parks Road
Oxford OX1 3PU, England, U. K.

R. W. CLAYTON

Seismological Laboratory, California Institute of Technology
Pasadena, CA 91125, U. S. A.

B. H. HAGER

Department of Earth, Atmospheric and Planetary Sciences
Massachusetts Institute of Technology
Cambridge, MA 02139, U. S. A.

M. A. SPIETH

Jet Propulsion Laboratory, California Institute of Technology
Pasadena, CA 91109, U. S. A.

C. V. VOORHIES

Geodynamics Branch Code 921, Goddard Space Flight Center
Greenbelt, MD 20771, U. S. A.

Astronomically-determined irregular fluctuations in the Earth's rotation vector on decadal time scales can be used to estimate the fluctuating torque on the lower surface of the Earth's mantle produced by magnetohydrodynamic flow in the underlying liquid metallic core. A method has been proposed for testing the hypothesis that the torque is due primarily to fluctuating dynamic pressure forces acting on irregular topographic features of the core-mantle boundary and also on the equatorial bulge. The method exploits (a) geostrophically-constrained models of fluid motions in the upper reaches of the core based on geomagnetic secular variation data, and (b) patterns of the topography of the CMB based on the mantle flow models constrained by data from seismic tomography, determinations of long wavelength anomalies of the Earth's gravitational field and other geophysical and geodetic data. According to the present study, the magnitude of the axial component of the torque implied by determinations of irregular changes in the length of the day is compatible with models of the Earth's deep interior characterized by the presence of irregular CMB topography of effective "height" no more than about 0.5km (about 6% of the equatorial bulge) and strong horizontal variations in the properties of the D" layer at the base of the mantle. The investigation is now being extended to cover a wider range of epochs and also the case of polar motion on decadal time scales produced by fluctuations in the equatorial components of the torque.

1. INTRODUCTION

Electric currents generated in the Earth's liquid metallic core are responsible for the main geomagnetic field and its secular changes (see *Jacobs*, 1987*ab*; *Melchior*, 1986; *Moffatt*, 1978*a*). The currents are produced by dynamo action involving irregular magnetohydrodynamic flow in the core. Concomitant dynamical stresses acting on the overlying mantle are invoked in the interpretation of the so-called "decadal" fluctuations in the rotation of the "solid Earth" (mantle, crust and cryosphere). Studies of these rotational manifestations of core motions bear directly on investigations of the structure, composition and dynamics of the Earth's deep interior (*Aldridge*, 1990; *Anufriev and Braginsky*, 1977; *Benton*, 1979;

Relating Geophysical Structures and Processes: The Jeffreys Volume
Geophysical Monograph 76, IUGG Volume 16

Edited by K. Aki and R. Dmowska

Eltayeb and Hassan, 1979; *Hide*, 1969; 1970; 1977; 1986; 1989; *Hide and Dickey*, 1991; *Hinderer et al.*, 1990; *Jault and Le Mouël*, 1989; 1990; *Lambeck*, 1980; 1988; *Moffatt*, 1977*b*; *Morrison*, 1979; *Paulus and Stix*, 1989; *Roberts*, 1972; *Rochester*, 1984; *Spieth et al.*, 1986; *Voorhies*, 1991*a*; *Wahr*, 1988].

Consider a set of body-fixed axes x_i, $i = 1, 2, 3$, aligned with the principal axes of the solid Earth and rotating about the center of mass of the whole Earth with angular velocity

$$\hat{\omega}_i = \hat{\omega}_i(t) = (\hat{\omega}_1, \hat{\omega}_2, \hat{\omega}_3) = \Omega\,(\hat{m}_1, \hat{m}_2, 1 + \hat{m}_3) \qquad (1.1)$$

Here t denotes time and Ω the mean speed of rotation of the solid Earth in recent times, 0.7292115 x 10^{-4} radians per second [*Cazenave*, 1986; *Lambeck*, 1980; *Moritz and Mueller*, 1987; *Munk and MacDonald*, 1960; *Rochester*, 1984]. Over time scales short compared with those characteristic of geological processes, the rotation of the Earth departs only slightly from steady rotation about the polar axis of figure, so that $\hat{m}_1$, $\hat{m}_2$, and $\hat{m}_3$ are all very much less than unity and $|\dot{m}_i| << \Omega$, where $\dot{m}_i \equiv d\hat{m}_i / dt$. Periodic variations in $\hat{\omega}_i$ on time scales less than a few years are caused by periodic lunar and solar tidal torques and related changes in the moment of inertia of the solid Earth. Irregular variations on these time scales are produced by atmospheric and oceanic torques due to tangential stresses in surface boundary layers and normal pressure forces acting on surface topography, and they are largely associated with seasonal, intraseasonal and interannual fluctuations in the total angular momentum of the atmosphere. When these rapid variations (including the Chandlerian wobble of the figure axis relative to the rotation axis) have been removed from the observational data, the smoothed time series

$$\omega_i = \Omega\,(m_1, m_2, 1 + m_3) \qquad (1.2)$$

that remains reveals (within the errors involved) the decadal variations, the axial component of which is illustrated in Fig. 1. Geophysicists have long argued that these decadal variations in m_3 are largely manifestations of angular momentum exchange between the core and mantle [*Jacobs*, 1987*ab*; *Jault and Le Mouël*, 1991; *Stoyko*, 1951; *Vestine*, 1952].

Expressions needed in the study of the variable rotation of the non-rigid solid Earth due to core-mantle coupling are readily obtained by standard methods based on Euler's dynamical equations (see e. g., *Munk and MacDonald*, [1960]). If $L_i^*(t)$, $i = 1, 2, 3$, is the fluctuating torque exerted by the core on the mantle then the axial component L_3^* satisfies [*Hide*, 1989]:

$$m_3 = -\Lambda_0\, d(\Delta\Lambda)/dt = L_3^*/\Omega\, C + \alpha_3 \qquad (1.3)$$

where C is the principal moment of inertia of the solid Earth about the polar axis, $\Lambda_0 \equiv 2\pi/\Omega$ is the average length of the day (LOD), $\Lambda(t) \equiv 2\pi/\omega_3$ and $\Delta\Lambda \equiv \Lambda(t) - \Lambda_0$. The quantity α_3, which can be calculated explicitly [*Hide*, 1989], represents secondary effects due to a variety of causes, such as fluctuations in the inertia tensor of the solid Earth (including changes associated with stresses responsible for L_i^* and to comparatively weak torques applied at the Earth's surface by the atmosphere and oceans on the relevant time scales).

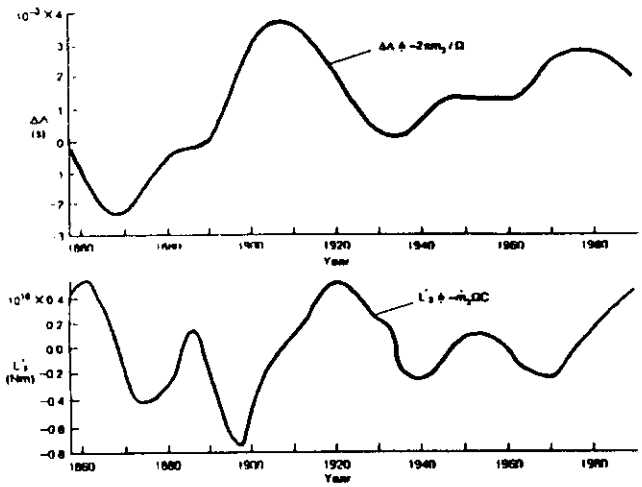

Fig. 1. Decadal variations in the length of day $\Lambda_0 + \Delta\Lambda(t)$ from 1855 to 1985 (upper curve) and corresponding variations in the axial component $L_3^*(t)$ of the torque L^* acting upon the solid Earth (lower diagram); see equation (1.3) and *Dickey et al.* [1989] or *Hide and Dickey* [1991]. More rapid variations (of tidal and atmospheric origin) were removed from the original time series by taking a ten-year running average.

2. The Torque Exerted by the Core on the Mantle

The fluctuating torque $L_i^*(t)$ exerted by the core on the overlying mantle is largely a consequence of (a) tangential stresses at the CMB associated with shearing motions in the thin (less than 1 m) viscous boundary layer just below the CMB, (b) normal dynamical pressure forces acting on the equatorial bulge and other (possibility) smaller and more irregular departures from spherical of the shape of the CMB, (c) Lorentz forces due to the flow of electric currents in the weakly-conducting lower mantle generated by the electromotive forces associated with the geodynamo processes in the core and (d) gravitational forces associated with horizontal density variations in the core and mantle and especially at the CMB [see *Hide*, 1969; *Jacobs*, 1987*ab*; *Jault and Le Mouël*, 1991; *Melchoir*, 1986; *Rochester*, 1984; *Voorhies*, 1991*a*]. Denote by $L_{i(+)}^*$ and $L_{i(-)}^*$ the respective contributions to L_i^* from regions where tractions act in the positive sense and from regions where tractions act in the negative sense and introduce the "canceling factor"

$$\gamma_i^* = \gamma_i^*(t) \equiv L_i^*/[L_{i(+)}^* - L_{i(-)}^*] \qquad (2.1)$$

By definition, each γ_i^* fluctuates about an average of zero and attains magnitudes less than or equal to unity. The accuracy with which L_i^* can be determined obviously depends on the value of $|\gamma_i^*|$, the most favorable situation being when $|\gamma_i^*| \sim 1$.

Rough dynamical arguments show that the pressure coupling associated with CMB topography might predominate over other effects [*Hide*, 1969]. The contribution made by viscous stresses is negligible on all but the most extreme assumptions about the viscosity of the core, but electromagnetic coupling, according to detailed studies by a number of investigators, might be adequate if the (unknown) electrical conductivity of the lower mantle were suffi-

ntly high and the toroidal magnetic field in the core concentrated a boundary layer just below the CMB [*Bullard et al.*, 1950; *ulus and Stix*, 1989; *Roberts*, 1972; *Rochester*, 1984]. So it is of rest to investigate the topographic contribution $L_i(t)$ (say) to $L_i^*(t)$ ng available geophysical data, in order to establish the extent to ich decadal variations in the Earth's rotation might reasonably be ibuted to topographic core-mantle coupling.

f p_s is the dynamical pressure associated with core motions u_s in the free stream just below the viscous boundary layer at the IB (u being the Eulerian flow velocity relative to a reference ne fixed to the solid Earth) and the CMB is the locus of points re the distance from the Earth's center of mass is $r = c + h(\theta, \phi)$, eing the mean radius of the CMB and (θ, ϕ) the co-latitude and gitude of a general point), then [see *Hide*, 1989; *Voorhies*, 1*a*].

$$L_i(t) = -c^2 \int_0^{2\pi} \int_0^{\pi} (r \times p_s \nabla h)_i \sin\theta \, d\theta \, d\phi \qquad (2.2)$$

$h \mid << c$ and $(\nabla_s h) << 1$. Here $\nabla_s \equiv c^{-1}(\hat{\theta}\, \partial/\partial\theta, \hat{\phi}\, cosec\theta\, \partial/\partial\phi)$, nd $\hat{\theta}$ are unit vectors in the directions of increasing θ and ϕ ectively, and r is the vector distance from the Earth's center of s. An important step in the analysis is the recognition of the fact the surface integral of $r \times \nabla_s(h\, p_s)$ over the whole CMB is equal ro, which leads to a more useful expression for $L_i(t)$, namely

$$L_i(t) = c^2 \int_0^{2\pi} \int_0^{\pi} (r \times h \nabla p_s)_i \sin\theta \, d\theta \, d\phi \qquad (2.3)$$

rly everywhere within the core, owing to the presence there of tric currents, Lorentz forces may be comparable in magnitude the Coriolis forces due to the Earth's rotation acting on core . But in the upper reaches of the core, within tens of kilometers e CMB, Lorentz forces should be about 10^{-2} times the Coriolis s or less, unless geodynamo action is confined to a thin bound- ayer just below the CMB or metallic electrical conductivities are ned at the base of the "solid" mantle. In regions where Lorentz s are negligible, geostrophic balance between the horizontal ponents of the pressure gradient and Coriolis forces should in to sufficient accuracy [*Backus and Le Mouël*, 1986; 1987; *ham and Jackson*, 1991; *Gire and Le Mouël*, 1990; *Hide*, 1986;); *Hills*, 1979; *Le Mouël*, 1984; *Voorhies*, 1991*a*]. Whence

$$2\bar{\rho}_s \Omega \cos\theta \, (-w_s, v_s) = -c^{-1}(\partial p_s/\partial\theta, \, cosec\theta \, \partial p_s/\partial\phi) \qquad (2.4)$$

re $\bar{\rho}_s$ is the horizontally averaged value of the density ρ in the r-reaches of the core. Here (v_s, w_s) are the (θ, ϕ) components , which are typically much greater in magnitude than u_r, the r- ponent of u_s. It follows from equations (2.3) and (2.4) that on ime scales of interest here, over which u_s may change signifi- y but h does not, that

$$\dot{L}_i(t) = -2\bar{\rho}_s \Omega c^3 \int_0^{2\pi} \int_0^{\pi} h(\theta,\phi)\, v_s(\theta,\phi,t) \sin^2\theta \cos\theta \, d\theta \, d\phi \qquad (2.5)$$

basic theoretical relationships needed are given by equation with $\alpha_i = 0$ and the working hypothesis that $L_i^* = L_i$, together equations (2.2) to (2.5). The integral on the right-hand side of tion (2.5) involves CMB topography $h(\theta, \phi)$. When dealing with the equatorial components of the torque and the polar motion they produce, the dominant contribution to h is the equatorial ϕ-independent bulge of the CMB, which corresponds to a 9 km difference between the equatorial and polar radii of the core. [e.g., *Herring et al.*, 1991]. But the equatorial bulge makes no contribution to the axial component L_3, which changes the LOD $\Lambda(t)$ (see equation (1.3)), so when dealing with such changes it is necessary to look in detail at features of h that depend on ϕ as well as θ. Over the past-twenty years various attempts have been made to infer $h(\theta, \phi)$ from seismology and from the pattern of long-wavelength gravity anomalies under various assumptions about the structure and rheology of the solid Earth, with more recent studies making use of results from seismic tomography; several hypothetical fields of $h(\theta, \phi)$ are now available, as discussed in Section 4 below.

The other quantity needed in the evaluation of $L_i(t)$ is either the field of pressure $p_s(\theta,\phi,t)$ or the field of horizontal flow $(v_s(\theta, \phi, t), w_s(\theta, \phi, t))$, which is related to p_s through equation (2.4). Geomagnetic secular variation data have been used by various workers to infer (v_s, w_s) by a method that invokes the geostrophic relationship (equation (2.4)) in combination with the equations of electrodynamics appropriate to the case when the mantle can be treated as a perfect electrical insulator of uniform magnetic permeability and the core as a perfect conductor, as we shall now discuss.

3. Velocity and Pressure Fields in the Core

Denote by $B(r, \theta, \phi, t)$ the value of the main geomagnetic field at a general point (r, θ, ϕ) at time t, and by $\dot{B} \equiv \partial B/\partial t$ the so-called geomagnetic secular variation. Determinations of B made at and near the Earth's surface at various epochs can be used to infer u_s, the Eulerian flow velocity just below the CMB [*Backus and Le Mouël*, 1986; 1987; *Benton*, 1981*ab*; *Benton and Celaya*, 1991; *Bloxham*, 1988; 1989; *Bloxham and Jackson*, 1991; *Courtillot and Le Mouël*, 1988; *Gire et al.*, 1986; *Gire and Le Mouël* 1990; *Gubbins*, 1982; *Lloyd and Gubbins*, 1990; *Voorhies*, 1986*ab*; 1987; 1991; 1992; *Voorhies and Backus*, 1985; *Whaler*, 1986; 1990; 1991; *Whaler and Clarke*, 1988]. From flows that are constrained to be tangentially geostrophic (see below), an estimate of the horizontal pressure gradient just below the CMB can be deduced through equations (2.4).

The first of the three reasonable key assumptions that underlie the method used is that the electrical conductivity of the mantle and magnetic permeability gradients there are negligibly small, so that B can be written as the gradient of a potential V satisfying Laplace's equation $\nabla^2 V = 0$. This facilitates the downward extrapolation of the observed field at and near the Earth's surface in order to obtain B and $\dot{B}$ at the CMB.

The second assumption is that the electrical conductivity of the core is so high that when dealing with fluctuations in B on time scales very much less than that of the Ohmic decay of magnetic fields in the core (which is several thousand years for global-scale features), B satisfies Alfven's "frozen flux" theorem [*Backus*, 1968; *Roberts and Scott*, 1965]. This is expressed by the equation

$$\partial B/\partial t = \nabla \times (u \times B), \qquad (3.1)$$

which may be shown to imply that the lines of magnetic force

emerging from the core are advected by the horizontal flow (v_s, w_s) just below the CMB. Accordingly, if $\boldsymbol{B} = (B_r, B_\theta, B_\phi)$, then B_r at the CMB satisfies

$$\frac{\partial B_r}{\partial t} + \frac{v_s}{c}\frac{\partial B_r}{\partial \theta} + \frac{w_s}{c\sin\theta}\frac{\partial B_r}{\partial \phi} = B_r\left[\frac{\partial u}{\partial r}\right]_{r_c} \tag{3.2}$$

Now equation (3.1) alone does not permit the unique determination of $\boldsymbol{u}$, from knowledge of $\boldsymbol{B}$ and $\dot{\boldsymbol{B}}$ at the CMB. Of the various additional considerations that have been employed to secure uniqueness, a physically plausible approach is to invoke the assumption we have already made in Section 2, namely that the flow in the upper reaches of the core is in geostrophic balance with the pressure field there [*Backus and Le Mouël*, 1986; 1987; *Hills*, 1979; *Jault et al.*, 1988; *Le Mouël*, 1984]. The corresponding radial vorticity balance can be expressed by the equation

$$\cos\theta\left[\frac{\partial u}{\partial r}\right]_{r_c} + \frac{v_s}{c}\sin\theta = 0, \tag{3.3}$$

which is readily deduced by eliminating p_s from equations (2.4) and using the mass continuity equation $\nabla \cdot \boldsymbol{u} = 0$ for flow in an effectively incompressible fluid.

Various groups of geomagnetic workers have produced maps of (v_s, w_s) and investigated the errors and uncertainties encountered in practice [*Bloxham and Jackson*, 1991]. In this study, we use ten flow models, two of which have been published elsewhere and eight of which were produced for this study. Four of these models are shown in Figure 2. Figure 2a shows model IIa of *Bloxham* [1989], a geostrophic model determined assuming steady flow and using a smoothly varying model of the magnetic field at the CMB for the interval 1975 - 1980. This model is expressed in terms of spherical harmonics through degree and order 14. The model shown in Figure 2b is model GVC1E6 of *Voorhies* [1991*a*; 1992], derived, assuming steady flow, using $\boldsymbol{B}$ and $\dot{\boldsymbol{B}}$ from the "Definitive Geomagnetic Reference Field" (DGRF) at epochs starting in 1980 and moving back to 1945 in 5-year intervals. This model incorporates spherical harmonic expansions up to degree and order 16 and provides a weighted variance reduction of 98.074%. *Voorhies* [1988] presented a series of models fit to the DGRF for shorter intervals of time. Model G6070.1, shown in Figure 2c, is a relatively smooth fit to the DGRF from 1960 - 1970. Model G8070.1, shown in Figure 2d, uses the same damping parameter to fit the DGRF data from 1980 - 1970. Other models of the G6070.*m*/G8070.*m* series (not shown here) for the same time intervals were used, with increasing index m corresponding to increasing roughness of the model flows.

These flow models, which were used to produce hypothetical flow fields $\boldsymbol{u}_s$ and corresponding pressure fields p_s, are all similar in appearance. *Voorhies'* [1988; 1991*a*; 1992] models CVC1E6 and G8070.1 are barely distinguishable in these plots, reflecting the fact that the models were fit using a similar procedure starting with the 1980 DGRF as the initial condition. The most apparent differences between these two models and the model of Bloxham [1989], appropriate for approximately the same time span as G8070.1, are beneath southern Africa and in the northwestern Pacific. The differences between *Voorhies'* [1988] models G8070.1 and G6070.1, fit to different epochs of the DGRF using identical procedures, are also small, being most easily seen beneath northern Siberia, Alaska, and the southeastern Pacific. Although the calculation of the time-varying core surface flows needed to model variations in p_s, (hence L_s) is straightforward, the similarity among these models demonstrates the care needed to estimate such variations reliably. In particular, there is as much variation between models fit to the same epoch by different workers as there is between models by a single worker of the flow for different epochs.

4. Topography of the Core-Mantle Boundary

The topography $h(\theta, \phi)$ of the CMB (see equation (2.3)) has been investigated using various techniques. The problem is complicated by the suspected presence of the D" layer at the base of the mantle: its variable mechanical and chemical properties make it difficult to separate the effects of D" and CMB topography [*Anderson*, 1989; *Bullen*, 1963; *Doornbos*, 1980; *Gubbins*, 1989; *Gudmundsson et al.*, 1990; *Gudmundsson and Clayton*, 1991, 1992; *Haddon*, 1982; *Hager et al.*, 1985; *Hager and Richards*, 1989; *Jacobs*, 1987*a*; *Jeanloz*, 1990; *Knittle and Jeanloz*, 1991; *Loper*, 1991; *Morelli and Dziewonski*, 1987]. Determinations of the amplitude and phase of the free-core nutation lead to an estimate of 0.5 km of excess ellipticity at the CMB [*Babcock and Wilkins*, 1988; *Gwinn et al.*, 1986; *Herring et al.*, 1985; 1986; 1991; *Kinoshita and Suchay*, 1990; *Reia and Moran*, 1988; *Wahr*, 1988]. While this topographic component does not affect L_s (and hence the LOD, see equation (1.3)), it may indicate the likely magnitude of the relief.

The most direct method (in principle) of estimating CMB topography is to examine variations in travel times of seismic waves that interact with the CMB. Core reflected phases such as PcP and phases that propagate through the core such as PKP and PKIKP are affected similarly by the presence of velocity anomalies in the mantle, which, for rays traversing the same path, affect the travel-times of both phases comparably. However, deformations of the CMB affect the two phases in opposite senses; in regions where $h < 0$, PcP travel times are increased owing to increased path length, but PKP and PKIKP travel times are reduced because a greater portion of the path is through the "faster" mantle material. Potentially, a joint investigation of data from both types of phase could lead to a unique determination of seismic properties of the CMB [*Morelli and Dziewonski*, 1987]. Unfortunately, the quality of the observations of PcP, PKP, and PKIKP travel times given in the International Seismic Centre (ISC) catalogue tends to be poor, both in terms of travel-time measurements and geographic distribution.

Morelli and Dziewonski [1987] boldly carried out inversions for CMB topography using PcP and PKPef phases. The models for these two phases showed a reasonable correlation, which they took as evidence that the inversions were successful, despite the potential pitfalls. They inverted both data sets together to determine a model of CMB topography through degree and order 4, with peak-to-peak amplitudes in excess of 10 km.

Gudmundsson and Clayton [1992] carried out a number of inversions of the ISC data for these phases, as well as the additional phases PKPab, PKPbc; and PKPde. They also investigated the

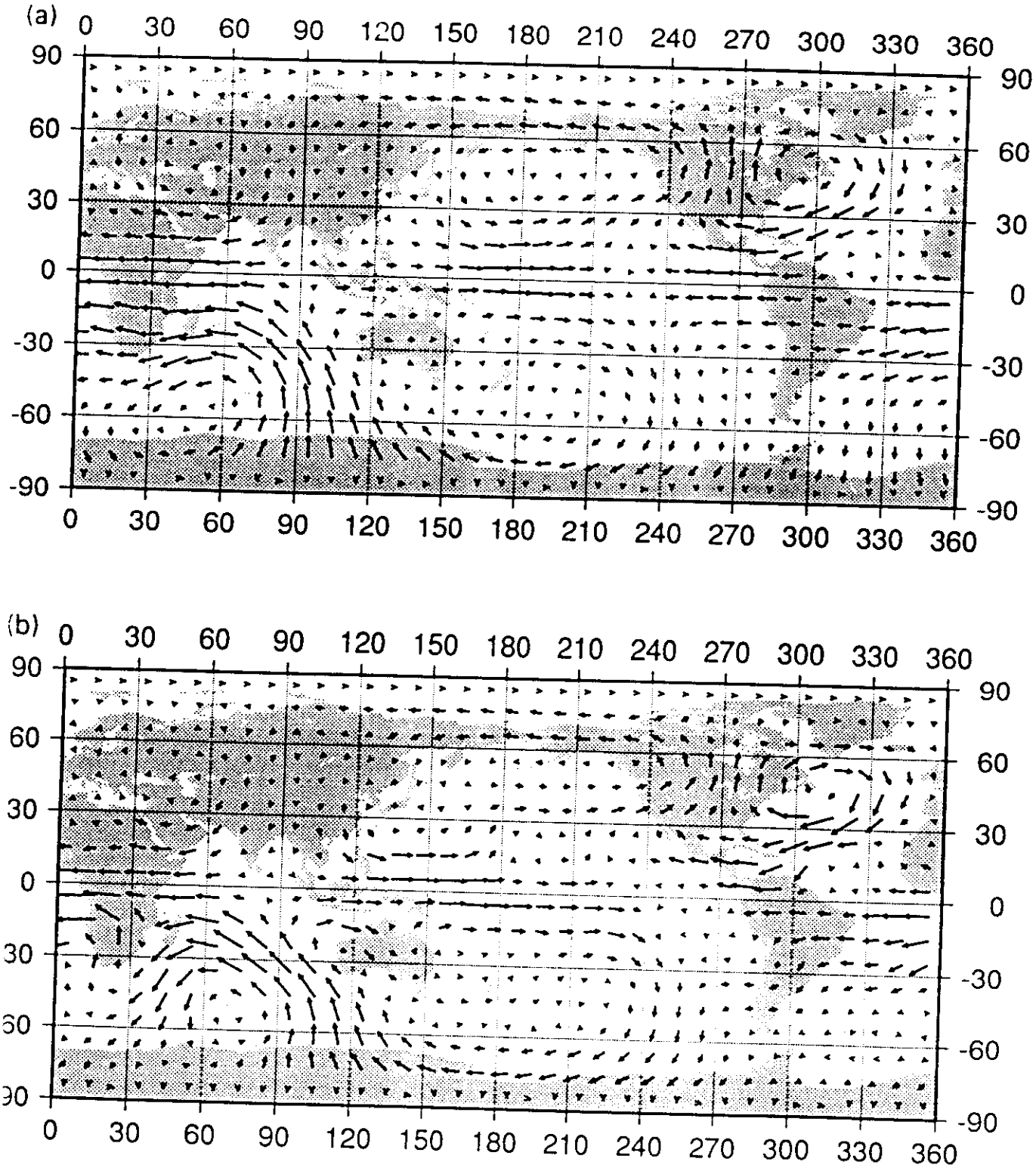

Fig. 2. Geostrophic flow fields estimated by *Bloxham* [1989] (2a), *Voorhies* [1991a] (2b) and *Voorhies* [1988] (2c and 2d). An arrow with a magnitude equal to the distance between grid points (10°) corresponds to a velocity of 20 km/year.

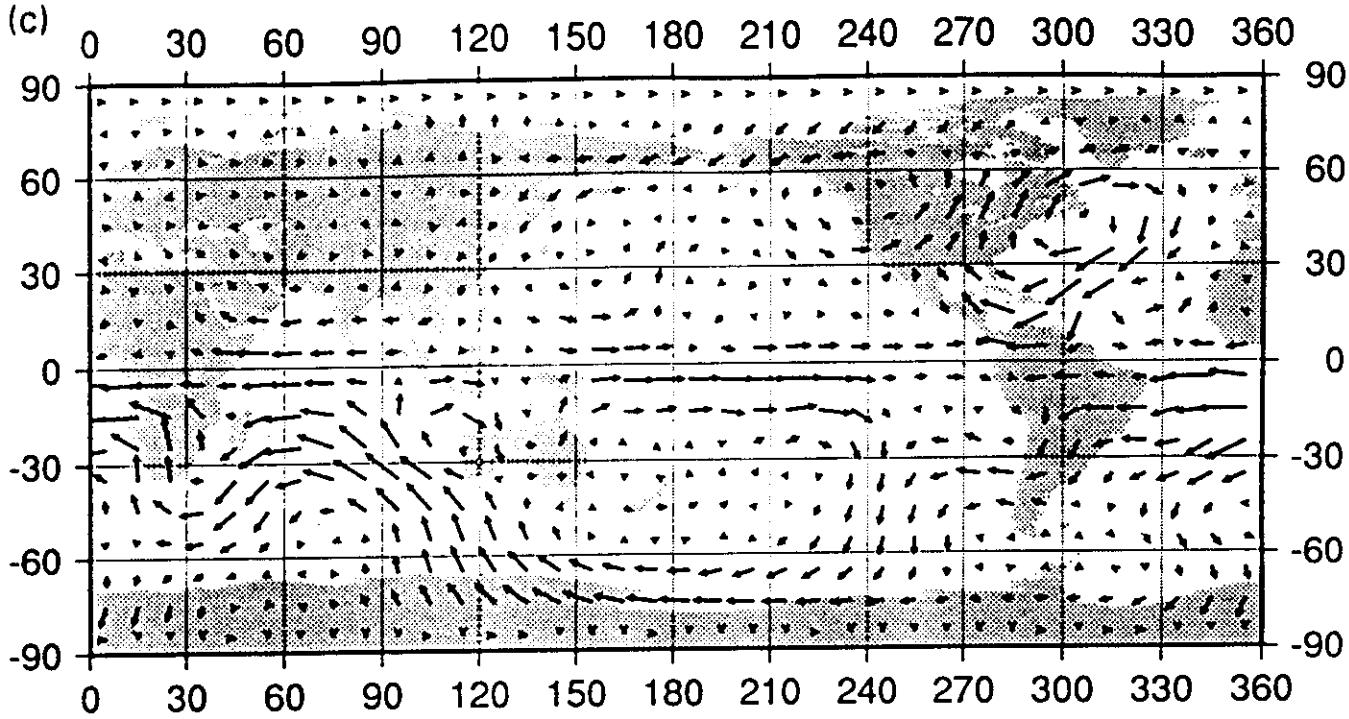

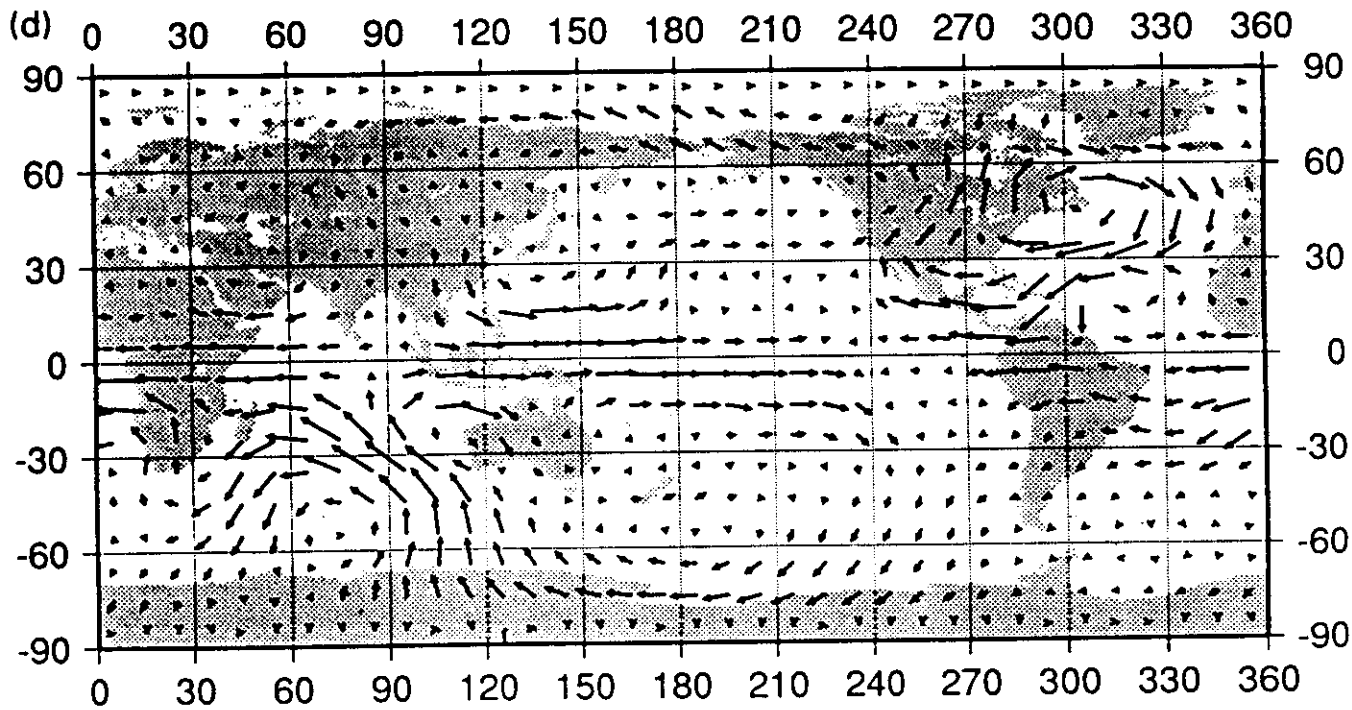

Fig. 2. (continued)

effects of including a horizontally-variable D" layer in their models. The CMB topography obtained for the different phases differs substantially. In addition, they found that by varying the "tradeoff" between the effects due to D" variations and CMB topography respectively, the amplitude of the ϕ-dependent part of h ranged from 1 km to 6 km. Their models were parameterized in terms of spherical harmonic expansions through degree and order 10, although they employed a "stochastic inverse," choosing the trade-off parameter to retain only 25 parameters (as measured by the trace of the resolution matrix) in their solution. The topography for one particular choice that includes the effects of variable velocity in the D" layer in the model parameterization (Figure 9 in *Gudmundsson and Clayton* [1992]), expanded through degree and order 4 for comparison with the model of *Morelli and Dziewonski* [1987], is illustrated in the top panel of Figure 3.

Another approach to modeling CMB topography is to use density variations inferred from lateral variations in seismic-wave velocities in the mantle or other geophysical inference to drive models of mantle flow. These models, which predict dynamically-maintained topography at the Earth's surface and at the CMB, are constrained by long-wavelength features of the geoid. This approach assumes that the seismic-velocity variations are caused by density variations (via temperature), to which they are linearly related. The mantle viscosity must also be specified, along with major chemical boundaries in the mantle, including the problematic D" layer. In a spherical harmonic expansion of $h(\theta, \phi)$ up to degree and order 9, models with no D" layer give amplitudes of the ϕ-dependent part of h up to 2.5 km (e.g., model WO of *Hager and Clayton* [1989]), nearly 25% of the equatorial bulge. On the other hand, models with a low viscosity and/or chemically distinct D" layer give much lower amplitudes. For example, the CMB topography for model WL of *Hager and Richards* [1989], a model which has a D" layer which has a low viscosity, but is not compositionally distinct from the overlying mantle, is shown in the bottom panel of Figure 3. It has an excess ellipticity compatible with the inferences from nutation studies. The model is dominated by long-wavelength variations, with a peak-to-peak amplitude of the topography of < 2 km.

Clearly, models of CMB topography differ more than do models of core flow. Thus, the comparison of the implied LOD variations with observed values on the basis of the method outlined in Section 1 has the potential to distinguish among classes of models such as those presented here.

5. PREDICTED TORQUES AND LENGTH-OF-DAY VARIATIONS

Estimates of the topographic torque exerted by the core on the mantle were produced from models of the flow fields in the outer core and the CMB topography via numerical integration of equation (2.5), and compared with values implied by the LOD determinations presented in Figure 1. Predicted LOD values obtained on the basis of equations (1.3) and (2.5) (with $\alpha_3 = 0$ and $L_3^* = L_3$) for 50 combinations of 10 different models of the flow field, (v_r, w_r), and 5 models of CMB topography, h, are given in Table 1. Four of the core flow models are those shown in Figure 2; the others represent additional models presented by *Voorhies* [1988] for the DGRF in the epochs 1980-1970 and 1960-1970. The models differ in the damping parameter used to control the roughness of the flow. For example, G6070.1 is the smoothest model for 1960 - 1970, while G6070.4 is the roughest. In addition to the two CMB topography models shown in Figure 3, we also used the model of *Morelli and Dziewonski* [1987], model WO of *Hager and Clayton* [1989], and the model of *Gudmundsson and Clayton* [1992] shown in Figure 3, but expanded through degree and order 10.

Core flow Model IIa of *Bloxham* [1989] assumes steady flow during the epoch 1975-1980, during which time the average value of L_3^* was -0.1×10^{18} Nm; the corresponding change in LOD is about −0.5 msec/decade. Models G8070.*m* of *Voorhies* [1988] assume steady flow starting in 1980, going back to 1970. During this interval, $\Delta\Lambda$ first increased, then decreased, with negligible net torque averaged over the decade. Models G6070.*m* of *Voorhies* [1988] assume steady flow between 1960 and 1970, corresponding to L_3^* of $\sim -0.2 \times 10^{18}$ Nm and a change in LOD of about +1 msec/decade. Model GVC1E6 of *Voorhies* [1991*a*] assumes steady flow starting in 1980, going back to 1945, with the fit to the data being better at later than at earlier times in this interval. An average torque of $\sim -0.1 \times 10^{18}$ seems appropriate for the interval over which this model best fits the geomagnetic data; this would correspond to a change in LOD of 0.5 msec/decade.

By chance, all combinations of flow models and topography models presented here give positive predictions for changes in LOD. (Other models we have used, not shown, give negative predictions.) The combinations using the seismological models of h, with irregular ϕ-dependent amplitudes of several kilometers, "predict" LOD changes much larger, some by over a factor of 100, than the observed changes. Much closer agreements with the magnitude of observed LOD changes were found in the case of combinations for model WL, which has irregular CMB topography < 1 km in amplitude, although the predicted changes are still a factor of 4 - 8 to large. For the topography models used here, *Bloxham's* [1989] flow model predicts the wrong sign of LOD variation during 1975 - 1980. *Voorhies'* [1988] models predict the correct sign for the decade represented by models G6070.*m*. The models for the epoch represented by models G8070.*m* predict too large changes in LOD; the observed value for this decade is about zero. But, as discussed next, we are more confident of the order of magnitude of the torques than their sign, so the differences for these different flow models may not be diagnostic.

There is of course concern about the effect of inadequacies in the flow and topography fields on "predicted" values of the LOD variations. The problem is illustrated in Figure 4, which presents maps of the spatial distribution of contributions to the L_3 torque, $2\bar{\rho}_s\Omega_0 c \sin\theta \cos\theta$, for the two flow models shown in Figures 3c and 3d, interacting with the topography shown in the bottom panel of Figure 2. As expected, a high degree of canceling is exhibited (see equation (2.1)). The net axial torque (and hence the LOD estimate) is the sum of these individual parts, which means it ends up being the small difference between two large numbers. For example, the total torque for the model in the top panel of Figure 4 is -1×10^{18} N-m (comparable to the that inferred for ~ 1900, as can be seen from Figure 1). A constant torque per unit area of -5×10^3 N/m

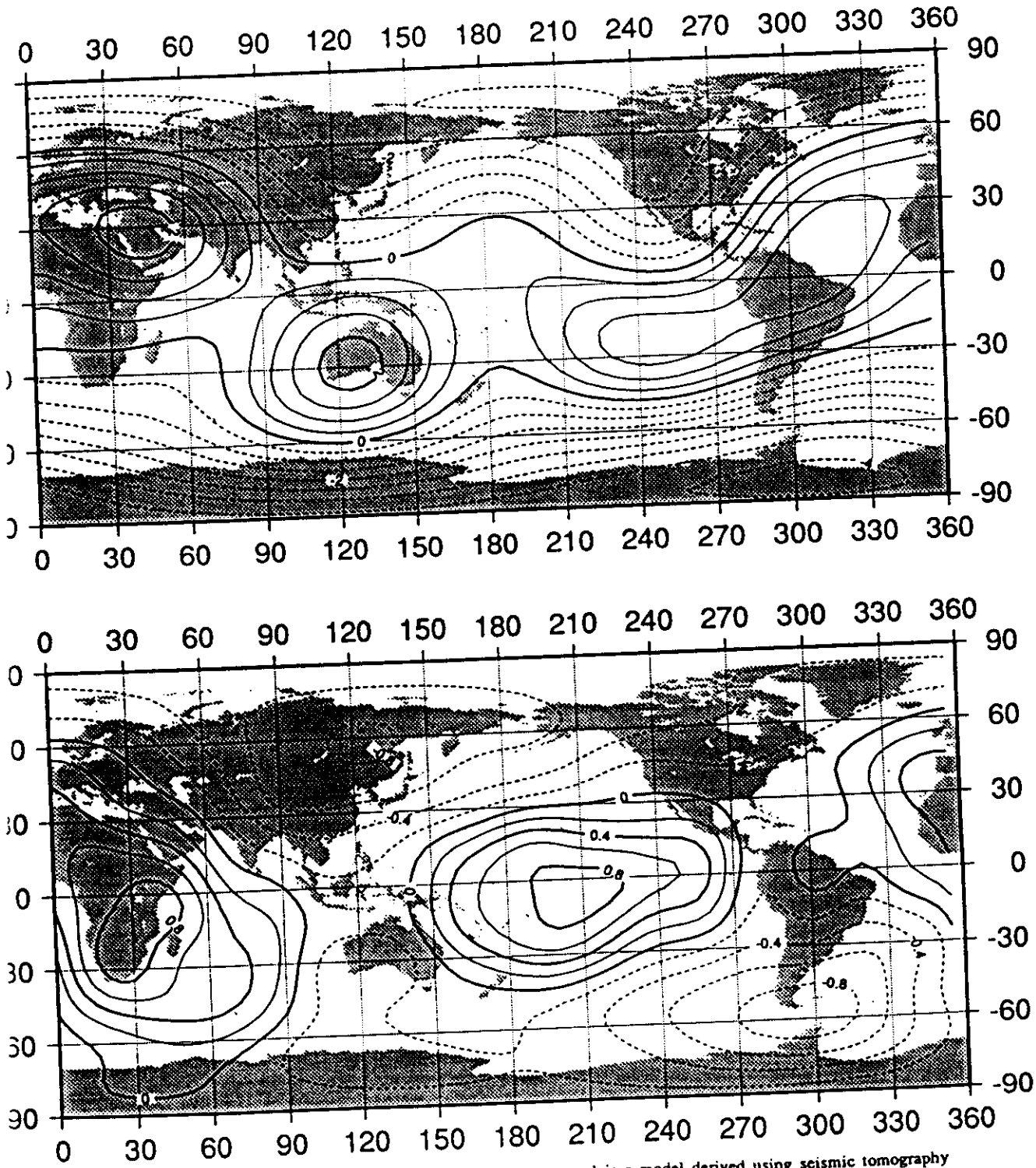

Fig. 3. Models of the topography of the CMB. The upper panel is a model derived using seismic tomography incorporating the effects of velocity variations in the D" layer above the CMB [*Gudmundsson and Clayton*, 1992]. The lower panel shows the dynamic topography inferred for model WL of *Hager and Richards* [1989]. Solid contours correspond to regions where the topography is upwarped towards the Earth's surface, while dashed contours represent regions where mantle is depressed into the core. The contour interval in the upper panel is 500 m; in the lower panel, 200 m.

TABLE 1. Predicted values of LOD variations for combinations of CMB topography models and geostrophic flow models discussed in the text.

$\Delta\Lambda$ (msec/decade)

CMB Topography \ Flow	Bloxham IIa [1989]	Voorhies GVC1E6 [1992]	Voorhies G6070.1 [1988]	Voorhies G8070.1 [1988]	Voorhies G6070.2 [1988]	Voorhies G8070.2 [1988]	Voorhies G6070.3 [1988]	Voorhies G8070.3 [1988]	Voorhies G6070.4 [1988]	Voorhies G8070.4 [1988]
Morelli & Dziewonski [1987]	143	115	110	133	115	131	97	120	58	112
Gudmundsson Clayton [1992] degree 1-4	85	71	66	75	59	81	47	80	33	78
Gudmundsson Clayton [1992] degree 1-10	88	70	64	73	57	77	46	75	34	78
Hager & Clayton WO [1989]	4.2	7.6	3.1	3.4	11	4.7	24	5.7	31	6.8
Hager & Richards WL [1989]	2.2	3.5	4.8	6.7	5.7	5.5	8.1	4.2	8.4	2.1

acting over the area of the CMB would result in a torque of this magnitude. The maximum amplitudes of the contributions to the equivalent torque integral plotted in Figure 4 are more than a factor of 100 greater than this average value.

The contributions to the torque integral for the two flow models at different epochs are similar, but there are discernable differences. For example, beneath southern Africa, the largest negative torque integral contribution for 1960 - 1970 has decreased in magnitude by 1980 - 1970, but the magnitude of the negative contribution south of India has increased. During the same interval, the contribution beneath Alaska changes sign, while the maximum over Manchuria splits into separated highs. Although these two flow models, and the patterns of torque contributions computed from them, are similar, the integrated effect of their small differences leads to calculated changes of LOD that differ by almost 2 msec/decade, comparable to the total predictions at the two epochs. Interestingly, the difference in LOD change predicted for these two models is comparable to the difference in LOD change observed for these two decades. But different flow models for the same epochs produce changes in predicted LOD comparable in magnitude, but opposite in sign. For this reason, we cannot assign very high significance to detailed LOD predictions. Indeed, it would probably be possible to construct an acceptable core flow model that exerts no net torque on the mantle [*Bloxham*, 1991; *Voorhies*, 1991*b*]. However, the order of magnitude supports the hypothesis that decadal fluctuations in LOD are largely effected by the topographic torque, even though the time-averaged torque is, of course, equal to zero. [*Hide*, 1969].

The effect of spherical harmonic degree truncation in the topography fields can be investigated by comparing the contributions in the torque integral and changes in length of day for two representations of the CMB topography model of *Gudmundsson and Clayton* [1992]. The first representation, shown in Figure 2, is expanded through degree and order 4. The second carries the expansion through degree and order 10. (Because only 25 parameters were used in their inversion, the amplitudes of the coefficients fall off fairly rapidly with harmonic degree.) As can be seen from Table 1, increasing the maximum degree and order from 4 to 10 has a very small effect on calculated LOD variations. Inspection of maps of the contributions to the torque integral calculated using *Voorhies'* flow model and these two topographic models (Figure 5) indicates that most of the features are well-represented by the smoother CMB models. The relative amplitudes of the contributions from different geographic regions vary, but the total torque remains almost constant. We take the stability of these estimates to indicate that contributions from higher harmonics (and their associated errors) are probably insignificant, owing to a high degree of cancellation at these scales (see equation (2.4)).

6. Discussion and Conclusions

The determination of the efficacy of topographic coupling is clearly fraught with practical difficulties. But the results of this paper demonstrate the usefulness of the method employed by providing independent evidence in favor of the hypothesis that topographic coupling can account for the observed decadal changes in LOD if $\bar{h}$, the rms. value of the ϕ-dependent portion of h, the topographic relief, is typically about 1 km in amplitude or possibly slightly less.

We emphasize that this value of $\bar{h}$ depends on the suppositions underlying the method. In particular, the velocity fields as determined from geomagnetic secular variation data (see Section 3) refer

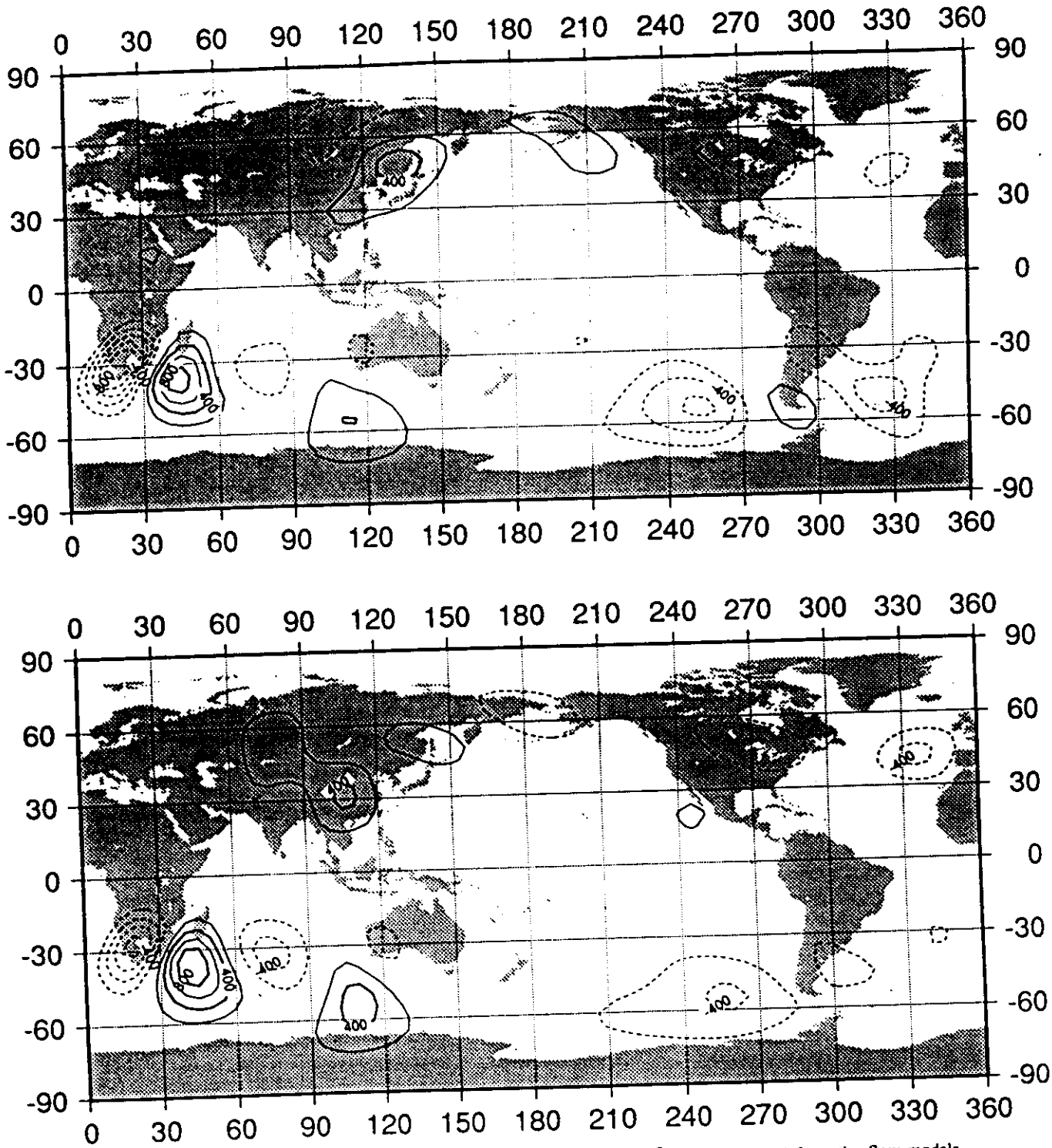

Fig. 4. The contributions to the L_3 component of torque, in units of 10^3 N/m, calculated from the flow models shown in Figure 2c and d interacting with the topography shown in the lower panel of Figure 3. Solid contours indicate positive contributions and dashed contours indicate negative contributions; the zero contour is not shown. The contour interval in both panels is 200 kN/m. The net change in the LOD is related to the integral of these contributions over the area of the CMB. A constant value of 200 kN/m, integrated over the area of the CMB, would give a torque of 0.3×10^{18} Nm and a variation in LOD of −1.4 msec/decade.

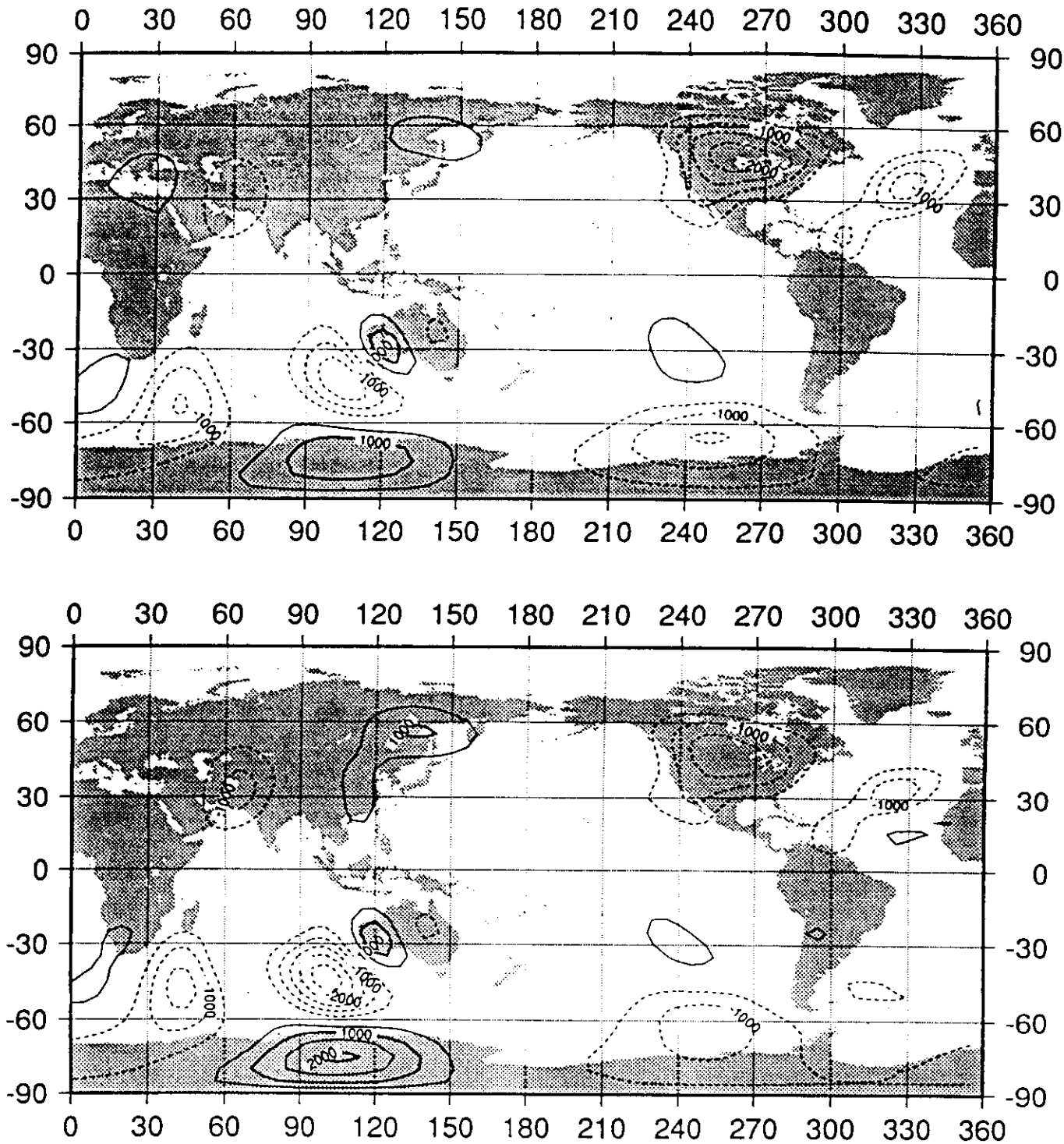

Fig. 5. The contributions to the L_3 component of torque, in units of 10^3 N/m, calculated from the flow model shown in Figure 2b interacting with the topography from the model of *Gudmundsson and Clayton* [1992] for two different degrees of truncation. The upper panel is for topography expanded through degree and order 4 (shown in the upper panel of Figure 3). The lower panel is for the model expanded through degree and order 10. Solid contours indicate positive contributions. The contour interval in both panels is 500 kN/m. The net change in the LOD is related to the integral of these contributions over the area of the CMB.

to the free stream at the top of the electrically-conducting liquid core. In calculating from these velocity fields the pressure fields acting upon topographic relief of the CMB, it has been assumed that the electrically-conducting core is in contact with the mantle over the whole of the CMB. This is probably a reasonable supposition, but it is interesting to speculate on the possibility that between the highly conducting core and the weakly conducting lower mantle there might exist a thin continuous layer or "pools" of weakly-conducting or insulating liquid which have escaped detection by seismic methods. The actual pressure field at the CMB might then differ from that given by equation (2.4) [*Hager and Richards*, 1989]. It would have to be determined from considerations of the dynamics of the hypothetical intermediate layer or pools, and the relationship between the two pressure fields might not be simple. If typical pressure gradients at the CMB were weaker than those at the top of the electrically-conducting core, then the value of $\bar{h}$ needed to produce the necessary torques on the mantle would have to be larger. However, the idea of an intermediate layer is not supported by a parallel study to the present one [R. Hide. and A. Jackson, in preparation], in which decadal polar motion induced by topographic core-mantle coupling is investigated.

As we have seen in Section 4, inferences concerning $\bar{h}$ can be drawn from direct seismic measurements and also from attempts to interpret the horizontal variations of the Earth's gravitational field in terms of density variations in the mantle maintained by slow convection there. In both cases, the implied value of $\bar{h}$ depends critically on the assumptions made concerning the properties of the lower mantle. Seismic measurements give values greater than 1 km unless there are substantial (~ 1%) lateral variations in seismic velocities in the zone just above the CMB. The most likely candidate is the D" layer of 100 - 300 km thickness. Consistent with this "scenario" are the mantle convection studies, which give $\bar{h}$ of about 1 km where a chemically-distinct or low viscosity layer in the D"-region is included, but a significantly greater value otherwise.

So far as future work on topographic core-mantle coupling is concerned, as better geophysical and geodetic data and models become available it will be necessary to repeat, refine, and extend the calculations and comparisons made in the present paper along the obvious lines already indicated. The results will have important implications not only for the nature of the stresses responsible for torques at the CMB and the structure of the lower mantle and CMB topography, but also, indirectly, for the magnetohydrodynamics of the core and the nature of the geodynamo. Dynamo "models" can be classified in terms of two characteristic features, namely (a) the average strength of the toroidal magnetic field in the core (which for "strong field" dynamos is typically much greater than that of the poloidal field, whereas for "weak field" dynamos the two field types are comparable in strength), and (b) whether or not dynamo action extends throughout most of the volume of the core or is confined to the upper reaches. Should more refined calculations either weaken the case for significant topographic coupling, or consistently indicate an excessive topographic couple, this would constitute evidence in favor of electromagnetic torques at the CMB produced by dynamo action concentrated just below the CMB.

Acknowledgements. We thank Don Anderson, Jean Dickey, Olafur Gudmundsson, David Stevenson, and Charles Yoder for helpful comments on various aspects of this work. We also thank Dr. Dickey and other members of the Space Geodesy Science and Applications Group of the Jet Propulsion Laboratory for facilitating this collaborative study. Jeremy Bloxham kindly provided coefficients for his core flow model. Partial support was provided by NASA grants NAG5-819 and NAG5-315 to RWC and BHH.

REFERENCES

Aldridge, K.D. (ed), Core-mantle interactions, *Surveys in Geophys., 11*, 329-353, 1990.

Anderson, D.L. *Theory of the Earth*, Oxford, Blackwell Scientific Publications, 1989.

Anufriev, A.P., and S.L. Braginsky, Influences of irregularities in the boundary of the Earth's core on fluid velocity and magnetic field, *Geomagn. Aeron., 17*, 492-496, 1977.

Babcock, A., and G. Wilkins, (Eds.) *The Earth's Rotation and Reference Frames*, Reidel, Dordrecht, 1988.

Backus, G.E., Kinematics of secular variation in a perfectly conducting core, *Philos. Trans. Roy. Soc., A263*, 239-263, 1968.

Backus, G.E., and J-L Le Mouël, The region of the core-mantle boundary where the geostrophic velocity field can be determined from frozen flux data, *Geophys. J. Roy. Astron. Soc., 85*, 617-628, 1986.

Backus, G.E., and J-L Le Mouël, The region of the core-mantle boundary where the geostrophic velocity field can be determined from frozen flux data, addendum, *Geophys. J. Roy. Astron. Soc., 88*, 321-322, 1987.

Benton, E.R., Magnetic probing of planetary interiors, *Phys. Earth Planet. Int., 20*, 111-118, 1979.

Benton, E.R., A simple method for determining the vertical growth rate of vertical motion at the top of Earth's outer core, *Phys. Earth Planet. Int., 24*, 242-244, 1981a.

Benton, E.R., Inviscid, frozen-flux velocity components at the top of Earth's core from magnetic observations at earth's surface: Part I. A new methodology, *Geophys. Astophys. Fluid Dyn., 18*, 154-174, 1981b.

Benton E. R., and M. A. Celaya, The simplest unsteady surface flow of a frozen flux core that exactly fits a geomagnetic field model, *Geophys. Res. Lett., 18*, 577-580, 1991.

Bloxham, J., The dynamical regime of fluid flow at the core surface, *Geophys. Res. Lett., 15*, 585-588, 1988.

Bloxham, J., Length-of-day variations, topographic core-mantle coupling, and the steady and time-dependent components of core flow (abstract), *Eos, Trans. AGU, 72*, 451, 1991.

Bloxham, J., Simple models of fluid flow at the core surface derived from geomagnetic field models, *Geophys. J. Int., 99*, 173-182, 1989.

Bloxham, J., and A. Jackson, Fluid flow near the surface of the Earth's core, *Rev. Geophys., 29*, 97-120, 1991.

Bullard, E.C., C. Freedman, H. Gellman, and J. Nixon, The westward drift of the Earth's magnetic field, *Phil. Trans. Roy. Soc., A243*, 67-92, 1950.

Bullen, K.E., *Introduction to the Theory of Seismology*, Cambridge University Press, Cambridge, 1963.

Cazenave, A., editor, *Earth Rotation; Solved and Unsolved Problems, NATO Advanced Institute Series C; Mathematical and Physical Sciences*, Boston, D. Reidel, 1986.

Courtillot, V., and J-L Le Mouël, Time variations of the Earth's magnetic field: From daily to secular, *Ann. Rev. Earth Planet. Sci., 16*, 389-476, 1988.

Dickey, J.O., T.M. Eubanks, and R. Hide, Interannual and decade flunctuations in the Earth's rotation, in *Variations in the Earth's Rotation, Geophysical Monograph Series*, edited by D.C. McCarthy, pp. 157-162, AGU, Washington, DC, 1990.

Doornbos, D.J., The effect of a rough core-mantle boundary found only on PKKP, *Phys. Earth Planet. Int., 21*, 351-358, 1980.

Eltayeb, I.A., and M.H.A. Hassan, On the effects of a bumpy core-mantle interface, *Phys. Earth Planet. Int., 19*, 239-254, 1979.

Gire, C., and J-L Le Mouel, Tangentially-geostrophic flow at the core-mantle boundary compatible with observed geomagnetic secular variation: The large-scale component of the flow, *Phys. Earth Planet. Int., 59*, 259-287, 1990.

Gire, C., J-L. Le Mouel, and T. Madden, Motions at the core surface derived from SV data, *Geophys. J. R. Astr. Soc., 84*, 1-29, 1986.

Gubbins, D., Finding core motions from magnetic observations, *Phil. Trans. Roy. Soc., A306*, 247-254, 1982.

Gudmundsson, O., and R.W. Clayton, A 2-D synthetic study of global traveltime tomography, *Geophys. J. Int., 106*, 53-68, 1991.

Gudmundsson, O., and R.W. Clayton, Some problems in mapping core-mantle boundary structure, *J. Geophys. Res.*, in press, 1992.

Gudmundsson, O., J.H. Davies, and R.W. Clayton, Stochastic analysis of global travel time data: Mantle heterogeneity and random errors in the ISC data, *Geophys. J. Int., 102*, 25-43, 1990.

Gwinn, C.R., T.A. Herring, and I.I. Shapiro, Geodesy by radio interferometry: Studies of the forced nutations of the Earth, 2. Interpretation, *J. Geophys. Res., 91*, 4755-4765, 1986.

Haddon, R. A. W., Evidence of inhomogeneities near the core-mantle boundary, *Phil. Trans. Roy. Soc., A306*, 61-70, 1982.

Hager, B. H., and R. W. Clayton, Constraints on the structure of mantle convection using seismic observations, flow models, and the geoid, in *Mantle Convection*, edited by W. R. Peltier, pp. 657-763, Gordon and Breach, New York, 1989.

Hager, B.H., R. W. Clayton, M. A. Richards, R. P. Comer, and A. M. Dziewonski, Lower mantle heterogeneity, dynamic topography and the geoid, *Nature, 313*, 541-545, 1985.

Hager, B.H., and M.A. Richards, Long wavelength variations in the Earth's geoid: Physical models and dynamical implications, *Philos. Trans. Roy. Soc., A328*, 309-327, 1989.

Herring, T.A., B. A. Buffett, P. M. Mathews, and I. I. Shapiro, Forced motions of the Earth: Influence of inner core dynamics: 3. Very long interferometry data analysis, *J. Geophys. Res., 96*, 8259-8273, 1991.

Herring, T.A., C.R. Gwinn, and I.I. Shapiro, Geodesy by radio interferometry: Corrections to the IAU 1980 nutation series, *Proc. Inter. Conf. Earth Rotation and Terrestrial Reference Frame, 1*, 307-328, Ohio State University, Columbus, 1985.

Herring, T.A., C.R. Gwinn, and I.I. Shapiro, Geodesy by radio interferometry: Studies of the forced nutations of the Earth 1. Data analysis, *J. Geophys. Res., 91*, 4745-4754, 1986.

Hide, R., Interaction between the Earth's liquid core and solid mantle, *Nature, 222*, 1055-1056, 1969.

Hide, R., On the Earth's core-mantle interface, *Quart. J. Roy. Meteorol. Soc., 96*, 579-590, 1970.

Hide, R., Towards a theory of irregular variations in the length of the day and core-mantle coupling, *Phil. Trans. Roy. Soc., A284*, 547-554, 1977.

Hide, R., Presidential address: The Earth's differential rotation, *Quart. J. Roy. Astron. Soc., 278*, 3-14, 1986.

Hide, R., Fluctuations in the Earth's rotation and the topography of the core-mantle interface, *Phil. Trans. Roy. Soc., A328*, 351-363, 1989.

Hide, R., and J.O. Dickey, Earth's variable rotation, *Science, 253*, 629-637, 1991.

Hide, R., and K.I. Horai, On the topography of the core-mantle interface, *Phys. Earth Planet. Int., 1*, 305-308, 1968.

Hills, R.G., Convection in the Earth's mantle due to viscous stress at the core-mantle interface and due to large scale buoyancy. Ph.D. thesis, New Mexico State University, Las Cruces, 1979.

Hinderer, J., D. Jault, and J-L Le Mouël, Core-mantle topographic torque: A spherical harmonic approach and implications for the excitation of the Earth's rotation by core motions, *Phys. Earth Planet. Int., 59*, 329-341, 1990.

Jacobs, J.A., (Ed.) *The Earth's Core*, 2nd ed., Academic Press Ltd., New York, 1987a.

Jacobs, J.A. *Geomagnetism*. 2 vols. Academic Press Ltd., New York, 1987b.

Jault, D., and J-L Le Mouël, The topographic torque associated with tangentially geostrophic motion at the core surface and inferences on the flow inside the core, *Geophys. Astrophys. Fluid Dyn., 48*, 273-296, 1989.

Jault, D., and J-L Le Mouël, Core-mantle boundary shape: Constraints inferred form the pressure torque acting between the core and mantle, *Geophys. J. Int., 101*, 233-241, 1990.

Jault, D., and J-L Le Mouël, Exchange of angular momentum between the core and mantle, *J. Geomag. Geoelect., 43*, 111-129, 1991.

Jault, D., C. Gire, and J-L Le Mouël, Westward drift, core motions and exchange of angular momentum between core and mantle, *Nature, 333*, 353-356, 1988.

Jeanloz, R., The nature of the Earth's core, *Ann. Rev. Earth Planet. Sci., 18*, 257-386, 1990.

Kinoshita, H., and J. Souchay, The theory of the nutation for the rigid Earth model of second order, *Celestial Mechanics, 48*, 187-265, 1990.

Knittle, E., and R. Jeanloz, Earth's core-mantle boundary: Results of experiments at high pressures and temperatures, *Science, 251*, 1438-1443, 1991.

Lambeck, K., *The Earth's Variable Rotation*, Cambridge University Press, London and New York, 1980.

Lambeck, K., *Geophysical Geodesy: The Slow Deformation of the Earth*, Oxford, Clarendon Press, 1988.

Le Mouël, J-L, Outer-core geostrophic flow and secular variation of the main geomagnetic field, *Nature, 311*, 734-735, 1984.

Lloyd, D., and D. Gubbins, Toroidal fluid motion at the top of the Earth's core, *Geophys. J. Int., 100*, 455-467, 1990.

Loper, D.E., The nature and consequences of thermal interactions twixt core and mantle, *J. Geomag. Geoelect., 43*, 79-91, 1991.

Melchior, P. *The Physics of the Earth's Core*. Pergamon Press, Oxford , 1986.

Moffatt, H.K., *Magnetic Field Generation by Fluid Motion*, Cambridge University Press, Cambridge, 1978a.

Moffatt, H.K., Topographic coupling at the core-mantle interface, *Geophys. Astrophys. Fluid Dyn., 9*, 279-288, 1978b.

Morelli, A., and A.M. Dziewonski, Topography of the core-mantle boundary and lateral homogeneity of the liquid core, *Nature, 325*, 678-683, 1987.

Moritz, H., and I.I. Mueller (Eds.), *Earth Rotation: Theory and Observation*, The Ungar Publishing Co., New York, 1987.

Morrison, L.V., Redetermination of the decade fluctuations in the rotation of the Earth in the period 1861-1978, *Geophys. J. Roy. Astron. Soc., 38*, 349-360, 1979.

Munk, W.H., and G.J.F. MacDonald, *The Rotation of the Earth*, Cambridge University Press, Cambridge, 1960.

Paulus, M., and M. Stix, Electromagnetic core-mantle coupling: The Fourier method for solving the induction equation, *Geophys. Astrophys. Fluid Dyn., 47*, 237-249, 1989.

Reid, M.J., and J.M. Moran, (Eds.) *The Impact of VLBI on Astrophysics and Geophysics*, Kluwer Academic Publishers, Dordrecht, 1988.

Roberts, P. H., Electromagnetic core-mantle coupling, *J. Geomag. Geoelect., 24*, 231-259, 1972.

Roberts, P.H., and S. Scott, On analysis of secular variation: 1 A hydromagnetic constraint, *J. Geomag. Geoelect., 17*, 137-151, 1965.

Rochester, M.G., Causes of fluctuations in the Earth's rotation, *Phil. Trans. Roy. Soc., A313*, 95-105, 1984.

Spieth, M.A. R. Hide, R. W. Clayton, B. H. Hager, and C. V. Voorhies, Topographic coupling of the core and mantle and changes in the length of the day (abstract), *Eos Trans. AGU, 67*, 908, 1986.

Stoyko, N., Sur les variations de champ magnetique et la rotation de la Terre, *C.R. Hebd. Seanc. Acad. Sci. Paris, 233*, 80-82, 1951.

Vestine, E.H., On variations of the geomagnetic field, fluid motions,

and the rate of the Earth's rotation, *Proc. Nat. Acad. Sci., 38*, 1030-1038, 1952.

Voorhies, C. V., Steady flows at the top of Earth's core derived from geomagnetic field models, *J. Geophys. Res., 91*, 12, 444-12, 466, 1986a.

Voorhies, C.V., Steady surficial core motions: an alternate method. *Geophys. Res. Lett., 13*, 1537-1540, 1986b.

Voorhies, C.V., The time-varying geomagnetic field, *Rev. Geophys., 25*, 929-938, 1987.

Voorhies, C.V., Probing surface core motions with DGRF models (abstract), *Eos Trans. AGU, 69*, 336, 1988.

Voorhies, C.V., Coupling an inviscid core to an electrically-insulating mantle, *J. Geomag. Geoelect., 43*, 131-156, 1991a.

Voorhies, C.V., On the joint inversion of geophysical data for models of the coupled core-mantle system, *NASA Tech Memo 104536*, 24pp., 1991b.

Voorhies, C. V., Implications of decade fluctuations in the length of the day for geomagnetic estimates of core surface flow and geodynamo experiments, in *Geophysical Monographs*, edited by J-L. Le Mouël, submitted, 1992.

Voorhies, C.V., and G.E. Backus, Steady flows at the top of the core from geomagnetic field models: the steady motions theorem. *Geophys. Astrophys. Fluid Dyn., 32*, 163-173, 1985.

Wahr, J. M., The Earth's rotation, *Ann. Rev. Earth Planet. Sci., 16*, 231-249, 1988.

Whaler, K.A., Geomagnetic evidence for fluid upwelling at the core-mantle boundary, *Geophys. Journ. Roy. Astron. Soc., 86*, 563-588, 1986.

Whaler, K.A., A steady velocity field at the top of the Earth's core in the frozen-flux approximation - errata and further comments, *Geophys. J. Int., 102*, 507-509, 1990.

Whaler, K.A., Properties of steady flows at the core-mantle boundary in the frozen-flux approximation, *Phys. Earth Planet. Int., 68*, 144-155, 1991.

Whaler, K.A., and S.O. Clarke, A steady velocity field at the top of the Earth's core in the frozen-flux approximation. *Geophys. J. Int., 94*, 143-155, 1988.

R. W. Clayton, Seismological Laboratory, California Institute of Technology, Pasadena, CA 91125. U. S. A.

B. H. Hager, Department of Earth, Atmospheric and Planetary Sciences, Massachusetts Institute of Technology, Cambridge, MA 02139, U. S. A.

R. Hide, Robert Hooke Institute, The Observatory, Clarendon Laboratory, Parks Road, Oxford 0X1 3PU, England, U. K.

M. A. Spieth, Jet Propulsion Laboratory, California Institute of Technology, Pasadena, CA 91109, U. S. A.

C. V. Voorhies, Geodynamics Branch Code 921, Goddard Space Flight Center, Greenbelt, MD 20771, U. S. A.

Published under the aegis of the AGU Books Board.

Library of Congress Cataloging-in-Publication Data

Relating geophysical structures and processes : the Jeffreys volume /
Keiiti Aki, Renata Dmowska, editors.
p. cm. — (Geophysical monograph ; 76) (IUGG ; v. 16)
ISBN 0-87590-467-X
1. Earth sciences—Mathematical models. 2. Geophysics—
Mathematical models.
I. Aki, Keiiti, 1930– II. Dmowska, Renata.
III. Series. IV. Series: IUGG (Series) ; v. 16.
QE43.R44 1993
550'.1'5118—dc20 93-28483
CIP

ISBN: 0-87590-467-X

ISSN: 0065-8448

Printed in the United States of America.

CONTENTS

Preface
K. Aki, R. Dmowska ix

Foreword
Helmut Moritz xi

1 **Jeffreys and the Earth**
Bruce A. Bolt 1

2 **The Ionosphere**
David R. Bates 11

3 **Hurricanes and Atmospheric Processes**
Yoshio Kurihara 19

4 **Upper Mantle Density Anomalies, Tectonic Stress in the Lithosphere, and Plate Boundary Forces**
Martin H. P. Bott 27

5 **A Simple Rheological Framework for Comparative Subductology**
Toshiko Shimamoto, Tetsuzo Seno, and Seiyo Uyeda 39

6 **Seismic Structure and Heterogeneity in the Upper Mantle**
B.L.N. Kennett 53

7 **Seismic Tomography and Geodynamics**
Adam M. Dziewonski, Alessandro M. Forte, Wei-jia Su, and Robert L. Woodward 67

8 **Topographic Core-Mantle Coupling and Fluctuations in the Earth's Rotation**
R. Hide, R. W. Clayton, B. H. Hager, M. A. Spieth, and C. V. Voorhies 107

9 **Chemical Reactions at the Earth's Core–Mantle Boundary: Summary of Evidence and Geomagnetic Implications**
Raymond Jeanloz 121

10 **Pressure-Temperature Regimes and Core Formation in the Accreting Earth**
Horton E. Newsom and Frederick A. Slane 129

TRANSITION FIELDS IN GEOMAGNETIC POLARITY REVERSALS: STORM TRACKS IN THE CORE!

By Raymond Hide
Oxford University

It is now widely accepted[1] on both quantitative and qualitative grounds that (*i*) the main magnetic fields of the Earth and other planets are due to ordinary electric currents circulating in the electrically conducting parts of their interiors, and (*ii*) these electric currents are produced and maintained against ohmic dissipation by the self-exciting magnetohydrodynamic (MHD) dynamo process first proposed by Larmor and subsequently elaborated by many others. The task of investigating such dynamos in detail, by solving the highly nonlinear equations of MHD under appropriate boundary conditions and comparing the results with manifold observations of planetary magnetic fields, is not yet feasible, for most theoretical research is of necessity concerned with mathematical analyses of systems very much simpler than the prototypes. But quite general considerations of the governing partial differential equations and of the boundary conditions under which they have to be solved can be used to expose the limitations of working hypotheses employed in the interpretation of observations and to guide future observational and theoretical research.

These equations comprise the usual equations of hydrodynamics and thermodynamics governing the Eulerian flow velocity **u**, pressure p, density ρ, temperature T, *etc.*, at a general point P, vector position **r** at time t, together with the 'pre-Maxwell' equations of electrodynamics governing the magnetic field **B**, electric current density **j**, *etc.*, in a moving medium, to be solved under the mechanical, thermal, and electromagnetic conditions imposed on the liquid core at its upper boundary by the overlying mantle and at its lower boundary by the solid inner core. It is readily shown, for example, that for every solution $(\mathbf{u}(\mathbf{r}, t), \mathbf{B}(\mathbf{r}, t))$ of the governing equations, there is a corresponding solution $(\mathbf{u}(\mathbf{r}, t), -\mathbf{B}(\mathbf{r}, t))$ (if the boundary conditions are independent of the sign of the magnetic field **B**). So, in some respects, it is not surprising, in retrospect at least, that the most striking property of the main geomagnetic field (as revealed by the study of fossilized field directions in igneous and sedimentary rocks) is that the geomagnetic dipole has reversed its polarity many thousands of times over geological history and that there is no significant bias towards one polarity or the other[2]. Reversals are sudden events, geologically speaking, lasting no more than tens of thousands of years, which is much less than typical intervals *between* reversals, which are highly variable in duration.

Owing to Coriolis forces associated with the Earth's rotation, core motions will be particularly sensitive not only to the presence of the solid inner core[3], but also to boundary conditions imposed at the core–mantle interface, such as horizontal temperature gradients and undulations in the shape of that interface associated with slow but time-dependent convective motions in the lower mantle[4]. Mantle flow is characterized by very much longer time scales — millions of years — than those associated with the general westward drift of features of the geomagnetic field and other direct manifestations of core motions. In particular, temporal and spatial characteristics of the geomagnetic field, such as the highly variable frequency of polarity reversals and detailed behaviour of transition fields, including the apparent tendency for virtual geomagnetic poles to follow certain tracks on the Earth's surface, would be *expected* to exhibit

THE OBSERVATORY, 115, 314–316 (1995).

properties that correlate well with geological processes, which in turn are reflected in geographical features, not the reverse.

These ideas bear on the use by palæomagnetic workers, starting in the 1950s, of the so-called 'geocentric axial dipole' (GAD) hypothesis, that when averaged over a few thousand years, owing to the westward drift, the geomagnetic field at the Earth's surface should be symmetric about the rotation axis and close in form to that of a hypothetical dipole placed at the centre of the Earth[1,2]. With the aid of the GAD hypothesis they were able from determinations of the fossilized inclination of the magnetic field in a wide variety of rocks to acquire important evidence for long-term continental drift and polar motion. Internal consistency of observations support the view that the hypothesis can be trusted as a rough first approximation, but it is still not widely appreciated that the basis of the hypothesis is largely empirical. Claims that the hypothesis has a secure basis in theory implicitly neglect the possibility of significant longitudinal variations in the boundary conditions imposed on motions in the liquid core by the regions with which it is in contact[4].

Notwithstanding the early success of the GAD hypothesis, the foregoing arguments indicate that when dealing with the interpretation of the detailed behaviour of transition fields during polarity reversals (and other aspects of the spatio-temporal behaviour of the geomagnetic field), the possibility that the observations reflect intrinsic behaviour of core motions under the influence of boundary conditions imposed by the mantle and the inner core should be taken seriously, as indeed some workers have done[5]. A different view is preferred by those who accept the suggestion that the electrical conductivity of the D″ layer at the bottom of the mantle can take very high values[6] (even comparable with that of the metallic core over the Pacific hemisphere) and attribute the observed properties of transition fields to electromagnetic screening in the D″ layer, implicitly assuming the GAD hypothesis holds with high precision. This view has been defended by one of its chief proponents as follows: "It is less easy to accept [the] idea [that] the core produces fields of different characteristics in different longitudes for times of the order of mantle convection", arguing that "the fundamental starting point in the discussion of core-mantle interactions is the explanation of irregular changes in the length of the day [on decadal time scales] by the interchange of angular momentum, between the core and the mantle. The rotation of the core relative to the mantle, seen clearly in the westward drift of the non-axial parts of the field in historical times, seems incompatible with the idea that the dynamo produces fields with characteristics [that] remain stationary with respect to the mantle for times long when compared to the lifetime of secular variation foci"[7].

It is instructive to apply this argument to another fluid system, namely Earth's atmosphere, which (like the core) exchanges angular momentum with the solid Earth, as evinced by pronounced irregular changes in the length of the day on sub-decadal time scales. The argument leads to the *incorrect* conclusion that longitudinal variations of atmospheric variables such as surface pressure, temperature, and wind velocity would average out to zero on timescales much longer than those characteristic of transient disturbances in the atmosphere (days to weeks). Maps of the mean state of the atmosphere over years and decades (see, *e.g.*, ref. 8) most certainly do not possess this property; indeed they show strong correlations with geographical features as do meteorological 'storm tracks'! Because the argument gives incorrect predictions for the atmosphere, it does not follow immediately that it must necessarily fail when applied

to the core, but it is clear that implicit in the argument are assumptions that would need to be justified. The main assumption, in my view, is the implicit neglect of the possibility that the core can support large-scale wave motions with phase speeds comparable with the speed of material motion in the core[3]. In such a system, stationary or quasi-stationary disturbances locked to 'geographical' features are readily produced.

As we have already seen, MHD flow in the core is influenced by electromagnetic as well as by thermal and mechanical boundary conditions imposed by the overlying mantle and the underlying solid inner core. So it follows that if certain regions (*e.g.*, the Pacific hemisphere of the D'' layer at the bottom of the mantle) consist of material of high electrical conductivity, then the magnetic field seen near the surface of the Earth would be affected not only by the screening effect of the conducting regions but also by their direct influence on the field produced in the core. However, the existence of such material may not be consistent with determinations of the 'magnetic' radius of the core from geomagnetic secular-variation data. The method[9] assumes that, to a first approximation, mantle conductivity can be neglected, and it gives for the magnetic radius of the core a value within no more than two per cent of the seismologically-determined value[10,11]. This near-agreement provides a constraint on models of the distribution of electrical conductivity in the mantle which might usefully be applied in future work on the interpretation of polarity reversals and transition fields.

This note summarizes the author's contribution to a Discussion Meeting on 'Geomagnetic Reversals: the Transition Fields and their Interpretation' held on 1994 January 14 at Savile Row, London. It is impossible to do justice to all the important observational material and theoretical ideas presented at the meeting (the proceedings of which have not been published), but extensive lists of relevant references can be found in two papers (refs. 12, 13) which have recently appeared.

References

(1) R. T. Merrill & M. W. McElhinny, *The Earth's Magnetic Field* (Academic Press, New York), 1983; J. A. Jacobs (ed.), *Geomagnetism* (4 volumes) (Academic Press, New York), 1987–91.
(2) J. A. Jacobs, *Reversals of the Earth's Magnetic Field* (Cambridge University Press), 1994.
(3) R. Hide, *Phil. Trans. R. Soc. London*, **A259**, 615, 1966.
(4) R. Hide, *Science*, 157, 55, 1967.
(5) C. Laj *et al.*, *Nature*, 351, 447, 1988.
(6) E. Knittle & R. Jeanloz, *Science*, 251, 1438, 1986.
(7) S. K. Runcorn, in D. B. Stone & S. K. Runcorn (eds.), *Flow and Creep in the Solar System: Observations, Modelling and Theory* (Kluwer, Dordrecht), 1993, p. 67.
(8) J. P. Peixoto & A. H. Oort, *Physics of Climate* (American Institute of Physics, New York), 1992.
(9) R. Hide, *Nature*, 271, 640, 1978.
(10) R. Hide & S. R. C. Malin, *Proc. R. Soc. London*, **A374**, 15, 1981.
(11) C. V. Voorhies & E. R. Benton, *Geophys. Res. Lett.*, 9, 258, 1982.
(12) D. E. Loper & T. Lay, *J. Geophys. Res.*, 100, 6397, 1995.
(13) G. A. Glatzmaier & P. H. Roberts, *Nature*, 377, 203, 1995.

Geophys. J. Int. (1996) 125, 599–607

Topographic core–mantle coupling and polar motion on decadal time-scales

R. Hide,[1,2] D. H. Boggs,[1] J. O. Dickey,[1] D. Dong,[1] R. S. Gross[1] and A. Jackson[3]

[1] *Space Geodetic Science and Applications Group, Jet Propulsion Laboratory, California Institute of Technology, Pasadena, CA 91109-8099, USA*
[2] *Department of Physics (Atmospheric, Oceanic and Planetary Physics), University of Oxford, Clarendon Laboratory, Parks Road, Oxford OX1 3PU*
[3] *School of Earth Sciences, University of Leeds, Leeds LS9 NJT*

Accepted 1996 January 10. Received 1996 January 9; in original form 1995 June 21

SUMMARY

Associated with non-steady magnetohydrodynamic (MHD) flow in the liquid metallic core of the Earth, with typical relative speeds of a fraction of a millimetre per second, are fluctuations in dynamic pressure of about 10^3 N m^{-2}. Acting on the non-spherical core–mantle boundary (CMB), these pressure fluctuations give rise to a fluctuating net topographic torque $L_i(t)$ $(i = 1, 2, 3)$—where t denotes time—on the overlying solid mantle. Geophysicists now accept the proposal by one of us (RH) that $L_i(t)$ makes a significant and possibly dominant contribution to the total torque $L_i^*(t)$ on the mantle produced directly or indirectly by core motions. Other contributions are the 'gravitational' torque associated with fluctuating density gradients in the core, the 'electromagnetic' torque associated with Lorentz forces in the weakly electrically conducting lower mantle, and the 'viscous' torque associated with shearing motions in the boundary layer just below the CMB. The axial component $L_3^*(t)$ of $L_i^*(t)$ contributes to the observed fluctuations in the length of the day [LOD, an inverse measure of the angular speed of rotation of the solid Earth (mantle, crust and cryosphere)], and the equatorial components $(L_1^*(t), L_2^*(t)) \equiv \mathbf{L}^*(t)$ contribute to the observed polar motion, as determined from measurements of changes in the Earth's rotation axis relative to its figure axis.

In earlier phases of a continuing programme of research based on a method for determining $L_i(t)$ from geophysical data (proposed independently about ten years ago by Hide and Le Mouël), it was shown that longitude-dependent irregular CMB topography no higher than about 0.5 km could give rise to values of $L_3(t)$ sufficient to account for the observed magnitude of LOD fluctuations on decadal time-scales. Here, we report an investigation of the equatorial components $(L_1(t), L_2(t)) = \mathbf{L}(t)$ of $L_i(t)$ taking into account just one topographic feature of the CMB—albeit possibly the most pronounced—namely the axisymmetric equatorial bulge, with an equatorial radius exceeding the polar radius by 9.5 ± 0.1 km (the mean radius of the core being 3485 ± 2 km, 0.547 times that of the whole Earth). A measure of the local horizontal gradient of the fluctuating pressure field near the CMB can be obtained from the local Eulerian flow velocity in the 'free stream' below the CMB by supposing that nearly everywhere in the outer reaches of the core—the 'polosphere' (Hide 1995)—geostrophic balance obtains between the pressure gradient and Coriolis forces. The polospheric velocity fields used were those determined by Jackson (1989) from geomagnetic secular variations (GSV) data on the basis of the geostrophic approximation combined with the assumption that, on the time-scales of the GSV, the core behaves like a perfect electrical conductor and the mantle as a perfect insulator.

In general agreement with independent calculations by Hulot, Le Huy & Le Mouël (1996) and Greff-Lefftz & Legros (1995), we found that in magnitude $\mathbf{L}(t)$ for epochs from 1840 to 1990 typically exceeds $|L_3(t)|$ by a factor of about 10, roughly equal to the ratio of the height of the equatorial bulge to that strongly implied for irregular topography by determinations of $L_3(t)$ (see Hide *et al.* 1993). But $\mathbf{L}(t)$ still apparently

falls short in magnitude by a factor of up to about 5 in its ability to account for the amplitude of the observed time-series of polar motion on decadal time-scales (DPM), and it is poorly correlated with that time-series. So we conclude that unless uncertainties in the determination of the DPM time-series from observations—which we also discuss—have been seriously underestimated, the action of normal pressure forces associated with core motions on the equatorial bulge of the core–mantle boundary makes a significant but not dominant contribution to the excitation of decadal polar motion. Other geophysical processes such as the movement of groundwater and changes in sea-level must also be involved.

Key words: core–mantle boundary, dynamics, Earth's core, Earth's interior, Earth's rotation, geomagnetism, planetary oblateness, topography.

INTRODUCTION

Electric currents generated in the Earth's liquid metallic core are responsible for the main geomagnetic field and its secular changes (see e.g. Merrill & McElhinny 1983; Jacobs 1987–1991). The currents are produced by dynamo action involving irregular MHD flow in the core. Concomitant dynamical stresses acting on the overlying mantle have been invoked by geophysicists as the main source of excitation of the so-called 'decadal' fluctuations in the speed of rotation of the 'solid Earth' (mantle, crust and cryosphere). It is possible that core motions make a detectable contribution to polar motion (i.e. the movement of the rotation axis of the solid Earth relative to the figure axis) on these time-scales. Studies of rotational manifestations of core motions have important implications, for they bear directly on the improvement of models of the structure, composition and dynamics of the Earth's deep interior, which have to reconcile a wide variety of geophysical observations (for references see Loper & Lay 1995).

Consider a set of body-fixed axes x_i $(i = 1, 2, 3)$ aligned with the principal axes of the solid Earth and rotating about the centre of mass of the whole Earth with angular velocity

$$\hat{\omega}_i = \hat{\omega}_i(t) = (\hat{\omega}_1, \hat{\omega}_2, \hat{\omega}_3) = \Omega(\hat{m}_1, \hat{m}_2, 1 + \hat{m}_3), \quad (1)$$

where t denotes time and Ω the mean speed of rotation of the solid Earth in recent times (0.7292115×10^{-4} rad s^{-1}) (see e.g. Munk & MacDonald 1960; Lambeck 1980; Rochester 1984; Moritz & Mueller 1987; Wahr 1988). Over time-scales that are short compared with those characteristic of geological processes, the rotation of the Earth departs only slightly from steady rotation about the polar axis of figure, so that $\hat{m}_1, \hat{m}_2, \hat{m}_3$ are all very much less than unity and $|\dot{\hat{m}}_i| \ll \Omega$, where $\dot{\hat{m}}_i \equiv d\hat{m}_i/dt$. Periodic variations in ω_i on time-scales less than a few years are forced by periodic lunar and solar tidal torques and related changes in the moment of inertia of the solid Earth. Irregular subdecadal variations are evidently produced largely by atmospheric and oceanic torques due to tangential stresses in boundary layers and normal (pressure) stresses acting on surface topography. These fluctuating stresses are associated with seasonal, intraseasonal and interannual fluctuations in the total angular momentum of the atmosphere (for references see Hide 1986; Hide & Dickey 1991; Eubanks 1993; Rosen 1993). When these rapid variations have been removed from the observational data, the smoothed time-series,

$$\omega_i(t) = \Omega(m_1(t), m_2(t), 1 + m_3(t)), \quad (2)$$

that remains (see Figs 1 and 2) represents the contributions of decadal variations to $\hat{\omega}_i(t)$. Errors and uncertainties in these determinations of $m_1(t)$ and $m_2(t)$ are discussed in Appendix A.

It is convenient at this stage to introduce the vector $\mathbf{L}_i^+(t)$, defined as the hypothetical torque acting on the solid Earth that would account for observed Earth-rotation fluctuations on decadal time-scales in the absence of other processes, such as changes in the inertia tensor of the solid Earth associated with the stresses responsible for $L_i^+(t)$ and also with the movement of groundwater, melting of ice, etc. Using standard methods (see e.g. Munk & Macdonald 1960; Lambeck 1980) it is readily shown that, to sufficient accuracy here (*cf.* Hide 1989),

$$\mathbf{L}^+(t) \equiv [L_1^+(t), L_2^+(t)] = \Omega^2(C^{(m)} - A^{(m)})[m_2(t), -m_1(t)], \quad (3)$$

where $C^{(m)} - A^{(m)} = 2.63 \times 10^{35}$ kg m^2, $C^{(m)}$ and $A^{(m)}$ being the principal moments of inertia of the solid Earth (about polar and equatorial axes through the Earth's centre of mass respectively). $C^{(m)}$ is 0.895 times the polar moment of inertia of the whole Earth, including the metallic core. Time-series of $L_1^+(t)$ and $L_2^+(t)$ are given in Fig. 2.

In this paper we investigate, as part of a continuing programme of research on Earth-rotation fluctuations, the extent to which the observed DPM can be accounted for by the fluctuating topographic torque $\mathbf{L}(t) \equiv [L_1(t), L_2(t)]$ associated with normal pressure forecasting on the equatorial bulge of the CMB. Our findings (see below) are in general agreement with those of independent and parallel studies by Hulot, Le Huy & Le Mouël (1996) and Greff-Lefftz & Legros (1995) extending earlier work by Hinderer *et al.* (1987), in which effects of irregular latitude-dependent topography as well as electromagnetic coupling and induced changes in the inertia tensor of the imperfectly rigid mantle are also investigated.

THE TOPOGRAPHIC TORQUE EXERTED BY THE CORE ON THE MANTLE

The fluctuating torque $L_i^*(t)$ exerted by the core on the overlying mantle is produced by:

(a) tangential stresses at the CMB associated with shearing motions in the thin (probably less than 1 m) viscous boundary layer just below the CMB;

(b) normal dynamic pressure forces acting on the equatorial

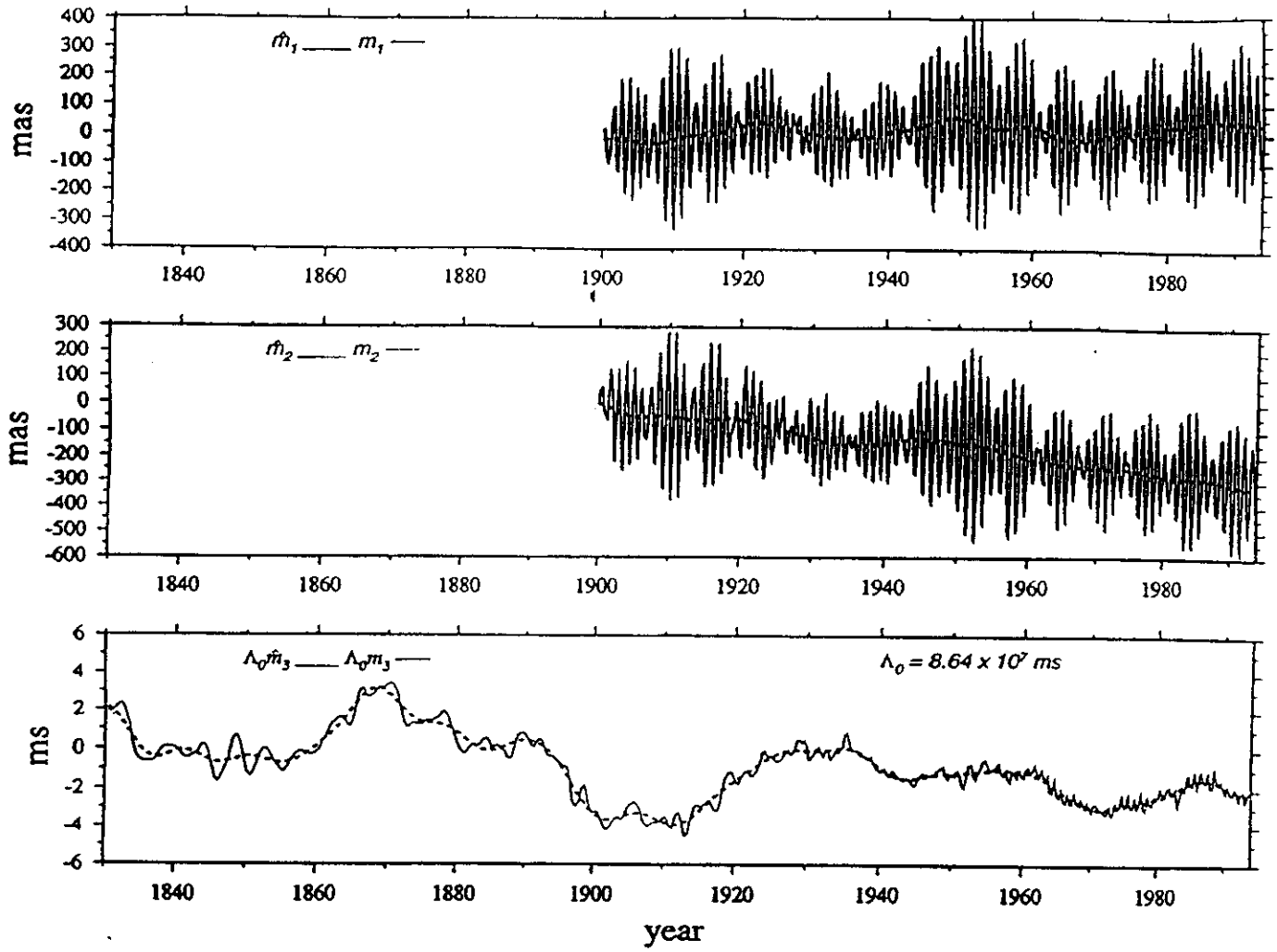

Figure 1. Time-series (solid lines) of the observed fluctuations in the Earth's rotation vector $\boldsymbol{\omega} \equiv \Omega[\hat{m}_1(t), \hat{m}_2(t), 1 + \hat{m}_3(t)]$ [see eq. (1) and Appendix A]. The top panel shows the x-component of polar motion, $\hat{m}_1(t)$, defined to be positive towards the Greenwich meridian, the middle panel shows the y-component of polar motion, $\hat{m}_2(t)$, defined to be positive towards 90°E longitude, and the bottom panel shows changes in the length of day $\hat{\Lambda}(t)$, which is related to $\hat{m}_3(t)$ by $\hat{\Lambda}(t) = -\Lambda_0 \hat{m}_3(t)$, where Λ_0 is the nominal length of day of 86 400 s. The dashed lines show the decadal variations obtained by applying a low-pass filter (cut-off period = 10 years) to the observed series (see also Fig. 2).

bulge and other (possibly) smaller and more irregular departures from sphericity of the shape of the CMB;

(c) Lorentz forces due to the flow of electric currents in the weakly conducting lower mantle generated by the electromotive forces associated with the geodynamo processes in the core; and

(d) gravitational forces associated with horizontal density variations in the core and mantle and especially with CMB topography (Jault & Le Mouël 1993; Eubanks 1993).

Dynamical arguments show that the pressure coupling associated with quite modest CMB topography could predominate over other effects (Hide 1969, 1986, 1989). While the contribution made by viscous stresses is negligible if, as is likely, the effective coefficient of kinematic viscosity of the core is less than about $10^4\ \mathrm{m^2\,s^{-1}}$, electromagnetic coupling might be quantatively significant if the (unknown) electrical conductivity of the lower mantle were sufficiently high. Gravitational coupling may turn out to be significant as well (see Jault & Le Mouël 1993; Hulot *et al.* 1996).

The axial component $L_3(t)$ of the topographic torque and its manifestation in decadal LOD variations have been considered in previous studies (e.g. Jault & Le Mouël 1990; Hide *et al.* 1993). Here we discuss the equatorial components $L_1(t)$ and $L_2(t)$ and their contribution to the decadal polar motion $m_1(t)$ and $m_2(t)$, a problem which, as noted above, has also been studied independently by Hinderer *et al.* (1987), Hulot *et al.* (1996) and Greff-Lefftz & Legros (1995), see also Hide (1989), with findings in general agreement with those of the present study. If p_s is the dynamic pressure associated with core motions $\mathbf{u} = \mathbf{u}_s = (u_s, v_s, w_s)$ in the free stream just below the viscous boundary layer at the CMB (u being the Eulerian flow velocity relative to a reference frame fixed to the solid Earth), and the CMB is the locus of points where the distance from the Earth's centre of mass is $r = c + h(\theta, \phi)$ (c being the mean radius of the CMB and (θ, ϕ) the co-latitude and longitude of a general point P), then

$$L_i(t) = -c^2 \int_0^{2\pi} \int_0^{\pi} (\mathbf{r} \times p_s \nabla_s h)_i \sin\theta \, d\theta \, d\phi \qquad (4)$$

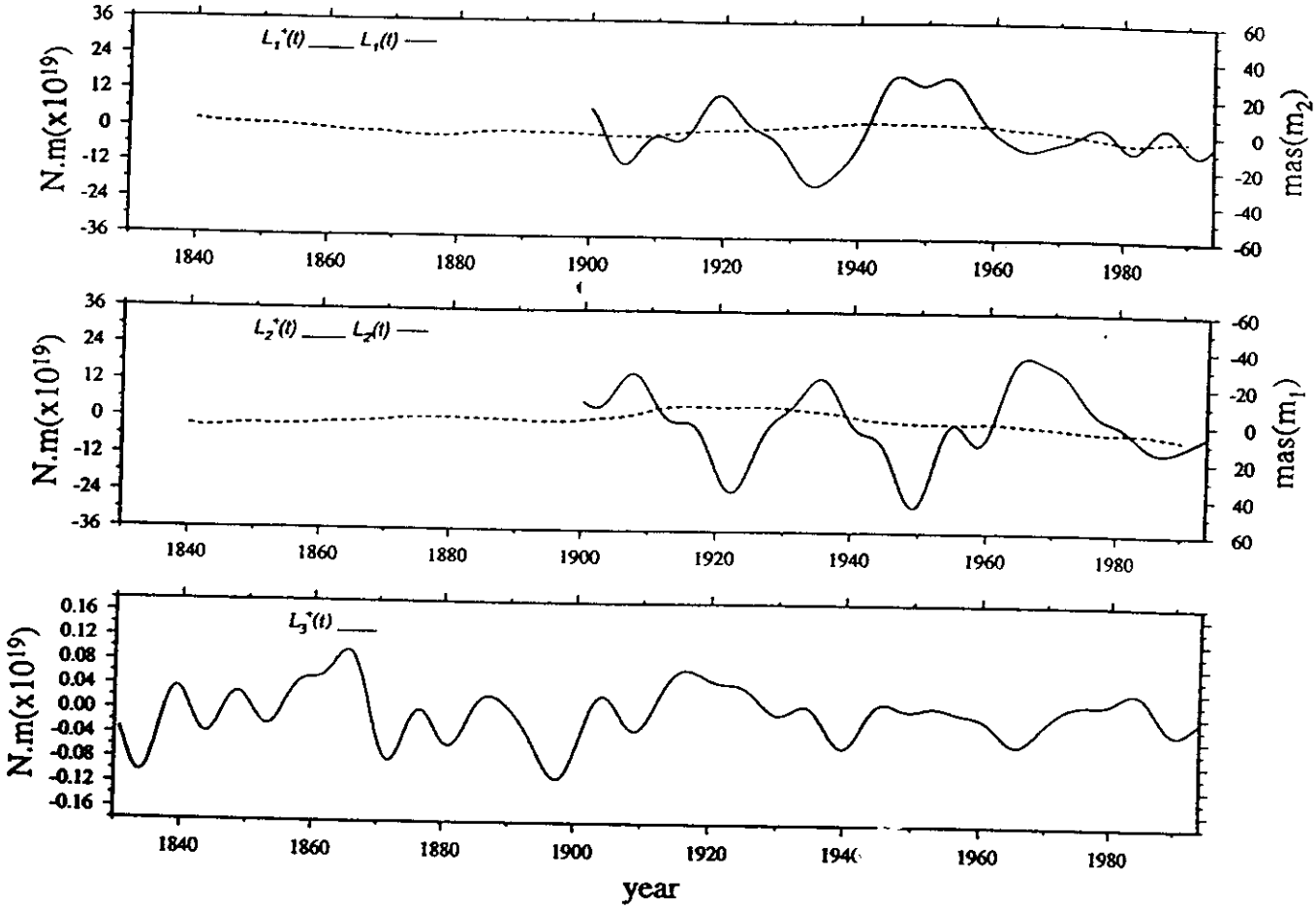

Figure 2. Time-series of the components ($L_1^*(t)$, $L_2^*(t)$, $L_3^*(t)$) of the equivalent torques implied by decadal components of ($\dot{m}_1(t)$, $\dot{m}_2(t)$, $1+\dot{m}_3(t)$) for a perfectly rigid mantle [see eqs (2) and (3) and Hide (1989)]. Also given (dashed lines) are the estimated time-series of the contribution made to ($\dot{m}_1(t)$, $\dot{m}_2(t)$) by the equatorial torque ($L_1(t)$, $L_2(t)$) (see eq. 23) due to the action on the equatorial bulge of the CMB of normal pressure forces associated with core motions in the case of a perfectly rigid mangle (see Fig. 3). A low-pass filter with a cut-off period of 10 years has been applied to all time series.

if $|h| \ll c$ and $|\nabla_s h| \ll 1$. Here $\nabla_s \equiv c^{-1}(\hat{\boldsymbol{\theta}}\partial/\partial\theta,\ \hat{\boldsymbol{\phi}}\ \mathrm{cosec}\,\theta\partial/\partial\phi)$, where $\hat{\boldsymbol{\theta}}$ and $\hat{\boldsymbol{\phi}}$ are unit vectors in the direction of increasing θ and ϕ respectively, and r is the vector distance from the Earth's centre of mass. Because $\mathbf{r}\times\nabla_s(hp_s)$ is a toroidal vector, with no radial components, its integral over the whole CMB is equal to zero (Hide 1989). This leads to a more useful expression for $L_i(t)$ in the present context (see below), namely

$$L_i(t) = c^2 \int_0^{2\pi}\int_0^{\pi} (\mathbf{r}\times h\nabla_s p_s)_i \sin\theta\, d\theta\, d\phi, \tag{5a}$$

with components

$$L_1 = -c^2 \int_0^{2\pi}\int_0^{\pi} h\left(\sin\theta\sin\phi\frac{\partial p_s}{\partial\theta} + \cos\theta\cos\phi\frac{\partial p_s}{\partial\phi}\right) d\theta\, d\phi, \tag{5b}$$

$$L_2 = c^2 \int_0^{2\pi}\int_0^{\pi} h\left(\sin\theta\cos\phi\frac{\partial p_s}{\partial\theta} - \cos\theta\sin\phi\frac{\partial p_s}{\partial\phi}\right) d\theta\, d\phi, \tag{5c}$$

$$L_3 = c^2 \int_0^{2\pi} h\left(\sin\theta\frac{\partial p_s}{\partial\phi}\right) d\theta\, d\phi. \tag{5d}$$

Given $h(\theta,\phi)$ and determinations of $p_s(\theta,\phi,t)$ on the CMB, $L_i(t)$ could be calculated directly using either eq. (4) or eq. (5). However, as in the case of the Earth's core and in other situations where p_s is *not* known from direct measurements but other information is available, such as $\mathbf{u}_s(\theta,\phi,t)$, it is still possible to estimate $L_i(t)$ by using the equations of fluid dynamics to relate the horizontal pressure gradient to 'observable' quantities. Owing to the Earth's rotation, Coriolis forces exert a strong influence on core flow (Elsasser 1939; Frenkel 1945; Inglis 1955). They should be in close 'geostrophic' balance with horizontal pressure gradients nearly everywhere within those regions of the core where Lorentz forces, which produce the strongest 'ageostrophic' effects (Hide 1956), are comparatively weak, and in 'magnetostrophic' balance in any regions where Lorentz forces are comparable in magnitude with Coriolis forces. Now the magnetic field in the core can be decomposed into 'toroidal' and 'poloidal' parts [Elsasser 1947; *cf.* eq. (12) below], where the former has no radial component and may exceed the latter in magnitude by as much as a factor of about 10 and give rise to magnetostrophic flow throughout most of the liquid core—the 'torosphere' (see Hide 1995)—but not in the outer reaches of the core—the 'polosphere'—where by definition the toroidal magnetic field

is no stronger than the poloidal field (see Le Mouël 1984; Hide 1995). With a fractional error of no more than about 10^{-2}, polospheric flow can be assumed geostrophic nearly everywhere, satisfying the equation

$$2\bar{\rho}_s\Omega\cos\theta[-w_s, v_s] = -c^{-1}[\partial p_s/\partial\theta, \operatorname{cosec}\theta\,\partial p_s/\partial\phi], \qquad (6)$$

where $\bar{\rho}_s$ is the average density over the spherical surface where $\mathbf{u} = \mathbf{u}_s$. Here (v_s, w_s), the (θ, ϕ) components of $\mathbf{u}_s$, are typically much greater in magnitude than u_s, the r-component of $\mathbf{u}_s$. It follows from eqs (5) and (6) that on the time-scales of interest here, over which $\mathbf{u}$ may change significantly but h does not,

$$[L_1(t), L_2(t)] = 2\bar{\rho}_s\Omega c^3 \int_0^{2\pi}\int_0^{\pi} h(\theta,\phi)[f_1(\theta,\phi,t), f_2(\theta,\phi,t)] \times \sin\theta\cos\theta\,d\theta\,d\phi, \qquad (7a)$$

where

$$[f_1, f_2] \equiv [v_s\cos\theta\cos\phi - w_s\sin\phi, v_s\cos\theta\sin\phi + w_s\cos\phi] \qquad (7b)$$

(Hide 1989, 1995; Jault & Le Mouël 1989; Voorhies 1991).

The basic theoretical relationships needed here are given by eqs (3–7). The integral on the right-hand side of eq. (7a) involves the CMB topography $h(\theta, \phi)$. The ϕ-independent mean equatorial bulge $h_0(\theta)$ (say) of the CMB corresponds to a 9.5 ± 0.1 km difference between the equatorial and polar radii of the CMB (see Denis & Ibrahim 1981; Gwinn, Herring & Shapiro 1986; Herring *et al.* 1991; *cf.* Moritz & Mueller 1987). If this is substantially larger than the typical vertical amplitude of irregular topographic features of the CMB [and there is evidence that this might be so from the study of decadal variations in the length of day, involving the evaluation of $L_3(t)$; see Jault & Le Mouël (1990); Hide *et al.* (1993)], then to a good first approximation we can replace $h(\theta, \phi)$ in eq. (7) by $h_0(\theta)$ [see eqs (17) and (18) below]. The other quantity needed in the evaluation of $L_i(t)$ is *either* the field of dynamical pressure $p_s(\theta, \phi, t)$ [see eqs (4) and (5) and Appendix B] *or* the field of horizontal flow $(v_s(\theta, \phi, t), w_s(\theta, \phi, t))$, which is related to p_s through eq. (6). Geomagnetic secular variation data have been used by various workers to infer (v_s, w_s) by a method that invokes geostrophic balance in combination with the equations of electrodynamics appropriate to the case when the mantle can be treated as a perfect electrical insulator of uniform magnetic permeability and the core as a perfect conductor, as we shall now discuss.

VELOCITY AND PRESSURE FIELDS IN THE CORE

Denote the value of the main geomagnetic field at a general point (r, θ, ϕ) at time t by $\mathbf{B}(r, \theta, \phi, t)$, and the geomagnetic secular variation (GSV) by $\dot{\mathbf{B}} \equiv \partial\mathbf{B}/\partial t$. Determinations of B made at and near the Earth's surface at various epochs can be used to infer $\mathbf{u}_s$, the Eulerian flow velocity just below the CMB (for references see Bloxham & Jackson 1991; Hulot, Le Mouël & Wahr 1992). In turn, estimates of the associated horizontal pressure gradient $c^{-1}(\partial p_s/\partial\theta, \operatorname{cosec}\theta\,\partial p_s/\partial\phi)$ there can be deduced by using eq. (6). The first of the three reasonable key assumptions that underlie the method used is that the electrical conductivity of the mantle and magnetic permeability gradients there are negligible, so that B can be written as the gradient of a potential V satisfying Laplace's equation $\nabla^2 V = 0$. This facilitates the downward extrapolation of the observed field at and near the Earth's surface in order to obtain B and $\dot{\mathbf{B}}$ at the CMB (see e.g. Jacobs 1987–1991). The second assumption concerns the time-scales of the GSV and the electrical conductivity of the core. Dynamo theory requires high but not perfect electrical conductivity, for it is impossible to change the magnetic flux linkage of a perfect conductor (Bondi & Gold 1950), in accordance with Alfvén's 'frozen flux' theorem. When dealing with fluctuations in B on time-scales very much less than that of the ohmic decay of magnetic fields in the core (which is several thousand years for global-scale features), however, Alfvén's 'frozen flux' theorem, in our notation

$$\partial\mathbf{B}/\partial t = \nabla\times(\mathbf{u}\times\mathbf{B}), \qquad (8)$$

should provide a good leading approximation, implying that the lines of magnetic force emerging from the core are advected by the horizontal flow (v_s, w_s) just below the CMB (Roberts & Scott 1965; Backus 1968). Accordingly if $\mathbf{B} = (B_r, B_\theta, B_\phi)$, then B_r at the CMB satisfies

$$\frac{\partial B_r}{\partial t} + \frac{v_s}{c}\frac{\partial B_r}{\partial\theta} + \frac{w_s}{c\sin\theta}\frac{\partial B_r}{\partial\phi} = B_r\left[\frac{\partial u}{\partial r}\right]_{r=c}. \qquad (9)$$

The last equation alone does not permit the unique determination of $\mathbf{u}_s$ from knowledge of B and $\dot{\mathbf{B}}$ at the CMB, so a third physically plausible assumption is needed. Effective uniqueness can be secured by making use of the assumption expressed by eq. (6) above, namely that, to a first approximation, polospheric flow is in geostrophic balance (Hills 1979; Le Mouël 1984; Le Mouël, Gire & Madden 1985; Backus & Le Mouël 1986; Gire & Le Mouël 1990; see also Bloxham & Jackson 1991; Hulot *et al.* 1992). This gives the additional equation

$$\cos\theta\left[\frac{\partial u}{\partial r}\right]_{r=c} + \frac{\sin\theta}{c}v_s = 0, \qquad (10)$$

which is obtained by eliminating p_s from eq. (6) and using the mass continuity equation

$$\nabla\cdot\mathbf{u} = 0 \qquad (11)$$

for flow of an effectively incompressible fluid.

Various groups of geomagnetic workers have produced maps of (v_s, w_s) based on this (and other) assumptions, and have investigated the errors and uncertainties encountered in practice (Bloxham & Jackson 1991; Hulot *et al.* 1992). Fields of B_r and $\dot{B}_r$ at $r = c$ deduced by Jackson (1989) for epochs going back to the year 1840 AD provided the basic B and $\dot{\mathbf{B}}$ input data for the present study. These were used to produce hypothetical 'geostrophic' flow fields $\mathbf{u}_s$, constructed using spherical harmonic expansions (see eqs 16–20) up to degree and order 14, which account for more than 90 per cent of the observed GSV (Jackson 1989).

TORQUE ON THE EQUATORIAL BULGE

For an effectively incompressible fluid, the Eulerian flow field $\mathbf{u}$ is solenoidal, by virtue of eq. (11), and can therefore be decomposed into a toroidal part (with no radial component) and a poloidal part as follows:

$$\mathbf{u} = \mathbf{u}_T + \mathbf{u}_P = \nabla\times(T^*\hat{\mathbf{r}}) + \nabla\times\nabla\times(P^*\hat{\mathbf{r}}), \qquad (12)$$

where $\hat{\mathbf{r}}$ is a unit vector in the direction of increasing r (cf. eq. 1).

If (u, v, w) are the (r, θ, ϕ) components of $\mathbf{u}$, then

$$u = \frac{-1}{r^2}\left[\frac{1}{\sin\theta}\frac{\partial}{\partial\theta}\left(\sin\theta\frac{\partial P^*}{\partial\theta}\right) + \frac{1}{\sin^2\theta}\frac{\partial^2 P^*}{\partial\phi^2}\right], \tag{13a}$$

$$v = \frac{1}{r\sin\theta}\frac{\partial T^*}{\partial\phi} + \frac{1}{r}\frac{\partial S^*}{\partial\theta}, \tag{13b}$$

$$w = -\frac{1}{r}\frac{\partial T^*}{\partial\theta} + \frac{1}{r\sin\theta}\frac{\partial S^*}{\partial\phi}, \tag{13c}$$

where $S^* \equiv \partial P^*/\partial r$. If $\mathbf{u} = \mathbf{u}_s = (u_s, v_s, w_s)$ in the free stream just below the CMB, where, for the purpose of this part of the calculation (but see Hide 1995, eq. 4.5), u_s can be set equal to zero and r equal to c, the mean radius of the CMB (*cf.* eq. 4), and $T^* = T$ and $S^* = S$ on $r = c$, then we have

$$v_s = \frac{1}{c\sin\theta}\frac{\partial T}{\partial\phi} + \frac{1}{c}\frac{\partial S}{\partial\theta}, \tag{14a}$$

$$w_s = -\frac{1}{c}\frac{\partial T}{\partial\theta} + \frac{1}{c\sin\theta}\frac{\partial S}{\partial\phi}. \tag{14b}$$

By the geostrophic relationship eq. (6),

$$\frac{\partial p_s}{\partial\theta} = (2\bar\rho\Omega c\cos\theta)w_s = (2\bar\rho\Omega)\left(-\cos\theta\frac{\partial T}{\partial\theta} + \frac{\cos\theta}{\sin\theta}\frac{\partial S}{\partial\phi}\right), \tag{15a}$$

$$\frac{\partial p_s}{\partial\phi} = -(2\bar\rho\Omega c\cos\theta\sin\theta)v_s = (2\bar\rho\Omega)\left(-\cos\theta\frac{\partial T}{\partial\phi} - \cos\theta\sin\theta\frac{\partial S}{\partial\theta}\right), \tag{15b}$$

from which it follows that T and S satisfy

$$\sin\theta\frac{\partial T}{\partial\phi} = (\cos^2\theta - \sin^2\theta)\frac{\partial S}{\partial\theta} + \cos\theta\sin\theta\frac{\partial^2 S}{\partial\theta^2} + \frac{\cos\theta}{\sin\theta}\frac{\partial^2 S}{\partial\phi^2}. \tag{15c}$$

The scalar quantities $T(\theta, \phi, t)$ and $S(\theta, \phi, t)$ and the topography $h(\theta, \phi)$ can be expressed as spherical harmonic expansions:

$$q = \sum_{n=0}^{\infty}\sum_{m=0}^{n}(q^c_{n,m}\cos m\phi + q^s_{n,m}\sin m\phi)P_{n,m}(\cos\theta), \tag{16}$$

where

$$(q^c_{n,m}, q^s_{n,m}) = (\tau^c_{n,m}, \tau^s_{n,m}) \quad \text{when } q = T, \tag{17}$$

$$(q^c_{n,m}, q^s_{n,m}) = (s^c_{n,m}, s^s_{n,m}) \quad \text{when } q = S, \tag{18}$$

$$(q^c_{n,m}, q^s_{n,m}) = (h^c_{n,m}, h^s_{n,m}) \quad \text{when } q = h. \tag{19}$$

Here $P_{n,m}(\cos\theta)$ are the associated Legendre polynomials of degree n and order m with the Schmidt semi-normalization

$$\int_0^\pi P_{n,m}(\cos\theta)P_{n',m}(\cos\theta)\sin\theta\,d\theta = 2(2-\delta_{m,0})\delta_{n,n'}/(2n+1), \tag{20}$$

where $\delta_{n,n'} = 1$ when $n = n'$, and $\delta_{n,n'} = 0$ when $n \neq n'$. (See Appendix B for a discussion of the spherical harmonic expansion of the pressure field p_s in terms of the coefficients of the expansions of T and S.)

In the case when the equatorial bulge is the sole topographic feature of the CMB to be considered, we have $h(\theta, \phi) = h_0(\theta)$, where

$$h_0(\theta) = h^c_{2,0}P_{2,0}(\cos\theta) = h^c_{2,0}\left[\frac{1}{2}(3\cos^2\theta - 1)\right]. \tag{21}$$

This gives $-3h^c_{2,0}/2$ for the difference between the equatorial and polar radii (9.5 ± 0.1 km, see above), so that

$$h^c_{2,0} = -(6.3 \pm 0.1) \times 10^3\ \text{m}. \tag{22}$$

The general expressions for (L_1, L_2) obtained when eqs (7) are combined with eqs (12–16) are quite complicated and will not be written down here (but see Appendix B). When $h(\theta, \phi) = h_0(\theta)$ given by eq. (21), the expressions simplify to the following:

$$(L_1, L_2) = -2\pi\bar\rho\Omega c^2 h^c_{2,0} \times\left[\frac{72\sqrt{3}}{35}(s^c_{2,1}, s^s_{2,1}) + \frac{32\sqrt{10}}{21}(s^c_{4,1}, s^s_{4,1})\right]. \tag{23}$$

The polar motion due to the action of geostrophic pressure forces acting on the equatorial bulge of the CMB in the case when the mantle is perfectly rigid could be derived by combining this equation with the equation obtained by setting $(L_1, L_2) = (L_1^+, L_2^+)$ in eq. (3). Alternatively, we can compare the time-series of $(L_1(t), L_2(t))$ as given by eq. (23) with those of $(L_1^+(t), L_2^+(t))$ implied by the observed polar motion through eq. (3). The results are shown in Figs 2 and 3, where in evaluating $m_1(t)$ and $m_2(t)$ we have taken

$$\bar\rho = 0.99 \times 10^4\ \text{kg m}^{-3}, \qquad \Omega = 7.29 \times 10^{-5}\ \text{rad s}^{-1},$$

$$c = 3.48 \times 10^6\ \text{m}, \qquad C^{(m)} - A^{(m)} = 2.63 \times 10^{35}\ \text{kg m}^2$$

(see e.g. Stacey 1992; Eubanks 1993), so that

$$2\pi\bar\rho\Omega c^2 h^c_{2,0} = -3.48 \times 10^{17}\ \text{kg s}^{-1}$$

and

$$[\Omega^2(C^{(m)} - A^{(m)})]^{-1} = 8.12 \times 10^{-28}\ \text{kg}^{-1}\,\text{m}^{-2}\,\text{s}^2$$

are the numerical values of these factors in eqs (23) and (3) respectively.

DISCUSSION AND CONCLUDING REMARKS

The axial component $L_3(t)$ of the net torque $L_i(t)$ on the mantle due to the action on topographic features $h(\theta, \phi)$ of the CMB of normal (pressure) stresses associated with core motions could, as shown in previous work, make a significant and possibly dominant contribution to observed decadal LOD fluctuations, even with longitudinal variations in h that are no bigger than 1 km in vertical amplitude and possibly even slightly less (Hide 1969; Jault & Le Mouël 1990; Hide *et al.* 1993). The equatorial bulge of about 10 km is likely to be the main topographic feature involved in producing the equatorial component $L(t)$ of $L_i(t)$, and it is not surprising therefore, as the calculations presented in this paper show (see Fig. 2 and Hide *et al.* 1993), that $|L(t)|$ typically exceeds $|L_3(t)|$ by a large factor. However, it is clear from Fig. 2 that $L(t)$ is about five times smaller in magnitude than the equatorial torque $L^+(t)$ inferred from the observed polar motion. Further analysis reveals that the series are uncorrelated as well.

In our study, the equatorial bulge is taken (for simplicity) to be the sole topographic CMB feature, and the resulting expression for the equatorial torque involves only the second- and fourth-degree spherical harmonic coefficients of the velocity field (see eq. 23). The second-degree harmonic clearly

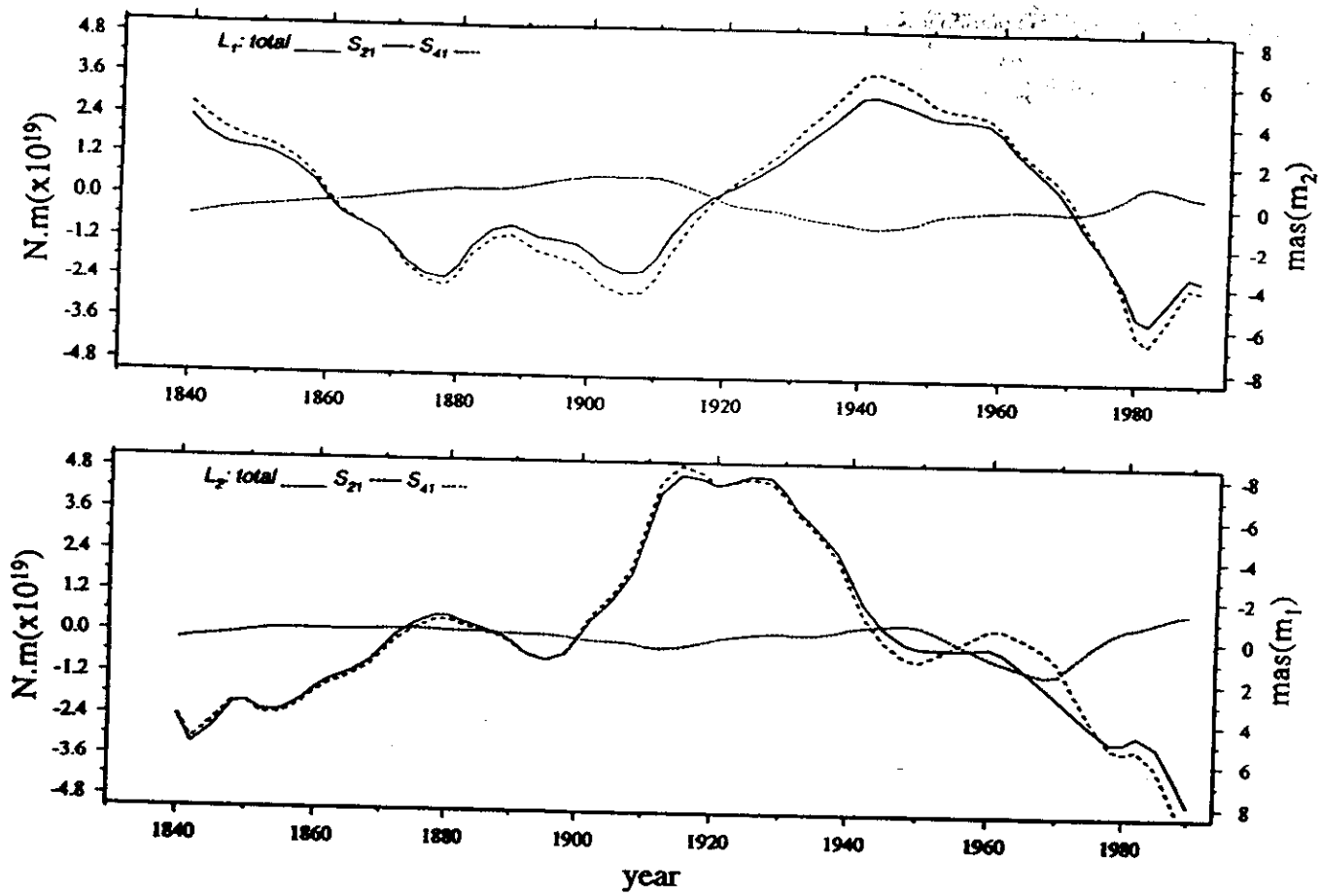

Figure 3. Time-series of the components $L_1(t)$ and $L_2(t)$ of the topographic torque produced by the action on the equatorial bulge of the CMB of normal pressure forces associated with core motions in the case of a perfectly rigid mantle (see eq. 23). Of the terms in the full spherical harmonic expansion of the pressure field (see Appendix B), only those corresponding to terms of degrees $n = 2$ and $n = 4$ in the poloidal part of the associated velocity field make non-zero contributions to $(L_1(t), L_2(t))$, namely $(L_1(t; n = 2), L_2(t; n = 2))$ and $(L_1(t; n = 4), L_2(t; n = 4))$; they are indicated in the diagram by dashed and dotted lines respectively. A low-pass filter with a cut-off period of 10 years has been applied to all time-series.

dominates (Fig. 3), so it is unlikely that uncertainties in the velocity fields used could account for the discrepancy. Our general findings concerning the inadequacy of topographic coupling in the excitation of decadal polar motions agree qualitatively with those of the above-mentioned work by Hulot *et al.* (1996) and Greff-Lefftz & Legros (1995), where effects due to irregular latitude-dependent topography, gravitational torques associated with the non-spherical shape of the CMB, and changes in the inertia tensor of the solid Earth produced by fluctuating horizontal pressure variations in the upper reaches of the core are also taken into account. The fluctuating electromagnetic torque on the mantle associated with core motions (see above) could, of course, be stronger than the topographic torque, but only under extreme assumptions concerning the (unknown) distribution and magnitude of the electrical conductivity of the lower mantle and of the toroidal part of the geomagnetic field just below the core–mantle boundary.

It is an old suggestion that the movement of air and water at and near the Earth's surface on relevant time-scales is involved in the excitation of DPM (see Wilson 1993), but quantitative studies are hard to make. The spectral characteristics of water movement are similar to that of DPM—red, and increasing sharply at decadal periods—whereas the air-mass excitation spectrum is white, i.e. flat (Kuehne & Wilson 1991). DPM observations imply an excitation showing linear polarization along the direction that would result from a uniform rise or fall of sea-level, implying that forcing is due, at least in part, to the redistribution of water mass (Wilson 1993). It will be necessary in future work, as better data become available, to re-investigate all possible excitation mechanisms, for it seems that the decadal polar motion is most likely caused by a variety of geophysical processes, with the topographic torque induced by the equatorial bulge producing a significant but not a dominant contribution.

ACKNOWLEDGMENT

This paper presents the results of one phase of research carried out at the Jet Propulsion Laboratory, California Institute of Technology, sponsored by the National Aeronautics and Space Administration. We also acknowledge helpful comments by Dr. Gauthier Hulot and an anonymous referee.

REFERENCES

Backus, G., 1968. Kinematics of geomagnetic secular variation in a perfectly conducting core, *Phil. Trans. R. Soc. Lond.*, A, 263, 239–266.
Backus, G. & Le Mouël, J.-L., 1986. The region of the core–mantle

boundary where a geostrophic velocity field can be determined from frozen-flux magnetic data, *Geophys. J. R. astr. Soc.*, 85, 617–628.

Bloxham, J. & Jackson, A., 1991. Fluid flow near the surface of the Earth's outer core, *Rev. Geophys.*, 29, 97–120.

Bondi, H. & Gold, T., 1950. On the generation of magnetism by fluid motion, *Mon. Not. R. astr. Soc.*, 110, 607–611.

Denis, C. & Ibrahim, A., 1981. On a self-consistent representation of Earth models, with application to the computing of internal flattening, *Bull. Géod.*, 55, 179–195.

Dickman, S.R., 1981. Investigation of controversial polar motion features using homogeneous International Latitude Service data, *J. geophys. Res.*, 86, 4904–4912.

Elsasser, W.M., 1939. On the origin of the Earth's magnetic field, *Phys. Rev.*, 55, 489–500.

Elsasser, W.M., 1947. Induction effects in terrestrial magnetism, Part III, Electric modes, *Phys. Rev.*, 72, 821–833.

Eubanks, T.M., 1993. Variations in the orientation of the Earth, in *Contributions of space geodesy to geodynamics: Earth dynamics*, pp. 1–54, eds Smith, D.E. & Turcotte, D.L., Am. Geophys. Un., Washington, DC.

Frenkel, J., 1945. On the origin of terrestrial magnetism, *C. R. Acad. Sci. USSR*, 49, 98–101.

Gire, C. & Le Mouël, J.-L., 1990. Tangentially-geostrophic flow at the core–mantle boundary compatible with the observed geomagnetic secular variation: the large-scale component of the flow, *Phys. Earth planet. Inter.*, 59, 259–287.

Greff-Lefftz, M. & Legros, H., 1995. Core–mantle coupling and polar motion, *Phys. Earth planet. Inter.*, 91, 273–283.

Gross, R.S., 1982. A determination and analysis of polar motion, *PhD thesis*, University of Colorado, Boulder, CO.

Gross, R.S., 1990. The secular drift of the rotation pole, in *Earth rotation and coordinate reference frames*, pp. 146–153, eds Boucher, C. & Wilkins, G.A., Springer-Verlag, New York, NY.

Gwinn, C.R., Herring, T.A. & Shapiro, I.I., 1986. Geodesy by radio interferometry: Studies of the forced nutations of the Earth 2. Interpretation, *J. geophys. Res.*, 91, 4755–4765.

Herring, T.A., Buffett, P.M., Mathews, P.M. & Shapiro, I.I., 1991. Forced nutations of the Earth: Influence of inner core dynamics. Very Long Baseline Interferometry data analysis, *J. geophys. Res.*, 96, 8259–8273.

Hide, R., 1956. The hydrodynamics of the Earth's core, *Phys. Chem. Earth*, 1, 94–137.

Hide, R., 1969. Interaction of the Earth's liquid core and solid mantle, *Nature*, 222, 1055–1056.

Hide, R., 1986. Presidential address: The Earth's differential rotation, *Q. J. R. astr. Soc.*, 27, 3–14.

Hide, R., 1989. Fluctuations in the Earth's rotation and the topography of the core–mantle interface, *Phil. Trans. R. Soc. Lond.*, A, 328, 351–363.

Hide, R., 1995. The topographic torque on the bounding surface of a rotating gravitating fluid and the excitation by core motions of decadal fluctuations in the Earth's rotation, *Geophys. Res. Lett.*, 22, 961–964 and 3563–3565.

Hide, R. & Dickey, J.O., 1991. Earth's variable rotation, *Science*, 253, 629–637.

Hide, R., Clayton, R.W., Hager, B.H., Spieth, M.A. & Voorhies, C.V., 1993. Topographic core–mantle coupling and fluctuations in the Earth's rotation, in *Relating geophysical structures and processes: The Jeffreys volume*, eds Aki, K. & Dmowska, R., *Geophys. Monog. Am. Geophys. Un.*, 76, 107–120.

Hills, R.G., 1979. Convection in the Earth's mantle due to viscous shear at the core–mantle interface and due to large-scale buoyancy, *PhD thesis*, New Mexico State University, Las Cruces.

Hinderer, J., Jault, D., Legros, H. & Le Mouël, J.-L., 1987. Geomagnetic secular variation, core motions and implications for the Earth's wobble, *Phys. Earth planet. Inter.*, 49, 121–132.

Hinderer, J., Jault, D., Legros, H. & Le Mouël, J.-L., 1990. Core–mantle topographic torque: a spherical harmonic approach and implications for the excitation of the Earth's rotation by core motions, *Phys. Earth planet. Inter.*, 59, 329–341.

Hulot, G., Le Mouël, J.-L. & Wahr, J.M., 1992. Taking into account truncation problems and geomagnetic model accuracy in assessing computed flows at the core–mantle boundary, *Geophys. J. Int.*, 108, 224–246.

Hulot, G., Le Huy, M. & Le Mouël, J.-L., 1996. Influence of core flows on the decade variations of the polar motion, *Geophys. astrophys. Fluid Dyn.*, in press.

Inglis, D.R., 1955, Theories of the Earth's magnetism, *Rev. Mod. Phys.*, 27, 212–248.

Jackson, A., 1989. The Earth's magnetic field at the core–mantle boundary, *PhD thesis*, University of Cambridge, Cambridge.

Jacobs, J.A., ed., 1987–91. *Geomagnetism* (4 volumes), Academic Press, London.

Jault, D. & Le Mouël, J.-L., 1989. Topographic torque associated with tangentially-geostrophic motion at the core surface and inferences on the flow inside the core, *Geophys. astrophys. Fluid Dyn.*, 48, 273–296.

Jault, D. & Le Mouël, J.-L., 1990. Core–mantle boundary shape: constraints inferred from the pressure torque acting between the core and mantle, *Geophys. J. Int.*, 101, 233–241.

Jault, D. & Le Mouël, J.-L., 1993. Circulation in the liquid core and coupling with the mantle, *Adv. Space Res.*, 13, 221–233.

Kuehne, J. & Wilson, C.R., 1991. Terrestrial water storage and polar motion, *J. geophys. Res.*, 96, 4337–4345.

Lambeck, K., 1980. *The Earth's variable rotation*, Cambridge University Press, Cambridge.

Le Mouël, J.-L., 1984. Outer-core geostrophic flow and secular variation of the Earth's magnetic field, *Nature*, 311, 734–735.

Le Mouël, J.-L., Gire, C. & Madden, T., 1985. Motions at the core surface in the geostrophic approximation, *Phys. Earth. planet. Inter.*, 39, 270–287.

Loper, D.E. & Lay, T., 1995. The core–mantle boundary region, *J. geophys. Res.*, 100, 6397–6420.

Merrill, R.T. & McElhinny, M.W., 1983. *The Earth's magnetic field*, Academic Press, London.

Moritz, H. & Mueller, I.I., 1987. *Earth rotation: theory and observation*, Ungar Publishing Company, New York, NY.

Munk, W.H. & MacDonald, G.J.F., 1960. *The rotation of the Earth*, Cambridge University Press, Cambridge.

Roberts, P.H. & Scott, S., 1965. On the analysis of the secular variation, 1: A hydromagnetic constraint: Theory, *J. Geomagn. Geoelect.*, 17, 137–151.

Rochester, M.G., 1984. Causes of fluctuations in the Earth's rotation, *Phil. trans. R. Soc. Lond.*, A, 313, 95–105.

Rosen, R.D., 1993. The axial momentum balance of Earth and its fluid envelope, *Surveys Geophys.*, 14, 1–29.

Stacey, F.D., 1992. *Physics of the Earth*, 3rd edn, Brookfield Press, Brisbane.

Voorhies, C.V., 1991. Coupling an inviscid core to an electrically-conducting mantle, *J. Geomagn. Geoelect.*, 43, 131–156.

Wahr, J.M., 1988. The Earth's rotation, *Ann. Rev. Earth planet. Sci.*, 16, 231–249.

Wilson, C.R., 1993. Contributions of water mass redistribution to polar motion excitation, in *Contributions of space geodesy to geodynamics: Earth dynamics*, pp. 77–82, eds Smith, D.E. & Turcotte, D.L., Am. Geophys. Un., Geodynamics Ser. Vol. 24, Washington, DC.

Wilson, C.R. & Vicente, R.O., 1980. An analysis of the homogeneous ILS polar motion series, *Geophys. J. R. astr. Soc.*, 62, 605–616.

Yumi, S. & Yokoyama, K., 1980. *Results of the International Latitude Service in a homogeneous system, 1899.9–1979.0*, Publication of the Central Bureau of the International Polar Motion Service and the International Latitude Observatory of Mizusawa, Mizusawa, Japan.

Zhao, M. & Dong, D., 1988. A new search for the secular polar motion in this century, in *The Earth's rotation and reference frames for*

geodesy and geodynamics, pp. 385–392, eds Babock, A.F. & Wilkins, G.A., Reidel, Dordrecht.

APPENDIX A: OBSERVATIONS OF POLAR MOTION

Studies of decadal variations in polar motion (see Fig. 1) rely heavily upon daily observations of the latitude of each of the five stations of the International Latitude Service (ILS), which are obtained by the technique of optical astrometry (see e.g. Yumi & Yokoyama 1980). Determinations of polar motion $(m(t), m_2(t))$ (see eq. 2) from monthly averages of these observations span the 80-year period 1899–1979. Analyses of this ILS polar-motion time-series show clear evidence of variability on decadal time scales (e.g. Wilson & Vicente 1980; Dickman 1981). The reality of this variability, however, has been called into question out of a concern about the contaminating effects of possible systematic errors occurring at individual stations (see e.g. Eubanks 1993). In particular, Zhao & Dong (1988) noticed that, when observations from the Ukiah ILS station are not used, the recovered DPM variations, although still present with about the same amplitude, are not as regular as when the polar motion is determined from all available observations. From this, they conclude that the apparent regularity of the decadal polar motion variations (i.e., the so-called 30-year Markowitz wobble) is an artefact of systematic errors in the Ukiah observations. We emphasize here that the study of Zhao & Dong (1988), although widely cited as concluding that the DPM variations are not real, in fact only questions the *regularity* of the observed variations, not their presence.

Gross (1982, 1990), recognizing the corrupting influence of systematic errors, developed a technique in which polar motion is recovered from the ILS variation of latitude observations by simultaneously solving for station-dependent systematic errors, leaving the polar-motion parameters free of such effects. The decadal variations evident in the polar-motion series that he obtained by this technique are nearly identical to that exhibited in the ILS series, leading him to conclude that these variations are real and not an artefact of systematic errors in the observations.

Space-geodetic determinations of polar motion began with the launch of the *Lageos I* satellite in 1976, May, and now span nearly 20 years. The POLE93 polar motion series analysed here is a Kalman filter-based combination of the ILS polar-motion series (spanning 1899–1979), the BIH (Bureau International de l'Heure) optical astrometric series (spanning 1962–1982), and space-geodetic polar motion measurements made by the techniques of SLR (satellite laser ranging) (spanning 1976–1993), VLBI (very long baseline interferometry) (spanning 1979–1993), and the GPS (global positioning system) (spanning 1991–1993). Since 1982, the polar motion values in POLE93 have therefore been based solely upon modern space-geodetic measurements. As seen in Figs 1 and 2, there is clear evidence of decadal-scale variability in the POLE93 polar-motion series since 1982. Furthermore, the post-1983 variability is consistent with similar-scale variability evident in this series during earlier epochs, thereby giving credence to this earlier variability.

The POLE93 series is used here since it is the most complete polar motion series currently available. The above discussion and previously cited studies indicate that the influence of systematic errors on the decadal variability evident in this series may affect the shape of the variations, but not the amplitude.

APPENDIX B: SPHERICAL HARMONIC EXPANSION OF PRESSURE FIELD

By virtue of the equivalence of eqs (4) and (5), which lead to eq. (7) for $L_i(t)$ in terms of $h(\theta, \phi)$ and $\mathbf{u}_s(\theta, \phi, t)$, it is possible to determine $L_i(t)$ without going through the stage of evaluating $p_s(\theta, \phi, t)$ directly (see Hide 1989). For the sake of completeness and other reasons, however, it is useful to relate, through eq. (6), the coefficients in the spherical harmonic expansions for $\mathbf{u}_s(\theta, \phi, t)$ (see eqs 14, 17 and 18) to those of the following expression for $p_s(\theta, \phi, t)$:

$$p_s(\theta, \phi, t) = \sum_{n=0}^{\infty} \sum_{m=0}^{n} (p^c_{n,m}(t) \cos m\phi + p^s_{n,m}(t) \sin m\phi) \times P_{n,m}(\cos\theta), \tag{B1}$$

where the $P_{n,m}(\cos\theta)$ are defined by Schmidt normalization given by eq. (20). The coefficients $p^s_{n,m}$ and $p^c_{n,m}$ can be expressed in terms of the spherical harmonic coefficients of $\mathbf{u}_s(\theta, \phi, t)$ as follows [see eqs (17) and (18); *cf.* Gire & Le Mouël (1990)]:

$$p^c_{n,m} = -2\bar{\rho}\Omega(C^{(-)}_{n,m} s^s_{n-2,m} + C^{(0)}_{n,m} s^s_{n,m} + C^{(+)}_{n,m} s^s_{n+2,m}), \tag{B2}$$

$$p^s_{n,m} = 2\bar{\rho}\Omega(C^{(-)}_{n,m} s^c_{n-2,m} + C^{(0)}_{n,m} s^c_{n,m} + C^{(+)}_{n,m} s^c_{n+2,m}), \tag{B3}$$

when $m > 0$, and

$$p^c_{n,0} = -2\bar{\rho}\Omega\left(\frac{n-1}{2n-1}\tau^c_{n-1,0} + \frac{n+2}{2n+3}\tau^c_{n+1,0}\right), \tag{B4}$$

the coefficients $s^c_{n,m}$, $s^s_{n,m}$, $\tau^c_{n,m}$, $\tau^s_{n,m}$ being equal to zero when $n < m$ and $m > 0$, in eqs (B2) and (B3).

$$C^{(-)}_{n,m} \equiv \frac{(n-1)(n-2)[(n-m)(n+m)(n-1-m)(n-1+m)]^{1/2}}{m(2n-1)(2n-3)}, \tag{B5}$$

$$C^{(0)}_{n,m} \equiv \frac{n(n+1)}{m(2n+1)}\left[\frac{(n+1-m)(n+1+m)}{(2n+3)} + \frac{(n-m)(n+m)}{(2n-1)}\right], \tag{B6}$$

and

$$C^{(+)}_{n,m} \equiv \frac{(n+2)(n+3)[(n+1-m)(n+1+m)(n+2-m)(n+2+m)]^{1/2}}{m(2n+3)(2n+5)}. \tag{B7}$$

In terms of the coefficients of pressure field, the torque acting on the main bulge at the CMB can be expressed as follows:

$$(L_1, L_2) = \frac{4\sqrt{3}\pi}{5} r^2 h_{2,0}(-p^s_{2,1}, p^c_{2,1}) \tag{B8}$$

(see Hinderer *et al.* 1990). It is readily demonstrated, using eqs (B2) and (B3), that eq. (B8) is consistent with the expression for the torque in terms of the velocity field given by eq. (23). Taking $h_{2,0}$ as $-2c\alpha_c/3$, where α_c denotes the ellipticity at CMB, our eq. (B8) is identical to the formula (22b) of Hulot *et al.* (1996).

Nonlinear Time Series and Chaos Vol. 2

CHAOS AND FORECASTING

Proceedings of the Royal Society Discussion Meeting

London 2–3 March 1994

Editor

Howell Tong

Institute of Mathematics and Statistics
University of Kent
UK

World Scientific

CHAOS and FORECASTING,
1995, ed. Howell Tong
Singapore: World Scientific
pages 175–198

CHAPTER 9

CHAOS IN GEOPHYSICAL FLUIDS

Raymond Hide
Department of Physics
(Atmospheric, Oceanic and Planetary Physics)
Clarendon Laboratory
Parks Road
Oxford OX1 3PU, England, U.K.

Abstract

Irregular buoyancy-driven flows occur in the atmospheres and fluid interiors of the Earth and other planets, and of the Sun and other stars, where they influence and often control the transfer of heat. Their presence is manifest in or implied by a wide variety of observed phenomena, including external magnetic fields generated by self-exciting magnetohydrodynamic (MHD) dynamo action. Based on the laws of classical mechanics, thermodynamics and, in the case of electrically-conducting fluids, electrodynamics, the governing mathematical equations are well known, but they are generally intractable owing to their essential nonlinearity. Computers play a key role in modern theoretical research in geophysical and astrophysical fluid dynamics, where ideas based on chaos theory are being applied in the analysis of models and the assessment of predictability. The aim of this paper is to provide a largely qualitative survey for non-specialists. The survey comprises two parts, namely a general introduction (Part I) followed by a discussion of two representative areas of research (Part II). Each of these areas is concerned with phenomena attributable to symmetry-breaking bifurcations caused by gyroscopic (Coriolis) forces, namely (a) large-scale waves and eddies in the atmospheres of the Earth, Jupiter and other planets (where, exceptionally, laboratory experiments have been influential), and (b) MHD dynamos. Various combinations of Faraday disk dynamos have been studied numerically as low-dimensional nonlinear electromechanical analogues of MHD dynamos, particularly in efforts to elucidate the complex time series of geomagnetic polarity reversals over geological time. The ability of the intensively-studied Rikitake coupled disk dynamo system to behave

chaotically appears to be a consequence of the neglect of mechanical friction, the inclusion of which renders the system structurally unstable.

Part I: General introduction

1. Buoyancy-driven flows

Flows in the atmospheres and interiors of the Earth and other planets and of the Sun and other stars are driven by buoyancy forces due to the action of gravity on spatial variations of density. These density variations are associated with temperature variations produced and maintained by differential heating and cooling, and they are modified by variations in pressure and chemical composition. Through their ability to transport ("advect" or "convect") heat in both horizontal and vertical directions such fluid flows influence and often control the overall heat balance and evolution of the systems within which they occur.

Buoyancy-driven flows derive their kinetic energy from gravitational potential energy, with heavier fluid tending to sink and lighter fluid to rise. Concomitant advection of heat in the vertical is always in the upward direction (unless the thermal coefficient of cubical expansion of the fluid is negative). Upward advection of heat by large-scale waves and jet streams in the lower reaches of the Earth's atmosphere–the troposphere–helps to maintain the vertical temperature gradient there at a value somewhat less than the adiabatic value. This in turn influences the scales and other characteristics of tropospheric flows, thereby providing a dynamically-important feedback mechanism. Horizontal advective heat transfer by this flow–and also by the currents driven in the underlying oceans by atmospheric surface winds and by buoyancy forces–keeps the equator-to-pole temperature difference at the Earth's surface at a fraction of the radiative equilibrium value that would otherwise obtain in order to balance differential solar heating.

The two general conditions for the occurrence of stable hydrostatic equilibrium–with no fluid flow and buoyancy forces everywhere balanced by pressure gradients alone (see (2.1) below) – are quite strict. The first is that density gradients nowhere possess a horizontal component, for otherwise fluid elements would experience gravitational torques, which cannot be balanced by pressure gradients. The second is that the vertical density gradient is either (a) "bottom heavy" (i.e. the "potential density" nowhere increases upwards (implying that the actual density everywhere decreases upwards at a rate less than the so-called "adiabatic gradient", which vanishes when the fluid is incompressible), or (b) "top- heavy" but of insufficient magnitude for buoyancy forces to be able to promote instability against inhibiting effects due to viscosity, thermal conduction and radiation, and also to gyroscopic (Coriolis) forces when the whole system is in general rotation, and to Lorentz forces when the fluid can conduct electricity and magnetic fields are present. When the first of these conditions is satisfied but the second is not, convection of the Rayleigh-Bénard type occurs, such

as the flow that gives rise to the "granular" appearance of the solar photosphere. Another example of Rayleigh - Bénard convection is the very slow flow – centimetres per year – in the highly viscous mantle of the Earth that geophysicists invoke to account for heat transfer there and also for various tectonic and other processes manifest in geophysical and geological data. When the second condition is satisfied but first is not, as in extensive regions of the atmospheres of the Earth and other planets, where the vertical density gradient is "bottom heavy" but there are impressed horizontal density gradients, flow must always occur no matter how small the magnitude of these gradients. Many factors determine the form and speed of the flow, and in the important case when Coriolis forces exert a dominant influence, the process of "sloping convection" can occur, in which the typical trajectory of a fluid element is inclined at an angle to the horizontal less than the slope of the surfaces of equal potential density. Through their differential action on the axial and non-axial components of the flow velocity vector, Coriolis forces tend to promote sloping convection, which is the dominant large-scale dynamical process in the extra-tropical regions of the Earth's atmosphere.

Irregularity characterizes the spatio-temporal behaviour of geophysical (and astrophysical) fluids, as evinced by both direct and, more commonly, indirect observations (see below). Attempts to interpret the observations in terms of underlying fluid - dynamical processes or to predict future behaviour require in the first instance the separation of manifestations in the data of effects due to random forcing (noise) of various kinds from any that might be attributable to deterministic chaos. The "predictability horizon" of a system exhibiting irregular behaviour depends *inter alia* upon the extent to which the underlying processes are dominated by deterministic chaos rather than by noise. In principle it should be possible to identify deterministic chaos in observational time series, by using sophisticated modern methods (see e.g. Drazin and King 1992, Ghil *et al.* 1991 Moon 1987, Mullin 1993, Ott 1993, Smith 1988, 1992, 1994, Thompson and Stewart 1986) developed for adducing evidence of low-dimensional attractors in the data. This can often be done in investigations of well-controlled laboratory systems (see e.g. Guckenheimer and Buzyna 1983, Haken 1981, Mullin 1993, Read 1993, Read *et al.* 1992), but it is more difficult or even impossible in the study of observational time series from geophysical and astrophysical fluids and other natural systems, owing to the inadequate length of available time series and to measurement errors. So other kinds of evidence for chaos must be sought, such as that afforded by constructing models of the prototype with varying degrees of simplification (see Section 2 below) and analyzing their behaviour. The clear identification in the prototype of regimes of behaviour determined by bifurcations at critical values of key parameters as revealed by the models would be evidence for chaos.

Optimism – albeit limited – shown by workers concerned with basic problems of predictability of the terrestrial atmosphere (see e.g. Ghil *et al.* 1991, Lorenz 1963, 1967, 1980, 1993, Mason *et al.* 1986, Monin 1972, Mullin 1993, Nicolis and Nicolis 1987, Palmer *et al.* 1994, Thompson, 1957, 1988, Webster and Keller 1975, White 1990) derives to some extent from the practical experience of weather forecasters and climatologists. Also influential according to the literature have been laboratory

experiments such as those carried out on sloping convection in a rotating fluid annulus subject to a steady axisymmetric temperature gradient (Hide 1953). In these experiments key parameters were identified and several flow regimes of varying degrees of spatial and temporal complexity were first delineated, ranging from steady axisymmetric flow through periodic and quasi-periodic non-axisymmetric flows to highly irregular "geostrophic turbulence". The quasi-periodic wave-like flows discovered in these experiments and termed "vacillation" have attracted some attention, but they have not yet been reproduced in satisfactory detail in numerical models (see e.g. Hignett *et al.* 1985, Lorenz 1963 (b), Quinet 1973, Thompson, 1988, White 1988). Elsewhere in this volume, Palmer *et al.* (1994) explain how modern ideas in the theory of deterministic chaos are guiding meteorologists armed with very powerful computers and highly sophisticated numerical models of the troposphere and the overlying stratosphere in their efforts to monitor global-scale atmospheric flow and forecast its future behaviour. Underlying such exercises is the implicit recognition of the possibility "intransitivity" and "multiple equilibria" (in modern parlance) (see Hide 1953) as well as other manifestations of essentially nonlinear and possibly chaotic behaviour such as hysteresis (see Fultz *et al.* 1959) in atmospheric flows. (For further references to laboratory studies and related work, see e.g. Buzyna *et al.* 1984, Ghil and Childress 1987, Hart 1986, Hide 1977, Hide and Mason 1975, Lewis 1992, Read 1988, Read *et al.* 1992, Smith 1994 and articles in Corby 1969, Hopfinger 1992, King and Mobbs 1991, Mullin 1993 and Roberts and Soward 1978.)

Owing to public demands for weather and climate forecasts, meteorologists enjoy abundant observations of wind velocity, pressure, temperature and other variables of direct dynamical relevance, collected frequently and systematically at many levels over the whole globe, and made available rapidly in "user friendly" form, making meteorologists the envy of workers in other areas of geophysical and astrophysical fluid dynamics. And for studying temporal fluctuations in one particularly important and revealing average property of the global atmospheric circulation, namely the total angular momentum, accurate surrogate data can be deduced from geodetic observations of fluctuations in the Earth's rotation vector (see Hide 1984, Hide and Dickey 1991, Rosen 1993). But in other areas of geophysical fluid dynamics such as the study of the atmospheres of other planets, observations are usually indirect in nature and of more restricted coverage in space and time, as they also are in studies of the oceans and of the Earth's atmosphere on the long time scales of interest to climatologists (see e.g. Berger *et al.* 1989, Ingersoll 1990, Ingersoll and Lyons 1993, James 1994, Neelin *et al.* 1994, Philander 1992, Saltzman and Verbitsky 1993, Sreenath 1993, Willebrand and Anderson 1993).

In the study of magnetohydrodynamic (MHD) flow in the Earth's liquid metallic core, where the main geomagnetic field is produced by self-exciting MHD dynamo action, the main observational data comes from magnetic measurements made at or near the surface of the Earth (see e.g. Jacobs 1987–91, 1994, Melchior 1986, also Part II below). Magnetic observations also provide the basis for studies of MHD flows in the electrically-conducting deep interiors of other planets such as Jupiter, Saturn, Uranus and Neptune and in the outer layers of the Sun (see e.g. Ness 1994,

Proctor and Gilbert 1994, Sonett *et al.* 1991, Stevenson 1983.) Additional data in the case of the Sun comprise a long time series of annual sunspot numbers, which exhibits nearly periodic oscillations with a dominant period of about eleven years. In the interpretation of these observations in terms of basic fluid-dynamical processes, highly simplified models analyzed by methods suggested by chaos theory are being applied with some success (e.g. Platt *et al.* 1993, Ruzmaikin *et al.* 1994, Weiss 1990, 1993, 1994).

Many essentially nonlinear phenomena are encountered in astronomy and geophysics (see e.g. Turcotte 1993), including earthquakes, the prediction of which is the topic of another paper in this session (Matsuzaki 1994). In the Part II of this article on chaos in geophysical fluids, two topics are selected for more detailed discussion, namely the study of (a) large-scale motions in planetary atmospheres, where laboratory studies have played a useful role, and (b) planetary magnetism, with emphasis on polarity reversals of the main geomagnetic field where theoretical work has to rely on mathematical modelling alone. The article reflects my own personal scientific interests and point of view. In preparing it I have relied heavily on my research library. This includes many reprints of papers from a wide range of journals, which colleagues have kindly sent to me over a period of more than forty years. A full bibliography citing all relevant original references would run to the editorially-unacceptable length of more than two hundred items, so I have included a selection of books, monographs and review articles where these original references can be found. Also it is impossible to reproduce here the many pictures and diagrams used to illustrate the lecture upon which this article is based.

2. Basic equations and modelling

Applying Newton's laws of motion to a fluid element of unit volume which at time t is located at the general point whose vector position is $\mathbf{r}$ in the chosen inertial frame of reference gives the equation

$$\rho\, D\mathbf{u}/Dt = -\nabla p - \rho\nabla V + \mathbf{F}\,. \tag{2.1}$$

Here ρ denotes the mass density of the fluid at P, $\mathbf{u}$ is the Eulerian flow velocity, and the operator

$$D/Dt \equiv \partial/\partial t + \mathbf{u}\,.\nabla \tag{2.2}$$

is the "substantial" time derivative following the moving fluid element. ∇p is the gradient of the pressure p, $-\nabla V$ is the acceleration due to gravity, and $\mathbf{F}$ represents all the other forces acting on the fluid element, including viscosity. In the case of electrically - conducting fluids, with which the subject of MHD is concerned, $\mathbf{F}$ also includes the Lorentz force $\mathbf{j} \times \mathbf{B}$ where $\mathbf{j}$ is the electrical current density at P and $\mathbf{B}$ the magnetic field. Continuity of matter is expressed by the equation

$$D\rho/Dt + \rho\nabla.\mathbf{u} = 0. \tag{2.3}$$

All these quantities, ρ, $\mathbf{u}$, p, V, $\mathbf{j}$ and $\mathbf{B}$ are in general functions of $\mathbf{r}$ and t. Equations (2.1) and (2.3) effectively comprise four scalar partial differential equations in twelve

scalar unknowns, namely ρ, p and V and the individual components of the three-dimensional vectors u, **B** and j, so additional equations are needed. When ∇V is variable the law of gravity is used to relate ρ and V; and when ρ is variable an equation of state relating ρ at P to the pressure p, entropy S, composition K and temperature T etc., is needed, together with transport equations for S, K, and T. These include the equation

$$(\partial/\partial t + \mathrm{u}.\nabla)(\rho cT) = J \tag{2.4}$$

expressing the heat balance of a fluid element of unit volume at P if c is the specific heat. Here the term $\mathrm{u}.\nabla(\rho cT)$ represents the contribution of advection to the heat balance and J represents all other contributions, including conduction and radiation.

Finally, in the case of MHD flows in electrically-conducting fluids, such as those found in planetary interiors and in stars, we need the equations of electrodynamics applied to a moving medium. These relate u, j and **B** implicit in (2.1) and bring in further variables such as the electric field vector **E** and the electric charge density θ at P. In the case of non-relativistic flows, **B** and j are related by Ampére's law $\nabla \times (\mathbf{B}/\mu) = \mathrm{j}$ (where μ is the magnetic permeability) and the other equations of electrodynamics (expressing the laws of Gauss, Faraday, etc.), which lead to the following equation involving the time rate of change of **B**:

$$\partial \mathbf{B}/\partial t - \nabla(\mathrm{u} \times \mathbf{B}) = -\nabla \times (\sigma^{-1}\nabla \times (\mu^{-1}\mathbf{B})) + \nabla \times \mathbf{Z}. \tag{2.5}$$

(cf. Moffatt 1978, Parker 1979). Here σ and **Z** are defined by a generalized Ohm's law applied to a moving medium:

$$\mathrm{j} = \sigma[\mathbf{E} + \mathrm{u} \times \mathbf{B} + \mathbf{Z}]. \tag{2.6}$$

The full set of nonlinear partial differential equation (PDE's) thus obtained is complete. In addition to c, μ and σ (see (2.3) and 2.5)), the equations include other coefficients needed to specify the physical properties of the fluid at a general point P at time t such as the coefficient of viscosity, thermal coefficient of cubical expansion, ratio of principal specific heats, coefficients of thermal conductivity, chemical diffusion, dielectric constant, etc. The mechanical, thermal and electromagnetic boundary conditions under which these equations must be solved in specific cases are also well known, at least in principle. They usually amount to the requirement that all dependent variables and their derivatives as well as certain fluxes be continuous everywhere. It follows that theoretical fluid dynamics is not handicapped primarily by incomplete knowledge of the basic equations to be solved! It is the intractability of these equations owing to their essential nonlinearity that causes the main difficulties. Nonlinearity can arise in important cases from the boundary conditions or from spatial and temporal variability in the various parameters such as viscosity in the governing equations. More commonly however it is advection that it is responsible, as expressed by the terms $(\mathrm{u}.\nabla)\mathrm{u}$, $(\mathrm{u}.\nabla)\rho$, $(\mathrm{u}.\nabla)(\rho cT)$ and $(\mathrm{u}.\nabla)\mathbf{B}$ implicit or otherwise on the left-hand sides of (2.1), (2.3), (2.4) and (2.5) respectively. In spite of these difficulties, thanks

to powerful modern computers and a wide range of new techniques in laboratory studies, where computers can be used in the control of apparatus and the analysis of data, the subject of fluid dynamics continues to develop as a lively branch of classical physics with many applications in engineering, geophysics and astronomy.

All mathematical modelling based on the above equations involves the simplification of both the equations and the boundary conditions governing the prototype being studied, and there is an art in constructing such models. In all cases the most sophisticated models such as those now used in numerical weather prediction involve minimal simplifications, still resulting in P.D.E's to be solved for all dynamical variables. At the other extreme are very highly simplified "low-dimensional" models governed by ordinary differential equations (O.D.E.s) usually expressing the time evolution of mean quantities such as spatially averaged velocity, temperature, magnetic field, etc. (see e.g. Lorenz 1963a, Moore and Spiegel 1966). Such models might be trustworthy when they are derived by rational arguments from the full P.D.E's, but the most highly simplified models used in the study of the behaviour of nonlinear systems can be irrational ones, for they are often based to some extent on intuition, giving errors which are hard to assess. Analyses of such models provide results which might be helpful with diagnostic studies of more complicated systems, but they always carry a "health warning". Nevertheless, in the right hands findings based on low-dimensional models can be brought to bear on truly quantitative studies of the prototype, just as metaphysical ideas, though non-scientific, can influence truly scientific work! The most favourable situation arises when the investigator has at his disposal the results not only from numerical integrations of a range of mathematical models but also from relevant laboratory studies. Recent books (e.g. Cvitanović 1984, Haken 1981, Mullin 1993) discuss examples of thermally-driven Rayleigh - Bénard convection and sloping convection (see Section 1 above and Part II below) and mechanically-driven motions such as Taylor-Couette flow. Useful numerical integrations were not available before high-speed computers were introduced and guidance then had to be sought solely from laboratory experiments and from limited and sometimes misleading findings based on linearized models.

There is also an art in the exploitation of results from mathematical or laboratory models in research on much more complicated and uncontrollable natural systems. In his celebrated monograph on the general circulation of the Earth's atmosphere, Lorenz (1967) devotes a whole chapter to the discussion of the results of laboratory experiments on sloping convection in cylindrical apparatus (see also Lorenz 1993). To paraphrase his concluding remarks, the laboratory experiments tell us more about planetary atmospheres in general than about the Earth's atmosphere in particular. They indicate the variety of flow patterns that can occur and the conditions favourable to each of these. Perhaps the most important contribution of laboratory experiments to the theory of the general circulation of the terrestrial atmosphere has been the separation of essential considerations from the minor and irrelevant. Condensation of water vapour, for example, may yet play an essential role in the Tropics but in temperate latitudes it appears to be no more than a modifying influence, since systems occurring in the atmosphere, including even cyclones and fronts, are found in the

laboratory system, where there is no analogue of the condensation process. Similar remarks apply to the topographic features of the Earth and the so-called "beta" effect (which represents the latitudinal variation of the Coriolis parameter associated with the near-spherical shape of the Earth) now appears to play a lesser rôle than had once been supposed by theoreticians. Certainly a numerical weather forecast would fail if the beta-effect were disregarded, but the beta-effect does not seem to be required for the development of typical atmospheric systems. The experiments emphasise the necessity for truly quantitative considerations. At the very least these must be sufficient to place the Earth's atmosphere in one of the régimes discovered in the experiments.

Most of the experiments to which he refers were carried out in the early 1950's (for references see e.g. Corby 1969, Hide and Mason 1975), but there have been many subsequent related studies (see e.g Drazin and King 1992, Guckenheimer and Buzyna 1983, Hide *et al.* 1994, Hignett *et al.* 1985, Hopfinger 1991, King and Mobbs 1991, Lorenz 1963, Nicolis and Nicolis 1987, Ott 1993, Quinet 1974, Read 1993, Read *et al.* 1992, Smith 1988, 1992, 1994, White 1988, 1990.) Modern work on sloping convection is based on the powerful combination of laboratory experiments and numerical models, and it is able to exploit some of the new methods of signal processing and time-series analysis to which chaos theory has given rise (see Section 1 above). In such work, where in the search for "low-dimensional attractors" in the output of transducers recording the behaviour of a system the acquisition of long time-series of high signal-to-noise ratio data is crucial, numerical models and laboratory models clearly have a key rôle to play. As already mentioned in Section 1, observational time series from natural geophysical fluid systems are usually much too noisy and limited in duration for chaos theory to be directly applicable in their interpretation.

Just as in meteorology it is of interest to know what the atmospheric general circulation would be like in the absence of various complicating effects such as the presence of continents and oceans, water vapour in the atmosphere, time-varying thermal forcing, etc. in the boundary conditions, a central question in geomagnetism concerns the extent to which it might be necessary to invoke complex thermal, mechanical and electrical boundary conditions imposed on the Earth's liquid metallic fluid core by very slow flow occurring in the highly viscous overlying mantle in order to account for observations such as the highly-variable frequency of polarity reversals of the main geomagnetic field. Should polarity reversals be regarded as being "forced" by irregular and fluctuating boundary conditions, or as an manifestation of "free" instabilities that would occur under simple and fixed boundary conditions? Modern research indicates that details of the pattern of the geomagnetic field at the surface of the Earth are manifestations of both "forced" and "free" processes. Edmond Halley raised money from the Crown at the end of the seventeenth century for the purpose of mapping this pattern (see Chapman 1941) with a view to predicting future changes, before the invention of the marine chronometer effectively solved the main practical problem which Halley had in mind, namely the accurate determination of geographical longitude at sea.

The very existence of the durable Great Red Spot in the atmosphere of Jupiter – more than three centuries after its discovery by Robert Hooke in 1665 – and of other long-lived dynamical features in the atmospheres of the major planets must have implications for theories of atmospheric predictability. Why are there more of these markings in the southern hemisphere of Jupiter than in the northern hemisphere? What is the rôle of these eddies in the heat balance of the atmosphere? To what extent should the eddies be regarded as "free" or "forced", and what (if any) is their relationship to the field of transient eddies within which they are embedded? Can we infer the vertical structure of Jupiter's atmosphere (or even just its depth) from the flow at the observable upper level? These and many other related questions pose key problems in the essentially nonlinear dynamics of geophysical fluids.

3. Symmetry breaking, heat transfer by geostrophic and magnetostrophic flows, and elastoid oscillations

It is inconvenient to use (2.1) when dealing with fluid flow in planets and stars, which usually rotate rapidly relative to an inertial frame. Owing to the rotation of the solid Earth with a period of 24 hours, points on the equator move in space at a speed some 40 times the typical speed (10 ms^{-1}) of atmospheric winds relative to the Earth's surface. The corresponding factor for ocean currents is even higher, about 4,000, and for the Earth's liquid metallic core it is higher still, about 10^6. For motions in the atmosphere of Jupiter, a planet with a diameter ten times that of the Earth and a rotation period as short as ten hours, the factor is more than 40. And even for the Sun, with a rotation period as long as a month but a diameter ten times that of Jupiter, linear speeds of rotation greatly exceed typical relative speeds of large-scale atmospheric flow. So we must refer our dynamical equations to a more convenient reference frame.

If we choose a frame that rotates steadily with angular velocity $\mathbf{\Omega}$ relative to an inertial frame, (2.1) has to be modified by adding the so-called Coriolis force $2\rho\mathbf{\Omega}\times\mathbf{u}$ to the left-hand side and replacing $-\nabla V$ by $\mathbf{g}$, which now includes centripetal effects. When $\mathbf{\Omega}$ is so large in magnitude that $|\,2\rho\mathbf{\Omega}\times\mathbf{u}\,|$ greatly exceeds the terms $|\,\rho\partial\mathbf{u}/\partial t\,|$ and $|\,\rho(\mathbf{u}.\nabla)\mathbf{u}\,|$ on typical time and space scales of the whole system, to a first approximation we can write

$$2\rho\mathbf{\Omega}\times\mathbf{u}\approx\mathbf{\Gamma}+\mathbf{F} \tag{3.1}$$

where

$$\mathbf{\Gamma}\equiv-\nabla p+\mathbf{g}\rho. \tag{3.2}$$

When $|\,\mathbf{F}\,|\ll|\,2\rho\mathbf{\Omega}\times\mathbf{u}\,|$, (3.1) reduces to

$$2\rho\mathbf{\Omega}\times\mathbf{u}\approx\mathbf{\Gamma}, \tag{3.3}$$

which expresses approximate "geostrophic" balance between Coriolis forces and dynamic pressure gradients in the horizontal. To a good approximation, large-scale flows occupying extensive regions in the oceans and in the atmospheres of the Earth and other planets (with the exception of slowly-rotating Venus) are either found or expected to be in geostrophic balance nearly everywhere. Exceptional regions are near

the equator, where the vertical component of Ω vanishes, and within narrow "fronts" and jet streams, where the nonlinear advective term $\rho(\mathbf{u}.\nabla)\mathbf{u}$ is typically comparable with $2\rho\Omega \times \mathbf{u}$ in magnitude. Indeed, the existence of such "detached shear layers" in rapidly - rotating fluids is implied by (3.3), which, being of lower order than the full equation, is diagnostic in character rather than prognostic, and therefore incapable of giving solutions that satisfy all the necessary boundary conditions (see Hide 1977). When the Lorentz force $\mathbf{j} \times \mathbf{B}$ makes the dominant contribution to $\mathbf{F}$ in (3.1) and is not negligible in magnitude in comparison with the Coriolis term, the equation becomes:

$$2\rho\Omega \times \mathbf{u} \approx \Gamma + \mathbf{j} \times \mathbf{B} \qquad (3.4)$$

This diagnostic equation expresses "magnetostrophic" balance of forces acting on individual fluid elements. Such balance nearly everywhere may be the main property that characterizes large-scale MHD flows in the electrically-conducting deep interiors of the planets, and also in the Sun and other stars.

Equation (3.3) is the basis of the meteorologist's "Buys-Ballot law" – stand with your back to the wind in the northern (southern) hemisphere and the low pressure is found to be on the left (right)! It follows from (3.3) that if the pattern of fluid flow $\mathbf{u}$ and the associated fields of p and ρ are symmetric about the axis of rotation, then the component of $\mathbf{u}$ perpendicular to the rotation axis is everywhere zero. This implies that any flow that is both axisymmetric and geostrophic cannot advect heat (or any other quantity) in directions that are perpendicular to the rotation axis. Such flows would therefore make no contribution to the overall heat balance of systems subject to axisymmetric applied heating and cooling. This result suggests, and experience based on many detailed studies of rapidly rotating laboratory systems and natural systems confirms (see Hide 1977), that large-scale non-axisymmetric flow capable of advecting heat perpendicularly to the rotation axis would develop in "generic" (i.e. typical) cases. We thus see a connection between the basic function of thermally-driven flows – namely heat transfer – and symmetry breaking which, from a theoretical point of view, can be associated with bifurcations produced by the action of Coriolis forces when $|\ \Omega\ |$ is large enough.

This symmetry breaking associated with geostrophy and heat transfer in generic systems provides a good starting point in the discussion of the role of rotation in the production of magnetic fields by MHD dynamo action in astronomical bodies such as the Earth and other planets (see Hide 1982). By a theorem due to Cowling and others (for references see Proctor and Gilbert 1994) no magnetic field with an axis of symmetry can be maintained by fluid motions against ohmic dissipation, so that a strictly axisymmetric pattern of fluid motion $\mathbf{u}$ and magnetic field $\mathbf{B}$ would be incapable of dynamo action. It is only possible to find non-decaying solutions to (2.5) (with $\mathbf{Z} = 0$) when the configuration of $\mathbf{B}$ has no axis of symmetry.

A magnetic field produced by self-exciting dynamo action can be regarded as having originated as an instability involving the amplification of a much weaker adventitious field through inductive action produced by fluid motion. Equilibration occurs when on average the rate at which buoyancy forces do work on the system is

balanced by ohmic and other types of energy dissipation. When the magnetic field is so weak that Lorentz forces are negligible, quasi-geostrophic non-axisymmetric flow is expected to occur. Dynamo action then amplifies the magnetic field, and various lines of evidence indicate that the field strength would typically build up until $\mathbf{j} \times \mathbf{B}$ is comparable in magnitude with $2\rho\Omega \times \mathbf{u}$ (see (3.3) and (3.4)), a process by which geostrophic balance gives way to magnetostrophic balance.

We now turn to an important general property of geophysical fluids which bears directly on their response to any kind of forcing, namely their ability to support wave motions and oscillations in which material particle displacements possess components parallel to the wave fronts (see e.g. Acheson and Hide 1973, Gill 1984, Hide and Stewartson 1972, Lighthill 1978). Ordinarily, the essential mechanical difference between a fluid and a solid is the inability of the former to resist an applied shear stress, rendering it unable to transmit energy and information by shear waves. But "elastoid" shear oscillations are possible in geophysical fluids owing to the action of Coriolis forces, Lorentz forces and, when the density distribution is "bottom heavy", buoyancy (Archimedes!) forces, associated respectively with general rotation, the presence of magnetic fields, and gravity. Elastoid oscillations are often generated by internal instabilities, and their properties, which include anisotropy and dispersion, are influenced by mutual interactions and by interactions with background flows and bounding surfaces. Nonlinear effects do not always increase the degree of disorder in a system, for in the remarkable soliton phenomenon nonlinear advection exactly cancels effects due to linear wave dispersion.

The elastoid oscillations encountered in studies of the oceans and of the atmospheres of the Earth and other planets include the so-called Rossby waves and Kelvin waves. Complex interactions between waves involving Coriolis and buoyancy forces and generated by internal instabilities are also seen in the non-axisymmetric flow régimes investigated in laboratory work on sloping convection. Even richer in variety are the elastoid oscillations encountered in studies of the electrically - conducting fluid interiors of planets and stars, where Lorentz forces arise. Of particular importance in magnetohydrodynamics is a special class of slow quasi-magnetostrophic oscillations in which Lorentz and Coriolis forces act in opposite directions. In the liquid metallic core of the Earth, the time scales of such oscillations could be comparable with those characteristic of the geomagnetic secular variation (decades to centuries), observations of which have been studied, often with a view to prediction, by geophysicists since the times of Halley and other early investigators (see Section 1 above).

This concludes the general introduction to chaos in geophysical fluids (see Hide 1994). In Part II below, two representative areas of research are discussed, both concerned with phenomena attributable to symmetry-breaking bifurcations caused by gyroscopic (Coriolis) forces. These are (a) waves and eddies in the atmospheres of the Earth, Jupiter and Saturn (where, exceptionally laboratory experiments have been influential), and (b) MHD dynamos, where effective laboratory experiments are not technically feasible.

Part II: Two representative areas of research

4. Sloping convection as a paradigm for large-scale waves and eddies in planetary atmospheres

Having presented a general introduction to research on chaotic flows in geophysical fluids we now turn to the first of two representative areas chosen for more detailed discussion (see summary above), namely large-scale waves and eddies in the atmospheres of the Earth, Jupiter and other planets. An important aim of research on motions in planetary atmospheres is to identify dynamical processes capable of accounting for the observations. To this end are needed *inter alia* investigations of model planetary atmospheres in which all the key parameters such as chemical composition, differential heating and cooling, size and rotation rate of the planet, mechanical and thermal conditions at bounding surfaces, etc. are varied systematically, and the findings compared with available observations of the actual planets. Comparatively few atmospheric scientists are engaged in such activities (see e.g. Ingersoll 1990, James 1994, Williams 1979), but there are signs that in future research such models and even better ones will be used to identify régimes of behaviour determined by bifurcations at critical values of basic parameters. This will be an important step in predictability studies where evidence of deterministic chaos must be sought (see Section 2 of Part I). In areas where they can be trusted, numerical models have obvious advantages in diagnostics studies over laboratory experiments, and the powerful combination of laboratory and numerical studies has contributed significantly to geophysical fluid dynamics during the past two decades and holds out great promise for future work as computers become even more effective (see e.g. Hignett *et al.*, 1985, White 1988). But it is worth recording that in spite of these advances, some of the main findings of laboratory experiments (see Part I) have not yet been reproduced satisfactorily in numerical models.

In the original annulus experiments (see Part I), where heat entered the systems by conduction *via* one of the side walls and left *via* the other side wall, non-axisymmetric upper level flows take the form of a jet-stream undulating in a wave-like pattern touching each side walls at m points, where m is the number of waves in the azimuthal direction. Theoretical considerations of the nature of this pattern led to a systematic attempt to change it by altering the thermal boundary conditions, in a series of experiments requiring the use of a fluid annulus subject to internal heating (for references see Hide and Mason 1975, Lewis 1992). With internal heating there are three important cases to consider, namely when all the heat is extracted *via* the inner wall, *via* the outer wall, and *via* both walls at roughly equal rates. In the first and second of these cases, the pattern consists of m waves extending as before across the annulus plus m eddies situated near the insulated wall (where no heat is extracted). In the third case, the waves are absent and the m eddies extend across the annulus. In all cases the eddies circulate in an anticyclonic sense (at the top surface). In accordance with the ideas being tested, cyclonic eddies are thermodynamically impossible in this case of internal heating and side-wall cooling, since they would have to be associated with a temperature gradient that would result in conductive heat flow *away* from the imposed sink of heat. By the same arguments in the case of *internal* cooling and side-wall heating all motions would be reversed: in particular the upper level eddies would then circulate in a *cyclonic* sense.

The waves and eddies are seen as playing a crucial rôle in two processes, namely the conversion of potential energy into kinetic energy and the horizontal advection of heat. They must also advect heat vertically upwards (see Section 1 above), a process which enables the system to control the horizontal scales of motion. The proposal that large oval atmospheric eddies on Jupiter and Saturn including Jupiter's anticyclonic Great Red Spot (GRS) and White ovals and the cyclonic "barges", are all manifestations of sloping convection has led to a variety of new investigations (for references see Hide *et al.*, 1994), all carried out with the aim of testing the proposal and extending our knowledge of sloping convection. It might seem surprising that dynamically-similar phenomena can be produced on length scales differing by such large factors, up to about 10^8, but quite general considerations of the processes that produce sloping convection can account for this similarity (see Hide 1977, Hide *et al.*, 1994). Central to these considerations is first the recognition that the flow in the main body of the fluid is nearly geostrophic almost everywhere. This requires that the so-called Ekman number ε_1 and Rossby number ε_2 satisfy

$$\varepsilon_1 \ll 1 \quad \text{and} \quad \varepsilon_2 \ll 1 \tag{4.1}$$

Here

$$\varepsilon_1 \equiv \nu/2\Omega \ \min\,(L^2, D^2) \ \text{and} \ \ \varepsilon_2 \equiv U/L\Omega \tag{4.2}$$

where ν is a measure of the effective coefficient of kinematic viscosity, U is a typical flow speed, $\Omega \equiv \mid \mathbf{\Omega} \mid$ and L and D are characteristic horizontal and vertical length-scales respectively. The other main consideration concerns the so-called Brunt-Väisälä frequency N with which a vertically-displaced fluid element would oscillate in a stably-stratified (i.e. bottom heavy) atmosphere in the absence of forces other than buoyancy forces. The essential balance of terms in the governing equations implies that

$$2\Omega L/ND \sim 1. \tag{4.3}$$

In the case of the Earth's atmosphere we can take $L \sim 3 \times 10^6 m$, $2\Omega \sim 10^{-4} s^{-1}$, $N \sim 2 \times 10^{-1} s^{-1}$ (the corresponding period $2\pi/N \sim 300$s) and $D \sim 10^4$m, we have $2\Omega L/ND \sim 1.5$. For typical laboratory experiments with quasi-geostrophic flows, $L \sim 10^{-1}$m, $2\Omega \leq 10 s^{-1}$, $0.1 s^{-1} \leq N \leq 1 s^{-1}$ and $3 \times 10^{-2}\text{m} \leq D \leq 3 \times 10^{-1}$m, the corresponding range of $2\Omega L/ND$ being $0 < 2\Omega L/ND \leq 300$, which includes values characteristic of all planetary atmospheres! For the South Tropical Zone of Jupiter's atmosphere, where the Great Red Spot is situated, we have $L \sim 10^7$m and $2\Omega \sim 10^{-4} s^{-1}$, so that $ND \sim 10^3 \text{ms}^{-1}$ if $2\Omega L/ND \sim 1$. This is not an outlandish value of ND but the extent to which it is consistent with observations is hard to judge, for little is known about the vertical structure of the Great Red Spot. In devising a strategy for research on the dynamics of planetary atmospheres other than the Earth's it has been

necessary to keep in mind that so far as planetary science is concerned the most useful conclusions are those bearing on the vertical structure of atmospheres and the nature of underlying regions, for most observations refer only to the outermost regions of the atmosphere. So it is appropriate to consider a wide range of dynamically-plausible processes and possible vertical structures. One could argue that the most important outcome of research in this area has been the attention given by fluid dynamicists to rapidly rotating fluids, and that the planetary features themselves might continue to remain enigmatic for many years to come. Useful determinations of N comprise one of the goals of the space-craft *Galileo* now on its way to Jupiter. Perhaps the collision of the comet *Shoemaker-Levy* with Jupiter starting in July 1994 (see e.g. Harrington *et al.*, 1994) will cause a perceptible disturbance from which further information about N can be deduced!

According to the "sloping convection paradigm" the principal phenomena in planetary atmospheres that would seem to have their counterparts in the above-mentioned laboratory studies and associated numerical models are the irregular large-scale wave motions observed in the Earth's atmosphere, the more regular large-scale wave motions in the atmosphere of Mars (the global circulation of which is occasionally interrupted by extensive dust storms, see e.g., Ingersoll and Lyons 1993), and the long-lived oval eddies occurring on scales ranging from 10^3–10^4 km in the atmospheres of Jupiter and of other major planets, as manifest in the complex patterns seen (by the reflected light of the Sun) at the visible cloud surface. Here is not the place to discuss the laboratory and numerical experiments in detail and to enumerate further proposed tests and various lines of existing evidence (such as high infra-red emission, implying descending motions, in a "collar" surrounding the Great Red Spot) in favour of the hypothesis. The hypothesis implies that the phenomena to which it applies are driven directly by buoyancy forces and contribute significantly to advective heat transfer. But mention should be made that in the laboratory studies the highest local Reynolds number UL/ν associated with fully-developed sloping convection is not large enough for shear instabilities to arise. Such instabilities would however occur on the vast scale of planetary atmospheres, and on the present hypothesis they may partially account for the highly irregular "turbulence" in which the Great Red Spot and other long-lived eddies are embedded. This view of the relationship between the turbulence and the long-lived eddies differs fundamentally from that held by other investigators in this lively area of research, who see the long-lived eddies as mechanically-driven features deriving their kinetic energy from the smaller-scale turbulent eddies through a nonlinear anticascade process (for references see Hide 1980, Hide *et al.*, 1994, Ingersoll 1990). It is possible that the zonal jets at the cloud levels in the atmospheres of Jupiter and Saturn owe their existence to deep-seated Rayleigh-Bénard convection (see e.g. Condie and Rhines 1994).

5. Low-dimensional analogues of self-exciting magnetohydrodynamic dynamos and geomagnetic polarity reversals

We conclude this paper with a brief account of an important process that occurs

in many geophysical and astrophysical fluid systems but (unlike sloping convection) cannot be reproduced and studied systematically on the small scale of the laboratory, namely the self-exciting MHD dynamo process. The reason for this can be seen by inspecting equation (2.5). The ability of fluid flow to amplify magnetic fields through the process of motional induction is expressed by the second term on the left-hand side of the equation. In magnitude this inductive term is typically of the order of

$$R_m \equiv U\hat{L}\mu\sigma \tag{5.1}$$

(the "magnetic Reynolds number) times the first term on the right-hand side of equation (2.5), which represents ohmic dissipation. Owing to the presence of the characteristic length scale $\hat{L}$ in the definition of R_m, when dealing with planets and stars it is found that quite slow motions in fluids of moderate electrical conductivity σ can give large values of R_m, which are impossible to achieve even with the highest practical values of U and σ attainable in the laboratory. So research on self-exciting dynamos has to be based on mathematical studies of the governing equations.

It is now generally accepted that the main magnetic fields of the Earth and other planets (Jupiter, Saturn, Uranus, Neptune and possibly Mercury) are generated by the self-exciting MHD dynamo mechanism operating in the electrically- conducting - but not necessarily metallic - fluid regions of their interiors. In the early 1950's, when the Earth was still the only planet known to possess a general magnetic field, geophysicists came round to the view that the magnitude of the field and its complex temporal variability implied that the dynamo mechanism must be at work in the Earth's liquid metallic core. It is known that slow relative motions of a rapidly - rotating fluid of low viscosity are strongly influenced by the action of Coriolis forces, which render the flow patterns highly anisotropic. So it was natural to assume that the near alignment between the Earth's magnetic and rotation axes must be a manifestation of such anisotropy, for the pattern of electric currents generated by dynamo action in the core will be related – albeit in a complicated way - to the pattern of fluid motions there. This general notion appeared to gain strength with the findings (starting in 1955 with ground-based observations of decametric and decimetric radiation from Jupiter and followed by NASA's highly successful *Pioneer* and *Voyager* missions to the outer solar system) that the magnetic axes of Jupiter and Saturn are at present closely aligned with their rotation axes. So dynamo theoreticians are being kept on their toes by the subsequent discovery from further *Voyager* observations that the planets Uranus and Neptune have highly eccentric magnetic fields (see Ness 1994)!

By re-examining in the light of these new findings the likely rôle of Coriolis forces in the dynamo process, it is possible to formulate a strategy (see Hide 1991) for future work towards the interpretation of the magnetic fields of all the planets which would not in the first instance involve straying too far from the current paradigm. But new mathematical methods will be needed that allow for the treatment of strong departures from axial symmetry in the instantaneous magnetic field. These methods are now in sight as geophysicists equipped with very powerful computers begin

the task of developing realistic numerical models. Systematic research with these models will include investigations of effects due to departures from axial symmetry in the boundary conditions, with a view in the first instance to interpreting certain important details of the geomagnetic field. But it would be wise in the study of the eccentric magnetic fields of Uranus and Neptune to see what progress can be made by examining "free" behaviour, without in the first instance invoking "forced" behaviour caused by non-axisymmetric boundary conditions.

The most striking property of the geomagnetic field is that the dipole has reversed its polarity many times over geological history. In certain respects this is not surprising, because for every solution $(\mathbf{B}(\mathbf{r},t),\ \mathbf{u}(\mathbf{r},t))$ of the MHD dynamo equations, $(-\mathbf{B}(\mathbf{r},t),\ \mathbf{u}(\mathbf{r},t))$, is also a solution. At about 7×10^5 years, the average interval between geomagnetic polarity reversals is very much longer, by a factor of about 100, than the duration of a reversal event, when the polarity changes sign. But the time series of reversals is highly irregular (see Jacobs 1994): there have been intervals as long as 3×10^7 years when the polarity apparently remained unchanged! It is likely that this general behaviour reflects to some extent *changing* boundary conditions at the surface of the core produced *inter alia* by mantle convection. It is also possible however that the time series of reversals includes manifestations of "deterministic chaos" typical of the behaviour of nonlinear systems operating under *fixed* boundary conditions.

It will not be possible to resolve such questions satisfactorily until full dynamo models have been investigated by solving the highly nonlinear partial differential equations of MHD under realistic boundary conditions (see Soward 1983). So far as polarity reversals are concerned, relevant studies to date have been largely concerned with the determination of the generic temporal behaviour of low-dimensional analogues. These satisfy nonlinear ordinary differential equations, which are readily integrated using quite modest computers. The first such analogue was proposed by Bullard (1955), who analyzed the behaviour of the simplest imaginable system, namely a Faraday disk dynamo consisting of a single disk and coil arrangement driven by a steady applied couple G. He was able to show that the current $I(t)$ in the system remained unidirectional and oscillated periodically but non-harmonically with amplitude and period which depend on the starting conditions. Malkus (1992) recognized that by introducing a resistive shunt between the disk and the coil into the Bullard system (a modification adumbrated by Bullard (1955), see also Allan (1962)) it was possible to produce equations with a degree of complexity known from previous work on nonlinear systems (e.g. Lorenz 1963, Moore and Spiegel 1966, see also Moon 1987, Thompson and Stewart 1986) to give rise to chaos, an expectation confirmed by Robbins (1977).

Much earlier, Rikitake (1958) introduced a system which has attracted much attention from mathematicians interested in the details of its chaotic behaviour, and also from geophysicists concerned with the interpretation of the statistical properties of the highly irregular time series of geomagnetic polarity reversals (for references see Jacobs 1994, Melchior 1986, Moffatt 1978, Parker 1979, Rikitake 1966, Turcotte 1993). Rikitake secured the same degree of complexity as in the shunted single disk dynamo by coupling two identical Bullard-type dynamos together. Dissipation due to ohmic heating is included in the Rikitake system, but as we shall see in what follows, an implicit assumption in previous work with that system, namely that dissipation due to mechanical friction may safely be neglected, appears to be unjustified. We conclude our discussion by showing that mechanical friction renders the dynamical behaviour of the Rikitake system "structurally unstable" (for definition see e.g. Thompson and Stewart 1986) and incapable of chaotic behaviour (see below).

The equations governing the Rikitake system are as follows (see e.g. Ghil and Childress 1987, Jacobs 1994, Moffatt 1978):

$$L dI_1/dt + RI_1 = M\Omega_1 I_2, \tag{5.2}$$

$$L dI_2/dt + RI_2 = M\Omega_2 I_1, \tag{5.3}$$

$$A d\Omega_1/dt = G - M I_1 I_2 \tag{5.4}$$

and

$$A d\Omega_2/dt = G - M I_2 I_1. \tag{5.5}$$

Here $(I_1(t),\ \Omega_1(t))$ are the current and angular speed of rotation of the disk in the first dynamo and $(I_2(t),\ \Omega_2(t))$ the corresponding quantities in the second dynamos; L and R respectively are the self-inductance and resistance of each dynamo, $2\pi/M$ is the mutual inductance of each coil and disk arrangement, and A is the moment of inertia of each disk. By measuring time t in units $(AL/GM)^{\frac{1}{2}}$, current in units $(G/M)^{\frac{1}{2}}$ and angular speed of rotation in units $(GL/AM)^{\frac{1}{2}}$, and writing

$$I_i = (G/M)^{\frac{1}{2}} X_i,\quad \Omega_i = (GL/AM)^{\frac{1}{2}} Y_i,\quad i = 1, 2, \tag{5.6}$$

equations (5.2) to (5.5) become

$$\dot{X}_1 + \gamma X_1 = Y_1 X_2, \tag{5.7}$$

$$\dot{X}_2 + \gamma X_2 = Y_2 X_1 \tag{5.8}$$

and

$$\dot{Y}_1 = \dot{Y}_2 = 1 - X_1 X_2, \tag{5.9}$$

where the dot denotes differentiation with respect to dimensionless time and

$$\gamma \equiv (AR^2/GLM)^{\frac{1}{2}}\ . \tag{5.10}$$

It follows from (5.9) that

$$Y_1 - Y_2 \equiv \Delta Y \tag{5.11}$$

remains constant.

Ito (1980) reported one of the most extensive of several detailed published theoretical studies (see Jacobs 1994, Moffatt 1978) based on these equations. The system has

two equilibrium points α and β with coordinates $(\pm\delta,\ \pm\delta^{-1},\ \gamma\delta^2)$ in the $(X_1,\ X_2,\ Y_1)$ phase space, where δ satisfies

$$\Delta Y \ = \ \gamma(\delta^2 - \delta^{-2}) \ . \tag{5.12}$$

To paraphrase a published summary of Ito's main findings, both equilibrium points α and β are unstable foci, and around them there is an attracting plane which traps all orbits starting from any point except those on the Y_1 axis. An orbit circles around α or β in this plane, irregularly travelling from an orbit around one point to one around the other. This corresponds to a reversal of the magnetic field. A phase diagram in the parameter space $(\gamma,\ \delta)$ shows various regions of periodic regime and a chaotic regime, with the transition from the former to the latter characterized by a succession of period-doubling bifurcations. Near the centre of the chaotic regime however there is an area of parameter space where reversals seldom occur and the dynamics are less disordered. The Markov entropy of the Lorenz map for the system has a sharp minimum in this parameter region, which Ito termed the "minimum entropy regime", concluding that the smallness and non-uniformity of the frequency of reversals as shown by the palaeomagnetic data suggest that the geodynamo is in such a state of minimum entropy.

This and related theoretical studies (see Jacobs 1994) cover wide ranges of γ and δ. In the work of Ito, for example, $0 < \gamma < 10$ and $1 < \delta < 6$. However the inclusion of mechanical friction in the Rikitake system appears to place restrictions on the possible values of δ that can be achieved. This is readily seen by adding the term $-k\Omega_1$ to the right-hand side of (5.4) and $-k\Omega_2$ to the right-hand side of (5.5), supposing for simplicity that k is constant, corresponding to linear mechanical friction. By subtracting one of the resultant equations from the other we find

$$Ad(\Omega_2 - \Omega_1)/dt = -k(\Omega_2 - \Omega_1) \tag{5.13}$$

which has solutions

$$[\Omega_2(t) - \Omega_1(t)] = [\Omega_2(t=0) - \Omega_1(t=0) \exp\,[-kt/A] \ . \tag{5.14}$$

It follows that $\Omega_2 - \Omega_1$ is no longer constant unless $k = 0$ or $t \to \infty$. Mechanical friction thus reduces $\Omega_2 - \Omega_1$ to zero, giving $\Delta Y = 0$; it damps out initial transients until δ takes the value unity (see (5.12)), at which chaotic behaviour cannot occur.

This result is one of several offshoots of an ongoing study, by the writer and Dr. D.J. Acheson, of single Faraday disk dynamos with additional electrical and mechanical elements (another being the discovery of simple novel reversing systems for which during the long interval of time between reversal events $I(t)$ remains virtually constant but $\Omega(t)$ does not). From this work, which was undertaken in the first instance with another geophysical (i.e. not the geodynamo) problem in mind, it became evident that, owing to structural instability the characteristic nonlinear relaxation oscillations of the Bullard dynamo give way under the influence of mechanical friction to steady solutions which (apart from the direction of the current) are independent

of the starting conditions, with the current equal to $\pm[(G - kR/M)/M]^{\frac{1}{2}}$ or zero according as $G > kR/M$ or $G \leq kR/M$, the corresponding values of the angular speed of rotation being R/M and G/K respectively. It should not be difficult in future research to take a variety of structurally-stable disk dynamo systems capable of chaotic behaviour and investigate the statistical and other properties of that behaviour in detail, for comparison with observed time series of geomagnetic polarity reversals.

Acknowledgements

Kindly commenting on the foregoing results, Professor N.O. Weiss has emphasized that in an early paper on the subject written (without the benefit of modern chaos theory) by Allan (1962), the equations for coupled disk dynamos with $k \neq 0$ are written down but not analyzed. The best known and most influential part of that paper (see e.g. Jacobs 1994) is Allan's detailed analysis of the case when $k = 0$, in which the chaotic behaviour of the Rikitake system was first demonstrated.

The author is grateful to the California Institute of Technology for the award of a Fairchild Distinguished Scholarship, during the tenure of which (October to December 1993) this invited review article was started.

References

Acheson, D.J. and Hide, R. 1973 *Repts. Prog. Phys.*, **36**, 159–221.

Allan, D.W. 1962 *Proc. Camb. Philos. Soc.*, **58**, 671–693.

Berger, A., Duplessy, J.-Cl. and Schneider, S.H. (eds.) 1989 *Climate change and geosciences.* Dordrecht: Reidel Publishing Company.

Buchler, J.R, Perdang, J.M. and Spiegel, E.A. (eds.) 1985 *Chaos in astrophysics.* Dordrecht: Reidel Publishing Company.

Bullard, E.C. 1955 *Proc. Camb. Philos Soc.*, **51**, 744–760.

Buzyna, G., Pfeffer, R.L. and Kung, R. 1984 *J. Fluid Mech.*, **145**, 337–403.

Chapman, S. 1941 *Occasional Notes Roy. Astron. Soc.*, **1** part 9, 122–134.

Condie, S.A. and Rhines, P.B. 1994 *Nature*, **367**, 711–713.

Corby, G. (ed.) 1969 *The global circulation of the atmosphere.* London: Royal Meteorological Society.

Cvitanović, P. (ed.) 1984 *Universality in chaos; a reprint selection.* Bristol: Adams

Hilger.

Drazin, P.G. and King, G.P. (eds.) 1992 *Interpretation of time series from nonlinear systems.* The Netherlands: North Holland.

Fultz, D., Long, R.R., Owens, G.V., Bohan, W., Kaylor, R. and Weil, J. 1959 *Meteorol. Monographs Amer. Meteorol. Soc.*, **4**, 1-104.

Ghil, M and Childress, S. 1987 *Topics in geophysical fluid dynamics: Atmospheric dynamics, dynamo theory and climate dynamics.* New York, Springer Verlag.

Ghil, M., Kimoto, M. and Neelin, J.D. 1991 *Rev. Geophys. Supplement*, 46-55.

Gill, A.E. 1982 *Atmosphere-ocean dynamics.* London: Academic Press.

Guckenheimer, J. and Buzyna, G. 1983 *Phys. Rev. Lett.*, **51**, 1438-1441.

Haken, H. (ed) 1981 *Chaos and order in nature.* New York: Springer Verlag.

Harrington, J., Le Beau, Jnr., R.P., Backes, K.A. and Dowling, T.E., 1994 *Nature*, **368**, 525-527.

Hart, J. 1986 *Physica D*, **20**, 350-362.

Hide, R. 1953 pp. 101-117 in *Fluid models in geophysics.* (ed. R.R. Long), Washington D.C.: U.S. Government Printing Office. (Also *Quart. J. Roy. Meteorol. Soc.*, **79**, 161.)

Hide, R. 1977 *Quart. J. Roy. Meteorol Soc.*, **103**, 1-28.

Hide, R. 1980 *The Observatory*, **100**, 182-193.

Hide, R. 1982 *Philos. Trans. Roy. Soc. London*, **A 306**, 223-234.

Hide, R. 1984 *Philos. Trans Roy. Soc. London*, **A 313**, 107-121.

Hide, R. 1991 *Geophys. Astrophys. Fluid Dyn.*, **62**, 183-189.

Hide, R. 1994 *Philos. Trans. Roy. Soc. London*, **A, 348**, (in the press).

Hide, R. and Dickey, J.O. 1991 *Science*, **253**, 629-637.

Hide, R., Lewis, S.R. and Read, P.L. 1994 *Chaos*, **4**, 135-162. (in the press).

Hide, R. and Mason, P.J. 1975 *Advances in Physics*, **24**, 47-100.

Hide, R. and Stewartson, K. 1972 *Rev. Geophys. and Space Phys.*, 10, 579-598.

Hignett, P., White, A.A., Carter, R.D, Jackson, W.D.N and Small, R. M 1985 *Quart Roy. Meteorol. Soc.*, **111**, 131-154.

Hopfinger, E.J. (ed.) 1991 *Rotating fluids in geophysical and industrial situations.* New York: Springer Verlag.

Ingersoll, A.P. 1990 *Science*, **248**, 308-315.

Ingersoll, A.P. and Lyons, J.R. 1993 *J. Geophys. Res.*, **98**, 10,951-10,961.

Ito, K. 1980 *Earth and Planet. Sci. Lett.*, **51**, 451-456.

Jacobs, J.A. (ed.) 1987-1991 *Geomagnetism* (4 volumes). New York: Academic Press.

Jacobs, J.A. 1994 *Reversals of the Earth's magnetic field.* Cambridge University Press.

James, I.N. 1994 *Introduction to circulating atmospheres.* Cambridge University Press.

King J.C. and Mobbs, S.D. (eds). 1991 *Waves and turbulence in rotating stratified fluids.* Oxford University Press.

Lewis, S.R. 1992 *Geophys. Astrophys Fluid Dyn.*, **65**, 31-55.

Lighthill, J. 1978 *Waves in fluids.* Cambridge University Press.

Lorenz, E.N. 1963(a) *J. Atmos. Sci.*, **20**, 130-141.

Lorenz, E.N. 1963(b) *J. Atmos. Sci.*, **20**, 448-464.

Lorenz, E.N. 1967 *The nature and theory of the general circulation of the Earth's atmosphere.* Geneva: World Meteorological Organization.

Lorenz, E.N. 1980 *Ann. New York Acad. Sci.*, **357**, 282-291.

Lorenz, E.N. 1993 *The essence of chaos.* London: U.C.L. Press Limited.

Malkus, W.V.R. 1972 *E.O.S. Trans. Amer. Geophys. Un.*, **53**, 617.

Mason, J., Mathias, P. and Westcott, J.H. (eds.) 1986 *Predictability in science and society.* London: The Royal Society.

Matsuzaki, M. 1994 *Philos Trans. Roy. Soc London*, **A 443**, (in the press

Melchior, P. 1986 *The physics of the Earth's core.* Oxford: Pergamon Press.

Moffatt, H.K. 1978 *Magnetic field generation in electrically-conducting fluids.* Cambridge University Press.

Monin, A.S. 1972 *Weather forecasting as a problem in physics.* Cambridge, Massachusetts: M.I.T. Press.

Moon, F.C. 1987 *Chaotic vibrations.* New York: John Wiley.

Moore, D.W. and Spiegel, E.A. 1966 *Astrophys. J.*, **143**, 871–887.

Mullin, T. (ed.) 1993 *The nature of chaos.* Oxford: Clarendon Press.

Neelin, J.D., Latif, M. and Jin, F.-F. 1994 *Ann Rev. Fluid Mech*, **26**, 617–659.

Ness, N.F. 1994 *Philos. Trans Roy . Soc. London*, **A**, 349. (in the press

Nicolis, C. and Nicolis, G. (eds.) 1987 *Irreversible phenomena and dynamical systems analysis in geosciences.* Dordrecht: D. Reidel Publishing Company.

Ott, E. 1993 *Chaos in dynamical systems.* Cambridge University Press.

Palmer, T.N., Buizza, R., Molteni, F., Chen, Y-Q. and Corti, S. 1994 *Philos Trans.Roy. Soc. London*, **A 443**, (in the press)

Parker, E.N. 1979 *Cosmical magnetic fields: their origin and activity.* Oxford: Clarendon Press.

Philander, G. 1990 *El Niño, la Niña and Southern Oscillation.* New York: Academic Press.

Platt, N., Spiegel, E.A. and Tresser, C. 1993 *Geophys. Astrophys. Fluid Dyn.*, **73**, 147–161.

Proctor, M.R.E. and Gilbert, A.D. (eds.) 1994 *Lectures on solar and planetary dynamos.* Cambridge University Press.

Quinet, A. 1974 *Advances in Physics*, **17**, 106–186.

Read, P.L. 1993 *Physica D*, **69**, 353–365.

Read, P.L., Bell, M.J., Johnson, D.W. and Small, R.M. 1992 *J. Fluid Mech.*, **238**, 599–632.

Rikitake, T. 1958 *Proc. Camb Philos. Soc.*, **54**, 89–105.

Rikitake, T. 1966 *Electromagnetism and the Earth's interior.* New York: Elsevier Publishing Company.

Robbins K.A. 1977 *Math. Proc. Cambridge Philos. Soc.*, **82**, 309–325.

Roberts, P.H. and Soward, A.M. (eds.) 1978 *Rotating fluids in geophysics.* London: Academic Press.

Rosen, R.D. 1993 *Surveys in geophysics*, **14**, 1–29.

Ruzmaikin, A., Feynman, J. and Robinson, R. 1994 *Solar physics*, **149**, 395–403.

Saltzmann, B. and Verbitsky, M.Y. 1993 *Climate dynamics*, **9**, 1–15.

Smith, L.A. 1988 *Phys. Lett.*, **A 133**, 283–288.

Smith, L.A. 1992 *Physica D*, **58**, 50–76.

Smith, L.A. 1994 *Philos Trans. Roy Soc. London*, **A** (in the press).

Sonett, C.P., Giampapa, H.S. and Matthews, M.S. (eds.) 1991 *The Sun in time.* Tucson: University of Arizona Press.

Soward, A.M. (ed.) 1983 *Stellar and planetary magnetism.* New York: Gordon and Breach Publishers.

Sreenath, N. 1993 *Systems representation of global climatic change.* New York, Springer Verlag.

Stevenson, D.J. 1983 *Repts. Prog Phys.*, **46**, 455–620.

Thompson, J.M.T. and Stewart, H.B. 1986 *Nonlinear dynamics and chaos.* Chichester: John Wiley and Sons.

Thompson, P.D. 1957 *Tellus*, **9**, 275–295.

Thompson, P.D. 1988 *J. Atmos. Sci.*, **45**, 1279–1282.

Turcotte, D.L. 1993 *Fractals and chaos in geology and geophysics.* Cambridge: University Press.

Webster, P.J. and Keller, J.L. 1975 *J. Atmos Sci.*, **32**, 1283–1300.

Weiss, N.O. 1990 *Philos. Trans. Roy. Soc. London*, **A 330**. 617–625.

Weiss, N.O. 1993 pp. 219-229 in *The cosmic dynamo.* F. Krause *et al.* (eds.). The Netherlands: International Astronomical Union.

Weiss, N.O. 1994 *Philos. Trans. Roy. Soc. London*, **A 443** (in the press).

White, A.A. 1988 *Meteorol. Mag.*, **117**, 54-63.

White, A.A. 1990 *Meteorol Mag.*, 119, 1-9.

Willebrandt, J. and Anderson, D.L.T. (eds.) 1993 *Modelling ocean climate interactions.* New York: Springer Verlag.

Williams, G.P. 1979 *J. Atmos. Sci.*, **36**, 932–968.

NONLINEAR TIME SERIES AND CHAOS

Editor: Howell Tong

Vol. 1: Dimension Estimation and Models
ed. H. Tong

Nonlinear Time Series and Chaos Vol. 2

CHAOS AND FORECASTING

Proceedings of the Royal Society Discussion Meeting

London **2–3 March 1994**

Editor

Howell Tong

Institute of Mathematics and Statistics
University of Kent
UK

World Scientific

venture. Last but not least, many thanks are due to Ms Jia-ling Leng, who assisted me with all stages of the editorial work.

Contents

Preface v

Orthogonal Projection, Embedding Dimension and Sample Size in Chaotic Time Series from a Statistical Perspective 1
B. Cheng and H. Tong

A Theory of Correlation Dimension for Stationary Time Series 31
C. D. Cutler

On Prediction and Chaos in Stochastic Systems 57
Q. W. Yao and H. Tong

Locally Optimized Prediction of Nonlinear Systems: Stochastic and Deterministic 87
L. A. Smith

A Poisson Distribution for the BDS Test Statistic for Independence in a Time Series 109
R. C. L. Wolff

Chaos and Nonlinear Forecastability in Economics and Finance 129
B. LeBaron

Paradigm Change in Prediction 145
A. S. Weigend

Predicting Nonuniform Chaotic Attractors in an Enzyme Reaction 161
L. F. Olsen, K. R. Valeur, T. Geest, C. W. Tidd, and W. M. Schaffer

Chaos in Geophysical Fluids 175
R. Hide

Chaotic Modulation of the Solar Cycle 199
S. M. Tobias and N. O. Weiss

Fractal Nature in Earthquake Phenomena and its Simple Models 213
M. Matsuzaki

Singular Vectors and the Predictability of Weather and Climate 249
T. N. Palmer, R. Buizza, F. Molteni, Y. Q. Chen, and S. Corti

Prediction as a Criterion for Classifying Natural Time Series 269
G. Sugihara

Measuring and Characterising Spatial Patterns, Dynamics and Chaos in Spatially-Extended Dynamical Systems and Ecologies 295
D. A. Rand

Non-Linear Forecasting and Chaos in Ecology and Epidemiology: Measles as a Case Study 321
B. T. Grenfell, A. Kleczkowski, S. Ellner, and B. M. Bolker

Chaos and Forecasting

GEOPHYSICAL RESEARCH LETTERS, VOL. 22, NO. 9, PAGES 1057-1059, MAY 1, 1995

Structural instability of the Rikitake disk dynamo

Raymond Hide[1]

Division of Geological and Planetary Sciences, California Institute of Technology, Pasadena, California 91125

Abstract. The Rikitake-type disk dynamo, consisting of two identical single Faraday-disk dynamos of the Bullard type coupled together, has been analyzed intensively for more than thirty years by: (a) mathematicians interested in its ability to behave chaotically, and (b) geophysicists needing low-dimensional electromechanical analogues of the geodynamo in their efforts to elucidate the complex time series of geomagnetic polarity reversals over geological time. Implicit in the theory is what now appears to be an unwarranted assumption, namely that mechanical friction is unimportant both qualitatively and quantitatively as a dissipative agency in comparison with ohmic effects, and can therefore safely be neglected. The assumption is inconsistent with the findings of the present study, which shows that mechanical friction can render the Rikitake dynamo "structurally unstable" and consequently incapable of producing chaotic oscillations. Research on low-dimensional analogues of the geodynamo should concentrate attention on structurally stable systems, with properties less dependent on the starting conditions.

Introduction

The most striking property of the geomagnetic field is that the dipole has reversed its polarity many times over geological history. At about 7×10^5 years, the average interval between geomagnetic polarity reversals is very much longer, by a factor of about 100, than the duration of a reversal event, when the polarity changes sign. But the time series of reversals is highly irregular (see *Jacobs* [1994]); there have been intervals as long as 3×10^7 years when the polarity apparently remained unchanged! It is likely that this general behavior reflects to some extent *changing* boundary conditions at the surface of the core produced *inter alia* by mantle convection, but it is possible that the time series of reversals also includes manifestations of "deterministic chaos" typical of the behavior of nonlinear systems operating under *fixed* boundary conditions (see e.g. *Lorenz* [1993]).

Such issues will not be fully resolvable until realistic dynamo models have been investigated by solving the highly nonlinear *partial* differential equations of magnetohydrodynamics (MHD) under realistic boundary conditions, a daunting task. Studies to date have been largely concerned with the determination of the generic temporal behavior of low-dimensional analogues satisfying nonlinear *ordinary* differential equations, which are readily integrated using quite modest computers. The first such analogue was proposed by *Bullard* [1955] who analyzed the behavior of the simplest imaginable system, namely a Faraday disk dynamo consisting of a single disk and coil arrangement driven by a steady applied couple G. He showed that the current $I(t)$ in the system remains unidirectional and oscillates periodically but non-harmonically with both amplitude and period dependent upon the starting conditions.

Malkus [1972] was able, by introducing a resistive shunt between the disk and coil in the Bullard dynamo, to produce a new system which over certain ranges of conditions exhibits non-periodic (i.e. chaotic) fluctuations in which (unlike the Bullard system) $I(t)$ can vary in sign (see e.g. *Robbins* [1977], *Ghil and Childress* [1987]).

Much earlier, *Rikitake* [1958] proposed a system which has attracted much attention from mathematicians interested in the details of its chaotic behavior, and also from theoretical geophysicists concerned with the interpretation of the statistical properties of the highly irregular time series of geomagnetic polarity reversals (for references see *Jacobs* [1994], *Moffatt* [1978], *Rikitake* [1966], *Turcotte* [1994]). Rikitake secured the same degree of complexity as in the shunted single-disk dynamo of Malkus and Robbins by coupling two identical Bullard-type dynamos together, with the rotating disk of the first component dynamo immersed in the magnetic field due to the current in the coil of the second component dynamo, and *vice versa*. Dissipation due to ohmic heating is included in the Rikitake system but, as we shall see in what follows, an assumption implicit in previous work with that system, namely that dissipation due to mechanical friction may safely be neglected, appears to be unjustified. Mechanical friction evidently renders the dynamical behavior of the symmetric Rikitake system "structurally unstable" (for exact definition see e.g. *Thompson and Stewart* [1986]) and incapable of chaotic behavior. Friction eliminates transients generated in the starting-up process (just as friction damps out oscillations of a simple pendulum produced by an initial disturbance). (The Bullard single-disk dynamo system is also rendered structurally unstable by mechanical friction, which damps out transient relaxation oscillations, giving steady solutions with only the sign of I dependent on the initial conditions.)

Analysis

The equations governing the Rikitake system are as follows (see e.g. *Ghil and Childress* [1987], *Jacobs* [1994], *Moffatt* [1978]):

$$L dI_1/dt + RI_1 = M\Omega_1 I_2 , \qquad (1)$$

$$L dI_2/dt + RI_2 = M\Omega_2 I_1 , \qquad (2)$$

$$A d\Omega_1/dt = G - MI_1 I_2 \qquad (3)$$

[1]Raymond Hide, 65 Charlbury Road, Oxford OX2 6UX, England, U.K.; Department of Physics, Clarendon Laboratory, University of Oxford, Parks Road, Oxford OX1 3PU, England, UK.
* Fax (0) 1865 - 811540

Paper number 95GL00779
0094-8534/95/95GL-00779$03.00

and

$$Ad\Omega_2/dt = G - MI_2J_1 . \quad (4)$$

Here the time-dependent variables $(I_1(t); \Omega_1(t))$ are respectively the current and angular speed of rotation of the disk in the first dynamo and $(I_2(t), \Omega_2(t))$ the corresponding quantities in the second dynamo; L and R respectively are the self-inductance and resistance of each dynamo, $2\pi/M$ is the mutual inductance of each coil and disk arrangement, and A is the moment of inertia of each disk. By measuring time t in units $(AL/GM)^{1/4}$ seconds, current in units $(G/M)^{1/4}$ Ampères and angular speed of rotation in units $(GL/AM)^{1/4}$ radians per second, and writing

$$I_i = (G/M)^{1/4}X_i , \Omega_i = (GL/AM)^{1/4}Y_i , i = 1 , 2 , \quad (5)$$

where X_i and Y_i are dimensionless functions of time, equations (1) to (4) become

$$\dot{X}_1 + \gamma X_1 = Y_1X_2 , \quad (6)$$

$$\dot{X}_2 + \gamma X_2 = Y_2X_1 \quad (7)$$

and

$$\dot{Y}_1 = \dot{Y}_2 = 1 - X_1X_2 . \quad (8)$$

Here the "dot" denotes differentiation with respect to dimensionless time and the dimensionless parameter

$$\gamma \equiv (AR^2/GLM)^{1/4} . \quad (9)$$

It follows from (8) that

$$Y_1 - Y_2 \equiv \Delta Y \quad (10)$$

remains constant and therefore equal to its initial value ΔY at $t = 0$.

Ito [1980] reported one of the most extensive of several detailed published theoretical studies (for references see *Jacobs* [1994], *Moffatt* [1978]) based on these equations. The system has two equilibrium points α and β with coordinates $(\pm\delta, \pm\delta^{-1}, \gamma\delta^2)$ in the (X_1, X_2, Y_1) phase space, where δ satisfies

$$\Delta Y = \gamma(\delta^2 - \delta^{-2}) . \quad (11)$$

To paraphrase a published summary of Ito's main findings, both equilibrium points α and β are unstable foci, and around them there is an attracting plane which traps all orbits starting from any point except those on the Y_1 axis. An orbit circles around α or β in this plane, irregularly traveling from an orbit around one point to one around the other. This corresponds to a reversal of the magnetic field. A phase diagram in the parameter space (γ,δ) shows various regions of periodic regime and a chaotic regime, with the transition from the former to the latter characterized by a succession of period-doubling bifurcations. Near the center of the chaotic regime however there is an area of parameter space where reversals seldom occur and the dynamics are less disordered. The Markov entropy of the Lorenz map for the system has a sharp minimum in this parameter region, which Ito termed the "minimum entropy regime", concluding that the smallness and non-uniformity of the frequency of reversals as shown by the palaeomagnetic data indicate that the geodynamo is in such a state of minimum entropy.

This and related theoretical studies (see *Jacobs* [1994]) cover wide ranges of γ and δ. In the work of Ito, for example, $0 < \gamma < 10$ and $1 < \delta < 6$. However the inclusion of mechanical friction in the Rikitake system appears to place a severe restriction on the possible values of δ that can be achieved. This is readily seen by adding the term $-k\Omega_1$ to the right-hand side of (3) and $-k\Omega_2$ to the right-hand side of (4), supposing for simplicity that k is constant, corresponding to linear mechanical friction. By subtracting one of the resultant equations from the other we find

$$Ad(\Omega_2 - \Omega_1)/dt = -k(\Omega_2 - \Omega_1) , \quad (12)$$

which has solutions

$$[\Omega_2(t) - \Omega_1(t)] = [\Omega_2(0) - \Omega_1(0)] \exp[-kt/A] . \quad (13)$$

This shows that $\Omega_2-\Omega_1$ is no longer constant and non-zero unless $k=0$. Mechanical friction reduces $\Omega_2-\Omega_1$ effectively to zero when $t >> A/k$, giving $\Delta Y=0$. Initial transients are attenuated until δ is equal to unity (see (11)), at which value chaotic behavior cannot occur!

It should not be difficult in any future research on disk dynamos to concentrate attention on structurally stable dynamos (possibly including unsymmetric Rikitake systems with unequal coefficients of mechanical friction) capable of chaotic behavior and investigate their statistical and other properties in detail, for comparison with the observed time series of geomagnetic polarity reversals and also with the output of sophisticated numerical dynamo models now being developed based on the equations of MHD. Since this paper was accepted for publication, Professor A.A. Ruzmaikin has drawn my attention to an extensive study of frictional and other effects in two-disk dynamo models (*Ershov et al.* [1989]) in which the findings of the present study are implicit. Professor N.O. Weiss has pointed out that in an early study of the Rikitake system (conducted without the benefit of modern chaos theory), *Allan* [1962] wrote down the equations for the case $k \neq 0$, but he did not analyze them. Indeed, the best known part of that paper (see e.g. *Jacobs* [1994]) is Allan's detailed analysis of the case $k=0$, in which he demonstrated that the Rikitake system (without mechanical friction) exhibits chaotic behavior, thereby stimulating great interest in that system amongst mathematicians and theoretical geophysicists!

Acknowledgement. This paper a by-product of a mathematical study of single-disk dynamos with various additional circuit elements carried out in collaboration with Dr David J. Acheson, with whom I have enjoyed helpful discussions. I am also indebted to the California Institute of Technology for the award of a Sherman Fairchild Distinguished Scholarship, during the tenure of which this article was written.

References

Bullard, E.C., The stability of a homopolar dynamo, *Proc. Cambridge Philos Soc.* 51, 744-760, 1955.

Ershov, S.V., G.G. Malinetskii, and A.A. Ruzmaikin, A generalized two-disk dynamo model, *Geophys. Astrophys. Fluid Dynam.* **47**, 251-277, 1989.

Ghil, M., and S. Childress, *Topics in geophysical fliud dynamics: Atmospheric dynamics, dynamo theory and climate dynamics*. New York, Springer Verlag, 1987.

Ito, K., Chaos in the Rikitake two-disk dynamo system, *Earth and Planet. Sci. Lett.* **51**, 451-456, 1980.

Jacobs, J.A., *Reversals of the Earth's magnetic field*. Cambridge: University Press, 1994.

Lorenz, E.N., *The essence of chaos*. London: U.C.L. Press Limited, 1993.

Malkus, W.V.R., Reversing Bullard's dynamo, *E.O.S. Trans. Amer. Geophys. Un.* **53**, 617.

Moffatt, H.K., *Magnetic field generation in electrically-conducting fluids*. Cambridge: University Press, 1978.

Rikitake, T., Oscillations of a system of disk dynamos, *Proc. Cambridge Philos. Soc.* **54**, 89-105, 1958.

Rikitake, T., *Electromagnetism and the Earth's interior*. New York: Elsevier Publishing Company, 1966.

Robbins K.A., A new approach to sub-critical instability and turbulent transitions in a simple dynamo. *Math. Proc. Cambridge Philos. Soc.* **82**, 309-325, 1977.

Thompson, J.M.T., and H.B. Stewart, *Nonlinear dynamics and chaos*. Chichester: John Wiley and Sons, 1986.

Turcotte, D.L., *Fractals and chaos in geology and geophysics*. Cambridge University Press, 1993.

(Received: 1 August 1994; accepted: 4 January 1995.)

GEOPHYSICAL RESEARCH LETTERS, VOL. 22, NO. 8, PAGES 961-964, APRIL 15, 1995
and VOL. 22, NO 24, PAGES 3561-3565, DEC. 15, 1995

The topographic torque on a bounding surface of a rotating gravitating fluid and the excitation by core motions of decadal fluctuations in the Earth's rotation

Raymond Hide[1]

Space Geodetic Science and Applications Group, Jet Propulsion Laboratory, California Institute of Techonology, Pasadena, California

Abstract. General expressions (with potential applications in several areas of geophysical fluid dynamics) are derived for all three components of the contribution made by the geostrophic part of the pressure field associated with flow in a rotating gravitating fluid to the topographic torque exerted by the fluid on a rigid impermeable bounding surface of any shape. When applied to the Earth's liquid metallic core, which is bounded by nearly spherical surfaces and can be divided into two main regions, the "torosphere" and "polosphere," the expressions reduce to formulae given previously by the author, thereby providing further support for his work and that of others on the rôle of topographic coupling at the core-mantle boundary in the excitation by core motions of Earth rotation fluctuations on decadal time scales. They also show that recent criticisms of that work are vitiated by mathematical and physical errors. Contrary to these criticisms, the author's scheme for exploiting Earth rotation and other geophysical data (either real or simulated in computer models) in quantitative studies of the topography of the core-mantle boundary (CMB) by intercomparing various models of (a) motions in the core based on geomagnetic secular variation data and (b) CMB topography based on seismological and gravity data has a sound theoretical basis. The practical scope of the scheme is of course limited by the accuracy of real data, but this is a matter for investigation, not *a priori* assessment.

Introduction

The local gradient ∇p of the instantaneous pressure $p(r, t)$ at a general point P in a gravitating fluid which rotates with angular velocity $\Omega(t)$ relative to an inertial frame of reference can be expressed formally as the sum of "gravitational," "geostrophic" and "ageostrophic" parts, $\nabla' p^{(\mathcal{V})}$, $\nabla' p^{(G)}$ and $\nabla' p^{(A)}$ (see (3.5) below), each satisfying a precise diagnostic relationship with the density $\rho(r, t)$, Eulerian relative flow velocity $u(r, t)$, magnetic field $B(r, t)$, etc. The relationship satisfied by $\nabla' p^{(G)}$ is

$$\nabla' p^{(G)}(r, t) \equiv -2\rho(r, t)\,\Omega(t) \times u(r, t). \qquad (1.1)$$

General expressions are derived below (see (4.1) to (4.5)) for all three components of the contribution $\Gamma_S^{(G)}(t)$ made by $\nabla' p^{(G)}$ to the instantaneous topographic torque $\Gamma_S(t)$ (where t denotes time) exerted by the moving fluid on a rigid impermeable bounding surface S of any shape through the action of normal pressure stresses p on S. The expressions are then applied to the Earth's liquid metallic core, which has nearly spherical bounding surfaces, extends from the solid inner core to the overlying solid mantle, and for certain dynamical purposes can be divided into two broad regions, the "pol(oid)osphere" and the "tor(oid)osphere" (see Fig. 1). The results provide further support for: (a) the author's proposal that in the excitation of fluctuations in the rotation of the mantle on decadal time scales by motions in the underlying core, topographic coupling is an important and possibly the predominant mechanism, (b) his ideas concerning the subtle but crucial role of Lorentz forces $j \times B$ (per unit volume, where $j(r, t)$ is the electric current density) in the dynamical processes involved, which depend *inter alia* on the dimensionless measure $R \equiv |\nabla' p^{(A)}|/|\nabla' p^{(G)}|$ (see (3.7)) of ageostrophic effects, and (c) the theoretical basis and preliminary findings of his scheme for exploiting Earth rotation data in quantitative investigations of the topography of the CMB, by intercomparing various models of motions in the polosphere (where $R \ll 1$ *nearly* everywhere) based on geomagnetic secular variation data, and various models of CMB topography based on gravity and seismological data. However certain geophysicists, whilst accepting (a) explicitly and (b) implicitly in their recent work on core dynamics, claim (see (2.2) below) that (c) "must be rejected," asserting that the scheme is "theoretically flawed" and "could provide no quantitative information about the CMB even with perfectly accurate geophysical data." The claim is thoroughly refuted by the present study as being inaccurate owing to demonstrable mathematical and physical errors. It is based on arguments that (i) not only fail to recognise the essentially diagnostic (but nonetheless dynamic) nature of the geostrophic relationship, but (ii) also suppose incorrectly that the axial component of $\Gamma_S^{(G)}(t)$ must be identically equal to zero (cf. (4.5)) even when quasi-geostrophic flow is largely confined to the polosphere (i.e., when $R \not\ll 1$ *nearly* everywhere in the torosphere), and (iii) overlook advection of angular momentum in an inaccurate attempt to provide a physical interpretation of the dynamical processes involved.

Decadal fluctuations in the Earth's rotation

The principal manifestation of time-varying fluid motions in the Earth's liquid metallic core is the main geomagnetic field, generated by the self-exciting magnetohydrodynamic dynamo process. The fluid motions also produce forces on the mantle which give rise *inter alia* to a fluctuating net torque $\Gamma^*(t)$. Geophysicists now accept that tiny but detectable irregular fluctuations in the magnitude of Ω, the vector rotation of the mantle with respect to an inertial frame, on decadal time scales are largely produced by the action of axial component $\Gamma^* \cdot \hat{z}$ (if $\hat{z}$ is a unit vector along the mean polar axis). It is also possible that the equatorial components of Γ^*, namely $\Gamma^* \cdot \hat{x}$ and $\Gamma^* \cdot \hat{y}$, contribute

[1]Raymond Hide, 65 Charlbury Road, Oxford OX2 6UX, England, U.K.; Department of Physics, Clarendon Laboratory, University of Oxford, Parks Road, Oxford OX1 3PU, England, U.K.

Paper number 95GL00539
0094-8534/95/95GL-00539$03.00

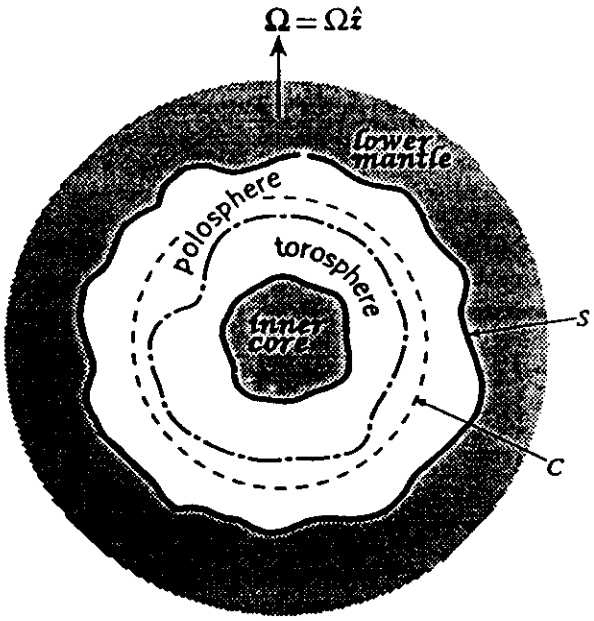

Figure 1. Schematic diagram illustrating the general system analyzed in this paper and the proposed division of the Earth's liquid metallic core into two main regions, the "pol(oid)osphere" and the "tor(oid)osphere" (which merge at the (non-spherical) "pol(oid)opause"), on the basis of the comparative strengths of the toroidal magnetic field B_T (which has no radial component and is largely confined to the core owing to the low electrical conductivity of the mantle) and the poloidal magnetic field B_P. In the polosphere $|B_T|$ is typically no larger than $|B_P|$ and in consequence polospheric flow is expected to be quasi-geostrophic nearly everywhere (see (3.7)). But in the torosphere $|B_T|$ by definition has its highest values which may be at least comparable with $|B_P|$ and may even exceed $|B_P|$ by as much as an order of magnitude, in which case torospheric flow would be highly non-geostrophic. Ω is the rotation vector of the mantle, S is the core-mantle boundary and C a general mathematical control surface used in the mathematical analysis presented in § 3 (see (1.1), (3.1) and (3.2)). Vertical scales of the bounding surfaces are greatly exaggerated. The position of the polopause is a matter for investigation, but its typical depth below the CMB may be much greater than $\bar{h}$ but much less than c (see (2.1)).

significantly to observed polar motion on decadal time scales. Here $\hat{x}$ and $\hat{y}$ are unit vectors along the x and y axes of a Cartesian frame of reference fixed in the mantle with its origin O located at the Earth's center of mass, with the x-axis pointing towards the Greenwich meridian where the longitude angle $\phi = 0$, and the y-axis in the direction $\phi = \pi/2$, see Fig. 1. The vector distance $r = r\hat{r}$ from O to a general point P satisfies $r = x\hat{x} + y\hat{y} + z\hat{z}$. (For general discussions of fluctuations in the Earth's rotation on all time scales and extensive lists of references, see *Munk and MacDonald* [1960], *Lambeck* [1980], *Melchior* [1986], *Moritz and Mueller* [1987], *Wahr* [1988], *Hide and Dickey* [1991] and *Eubanks* [1993].)

The forces that contribute to $\Gamma^*(t)$ are of four types, namely (a) tangential viscous stresses in the thin frictional (Ekman-Hartmann) boundary layer at the CMB, (b) Lorentz forces associated with electric currents induced in the weakly-conducting mantle by core processes, (c) non-radial buoyancy forces associated with gravitational interactions between the heterogeneous core and mantle (*Jault and LeMouël* [1990]), and (d) normal pressure forces acting on topographic features ("bumps") on the CMB, which are able to exert a net torque on a non-spherical surface (see *Hide* [1969, 1977(a), 1986]; *Hide et al.* [1993], *Hinderer et al.* [1990], *Jault and LeMouël* [1991], *Voorhies* [1991]). Denote by $\Gamma(t)$ the contribution to $\Gamma^*(t)$ associated with topographic coupling, a mechanism first proposed by *Hide* [1969] who (a) argued that bumps no higher than about a kilometre might suffice to account for the magnitude of $\Gamma^*_z\hat{z}$ implied by observations of decadal variations in the length of the day even with a high degree of instantaneous cancelling between positive and negative couples (see *Hide et al.* [1993, especially (2.1)]), (b) outlined a strategy for research on the essential fluid dynamical processes involved (see *Hide* [1977(a)], *Anufriev and Braginsky* [1977], *Eltayeb and Hassan* [1979], *Moffatt* [1978], *Kuang and Bloxham* [1993]), and (c) proposed and implemented a method (independently put forward by Professor J-L LeMouël) for determining $\Gamma(t)$ from geomagnetic and other geophysical data (*Hide* [1986, 1989, cited as H89], *Hide et al.* [1993], *Hinderer et al.* [1990], *Jault and LeMouël* [1991]).

Suppose that the CMB is the locus of points where $r = c + h(\theta, \phi)$, where c = 3486km is the mean radius of the CMB, and introduce the dimensionless parameter

$$\delta \equiv \bar{h}/c \tag{2.1}$$

where $\bar{h}$ is the rms value of $h(\theta, \phi)$. It is unlikely that $\bar{h}$ exceeds the height of the equatorial bulge of the CMB, about 10^4m, (see *Gwinn et al.* [1986]), so that $\delta \leq 3 \times 10^{-3}$. Define a spherical surface $r = c - \Delta$ in the free stream near the top of the polosphere and suppose that the Eulerian flow velocity $u = u_1$ on that surface, with components (u, v, w) in the (r, θ, ϕ) directions equal to (u_1, v_1, w_1). Here u_1 is typically much less than v_1 and w_1 in magnitude, by a factor δ, and can be neglected for some purposes, but not all (see e.g. (4.5) below). Expressions for all three components of $\Gamma(t)$ to leading order in R in the polosphere and in δ are given in terms of (u_1, v_1, w_1) by equations (2.1, 2.8, 2.9 H89), where R is a measure of ageostrophic contributions to the momentum equation (see (3.7) below).

Many geophysicists now accept that topographic torques may be important and possibly even dominant, but unsubstantiated criticisms of the validity of the author's expression for $\Gamma_z\hat{z}$ (see (2.9 H89)) have been voiced in well-publicized abstracts of papers presented at various recent scientific meetings. Thus:

> (a) "...although such calculations (based on the z component of (2.9 H89)) are essentially kinematic in nature, dynamical considerations show that they are flawed, since geostrophic flow cannot in itself results in topographic coupling"; (b) "(Hide's) scheme (would be) inapplicable even if we had perfect knowledge of the core flow and topography (for) geostrophic balance precludes the transfer of angular momentum, so, for a core in geostrophic balance, the (instantaneous axial component) of the topographical couple is (identically) zero"; (c) "maps of the fluid flow at the core surface and length of day observations have been used (by *Hide et al.*, [1993]) to place a constraint on the amplitude of topography at the core surface. We argue...that such constraints have been wrongly applied...."; and (d) "the geostrophic pressure yields no information on the topographical torque". (2.2)

(see e.g. *J. Bloxham et al., EOS Trans. Am Geophys. Un. Supplement*, April 20, 1993, p. 51; November 1, 1994, pages 58

and 84). These statements are vitiated by demonstrable mathematical and physical errors in the arguments upon which they are based. They stem from misconceptions concerning the dynamical processes involved, and from an expression for $\Gamma_s \cdot \hat{z}$, namely $\Gamma_s \cdot \hat{z} = 0$, which is incorrect owing apparently to an elementary but crucial mathematical error in its derivation. $\Gamma_s \cdot \hat{z}$, is certainly *not* identically equal to zero in the situation envisaged by the critics, namely when quasi-geostrophic balance is confined to the polosphere (see (4.5) below). And the statements fail to take into account of the essentially diagnostic (as opposed to prognostic, see *Hide* [1977, 1982]) nature of the geostrophic relationship, and would in the author's view be unacceptable on that basis alone. Bernoulli's celebrated equation (see e.g. *Birkhoff* [1960]), is another useful diagnostic expression in fluid dynamics whose poor prognostic properties can lead to highly erroneous conclusions, as in the well-known d'Alembert paradox concerning the drag on a moving body in a fluid of low viscosity.

Expressions for the topographic torque

Denote by $p(r, t)$ the pressure at a general point P and by S the closed surface (see Fig. 1) that coincides with the "CMB," the shape of which in the following general analysis need not be nearly spherical. The topographic torque $\Gamma_s(t)$ exerted by the fluid "core" on the overlying "solid mantle" is

$$\Gamma_s(t) = \iint_S p(r,t)\, r \times dS \tag{3.1}$$

where the integral is taken over the whole of S, the vector element of area dS of which is directed generally away from O. Clearly $\Gamma_s(t) = 0$ for a sphere r = constant, for then $r \times dS = 0$ everywhere. Also equal to zero would any component of $\Gamma_s(t)$ in a direction about which S were a figure of revolution.

Introduce mathematical control surfaces C within the fluid "core" where by definition C-surfaces are spherical and centered on O (i.e. r = constant on C), see Fig. 1; the pseudo-torque

$$\Gamma_C(t) \equiv \iint_C p(r,t)\, r \times dS \tag{3.2}$$

is therefore equal to zero. It follows from (3.1) and (3.2) and a well-known vector identity that

$$\Gamma_s(t) = \iiint_{S\text{-}C} r \times \nabla p(r,t)\, d\tau \tag{3.3}$$

where $d\tau$ is the volume element and the integral is taken over the whole volume of fluid lying between the surface S (the "CMB") and the spherical mathematical control surface C lying at or below $r = c - \Delta$ (see (2.1)).

An expression for ∇p can be obtained from the equations of fluid dynamics. For our purposes it is sufficient to consider the equations of mass continuity and momentum. The first of these is $\partial\rho/\partial t + \nabla \cdot \rho u = 0$, which can be written

$$\nabla \cdot U = 0 \tag{3.4}$$

(if $U \equiv \rho u$) without fear of serious error when dealing with highly subsonic motions. The second is conveniently written as follows:

$$\nabla p + 2\Omega\hat{z} \times U + \rho\nabla V = A \tag{3.5}$$

where V is the potential due to gravity and centripetal effects and A comprises all the "ageostrophic" terms. Thus

$$A = A(r,t) \equiv j \times B + F_{visc} - \rho\dot{\Omega} \times r - \rho\,[\partial u/\partial t + (u \cdot \nabla)\, u]\,, \tag{3.6}$$

where the Lorentz force (per unit volume), $j \times B$, is the largest contribution to A in the core outside the thin Ekman-Hartmann viscous boundary layers (see *Hide* [1977(a)]). F_{visc} is the viscous force, $\rho\,\dot{\Omega} \times r$ is a "fictitious" force associated with time-variations in Ω (since $\dot{\Omega} \equiv d\Omega/dt$), and $\rho\,[\partial u/\partial t + (u \cdot \nabla)u]$ is the acceleration of a moving fluid element relative to the rotating reference frame. The flow would be *strictly geostrophic* in regions where the dimensionless parameter

$$R \equiv |A| / |2\Omega \times U| \tag{3.7}$$

is equal to zero, *quasi-geostrophic* in regions where $0 < R \ll 1$, and *non-geostrophic* where $R \not\ll 1$.

Since $\nabla p = A - \rho\nabla V - 2\Omega\hat{z} \times U$, it is convenient to write

$$\Gamma_s(t) = \Gamma_s^{(A)}(t) + \Gamma_s^{(V)}(t) + \Gamma_s^{(G)}(t) \tag{3.8}$$

where (see (3.3))

$$\Gamma_s^{(A)} \equiv \iiint_{S\text{-}C} r \times A\, d\tau \tag{3.9}$$

is the contribution to Γ_s associated with the ageostrophic terms in the momentum equation,

$$\Gamma_s^{(V)} \equiv -\iiint_{S\text{-}C} r \times \rho\nabla V d\tau \tag{3.10}$$

is the contribution associated with the non-radial components of ∇V, and

$$\Gamma_s^{(G)} \equiv -2\Omega \iiint_{S\text{-}C} r \times (\hat{z} \times U)\, d\tau \tag{3.11}$$

is the contribution associated with what we here term the "geostrophic pressure field" $p^{(G)}$.

The geostrophic contribution to the topographic torque

Making use of a well-known vector identity and the facts that $2(r \cdot U) = \nabla \cdot (r^2 U)$ and $\nabla \cdot U = 0$ (see (3.4)), (3.11) gives

$$\Gamma_s^{(G)} = 2\Omega \iiint_{S\text{-}C} z\,(U_x\hat{x} + U_y\hat{y} + U_z\hat{z})\, d\tau \tag{4.1}$$

where $U = (U_x\hat{x} + U_y\hat{y} + U_z\hat{z}) = \rho(r,t)(u_y\hat{x} + u_y\hat{y} + u_z\hat{z})$. The validity of (2.8 H89) can be demonstrated by noting that the exact equation (4.1) reduces to (2.8 H89) when terms of second order and higher in the small quantity δ (see (2.1)) are neglected. In carrying out the comparison, the volume of integration is taken to extend outward from that spherical control surface C where $r = c - \Delta$, in the "free stream" (see (2.1)), to the CMB where $r = c + h(\theta, \phi)$, and expressing (u_x, u_y, u_z) in terms of (u_r, u_θ, u_ϕ).

A more revealing comparison can be made by noting first that in virtue of (3.4) and the vanishing of $U \cdot dS$ everywhere on the impermeable and rigid surface S (but not on C!):

$$\Gamma_s^{(G)} \cdot \hat{x} = -2\Omega\,\Big[\iint_C xz\, U \cdot dS + \iiint_{S\text{-}C} xU_z d\tau\Big], \tag{4.2}$$

$$\Gamma_s^{(G)} \cdot \hat{y} = -2\Omega\,\Big[\iint_C yz\, U \cdot dS + \iiint_{S\text{-}C} yU_z d\tau\Big], \tag{4.3}$$

$$\Gamma_s^{(G)} \cdot \hat{z} = -\Omega \iint_C z^2 U \cdot dS. \tag{4.4}$$

In general, none of these components of $\Gamma_s^{(G)}$ is identically equal to zero. We note here in passing that (4.4) refutes the assertion in (2.2b).

The physical interpretation of (4.4) becomes evident when it is re-written as

$$\Gamma_s^{(G)} \cdot \hat{z} = \iint_C \left[\rho\,\Omega(x^2 + y^2)\right] u \cdot dS \equiv Q_C \text{ (say)} \tag{4.5}$$

(remembering that $x^2 + y^2 + z^2 = r^2$ and r = constant on C). The quantity in the square bracket in the integrand is the axial

component of the angular momentum of a fluid element of unit volume at a distance $(x^2 + y^2)^{1/2}$ from the z–axis associated with its rotation about that axis, and Q_C is therefore the rate of advection of that quantity across the surface C. The equivalence to first order in δ of (2.8 H89) to the more general equation (4.4) (or (4.5)) is readily demonstrated along the same lines as those followed when comparing (4.1) with (2.8 H89). Thus, we take C to be the surface where $r = c - \Delta$ and infer the radial motion on C by applying the boundary condition that $\mathbf{u}.d\mathbf{S} = 0$ on the CMB, where $r = c + h(\theta, \phi)$. It is important to note that whilst this radial motion can safely be neglected to leading order in the equation of motional induction when deducing core motions from geomagnetic secular variation data (see (4.1 H89), also *Bloxham and Jackson* [1991, equation (38)] and *Backus and LeMouël* [1987]), it is certainly non-zero in general and plays a crucial role in angular momentum transfer and torque balance!

Possibly the simplest model of the Earth's liquid core that one could imagine for the purpose of an exercise in estimating $\Gamma(t)$ from first principles would comprise a largely quasi-geostrophic polosphere within which R_P, the average value of R, satisfies $R_P \ll 1$ (see (3.7)), and a possibly non-geostrophic torosphere where R_T (the average value of R there) may be significantly larger than R_P, even of order unity or greater. $\Gamma_S^{(G)}$ would then provide a good leading approximation to Γ (with errors no more than R_P), and only in very special circumstances would $\Gamma_S^{(G)} \cdot \hat{\mathbf{z}}$ vanish, namely when $R_T \ll 1$ and the shape of the interface between the liquid core and the underlying solid inner core is a figure of revolution about the z-axis!

Beyond the scope of the present short article is (a) the inclusion of all the details of the analysis leading to the general expressions deduced in §§ 3 and 4, and (b) full discussions of their implications for realistic models of the core and also for theoretical studies of the dynamics of oceans and atmospheres of the Earth and other planets. These matters will have to be treated elsewhere.

Acknowledgment. It is a pleasure to acknowledge the scientific hospitality and helpful discussions with members of the Space Geodetic Science and Applications Group of Jet Propulsion Laboratory during a visit when this paper was written.

References

Anufriev, A. P. and S. I. Braginsky, Influences of irregularities in the boundary of the Earth's core on fluid velocity and magnetic field, *Geomagn. Aeron.* , 17, 492-496, 1977.

Backus, G. E. and J-L. LeMouël, The region of the core-mantle boundary where the geostrophic velocity field can be determined from frozen flux data, addendum, *Geophys. J. Roy. Astron. Soc.*, 88, 321-322, 1987.

Birkhoff, G., *Hydrodynamics; a study in logic, fact and similitude*, Princeton University Press, 1960.

Bloxham, J., and A. Jackson, Fluid flow near the surface of the Earth's core, *Rev. Geophys.*, 29, 97-120, 1991.

Eltayeb, I. A., and M. H. A. Hassan, On the effects of a bumpy core-mantle interface, *Phys. Earth Planet. Int.* 19, 239-254, 1979.

Eubanks, T. M., Variations in the orientation of the Earth, pp. 1-54 in *Contributions of space geodesy to geodynamics* (eds. D. E. Smith and D. L. Turcotte), Geodynamics Series Vol. 24, American Geophysical Union, Washington, D.C., 1993.

Gire, C., and J-L. LeMouël, Tangentially-geostrophic flow at the core-mantle boundary compatible with observed geomagnetic secular variation: the large-scale component of the flow, *Phys. Earth Planet Int.*, 59, 259-287, 1990.

Gwinn, C. R., T. A. Herring, and I. I. Shapiro, Geodesy by radio interferometry: Studies of the forced nutations of the Earth, 2. Interpretation, *J. Geophys. Res.*, 91, 4755-4765, 1986.

Hide, R., Interaction between the Earth's liquid core and solid mantle, *Nature*, 222, 1055-1056, 1969.

Hide, R., Towards a theory of irregular variations in the length of the day and core-mantle coupling, *Phil. Trans. Roy. Soc. Lond.*, A284, 547-554, 1977(a).

Hide, R., Experiments with rotating fluids (Presidential address), *Quart. J. Roy. Meteorol. Soc.*, 103, 1-28, 1977(b).

Hide, R., "On the rôle of rotation in the generation of magnetic fields by fluid motions," *Philos. Trans. Roy. Soc. Lond.* A 306, 223-234, 1982.

Hide, R., Presidential Address: The Earth's differential rotation, *Quart. J. Roy. Astron. Soc.*, 278, 3-14, 1986.

Hide, R., Fluctuations in the Earth's rotation and the topography of the core-mantle interface, *Phil. Trans. Roy. Soc. Lond.*, A328, 351-363, 1989; cited as H89.

Hide, R., R. W. Clayton, B. H., Hager, M. A., Spieth, and C. V., Voorhies,, Topographic core-mantle coupling and fluctuations in the Earth's rotation, in *Relating geophysical structures and processes, The Jeffreys volume* (edited by K. Aki and R. Dmowska), *Geophys. Monog. Am. Geophys. Un.*, 76, 107-120, 1993.

Hide, R., and J. O. Dickey, Earth's variable rotation, *Science*, 253, 629-637, 1991.

Hinderer, J., D. Jault, and Legros, H., J-L. LeMouël, Core-mantle topographic torque: A spherical harmonic approach and implications for the excitation of the Earth's rotation by core motions, *Phys. Earth Planet. Int.*, 59, 329-341, 1990.

Jault, D., and J-L. LeMouël, "Core-mantle boundary shape: Constraints inferred from the pressure torque acting between the core and mantle," *Geophys. J. Int.*, 101, 233-241, 1990.

Jault, D., and J-L. LeMouël, "Exchange of angular momentum between the core and mantle, *J. Geomag. Geoelect.*, 43, 111-129, 1991.

Kuang, W., and J. Bloxham, The effect of boundary topography on motions in the Earth's core, *Geophys. Astrophys. Fluid Dynam.*, 72, 161-195, 1993.

Lambeck, K., *The Earth's variable rotation*, Cambridge Univ. Press, London and New York, 1980.

Moffatt, H. K., Topographic coupling at the core-mantle interface, *Geophys. Astrophys. Fluid Dyn.*, 9, 279-288, 1978.

Moritz, H., and I. I. Mueller, *Earth rotation: Theory and observation*, The Ungar Publishing Co., New York, 1987.

Munk, W. H., and G. J. F. MacDonald, *The rotation of the Earth*, Cambridge University Press, 1960.

Voorhies, C. V., "Coupling an inviscid core to an electrically-insulating mantle," *J. Geomag. Geoelect.*, 43, 131-156, 1991.

Wahr, J. M., The Earth's rotation, *Ann. Rev. Earth Planet Sci.*, 16, 231-249, 1988.

Received: August 9, 1994
Revised: February 1, 1995
Accepted: February 6, 1995

GEOPHYSICAL RESEARCH LETTERS, VOL. 22, NO. 24, PAGES 3561-3562, DECEMBER 15, 1995

Comment on "The topographic torque on a bounding surface of a rotating gravitating fluid and the excitation by core motions of decadal fluctuations in the Earth's rotation"

plus reply by R. Hide!

Jeremy Bloxham and Weijia Kuang

Department of Earth and Planetary Sciences, Harvard University

Understanding the mechanism of angular momentum exchange at the core-mantle boundary is important not only because it results in observed changes in the rotation rate of the solid Earth over periods of a few decades but also because of the constraint that the angular momentum exchange places on the fluid flow and dynamo process in the fluid outer core. Of the various candidate mechanisms for this angular momentum exchange, topographical core-mantle coupling, which was first proposed by *Hide* [1969] and which arises from the action of normal pressure forces on core-mantle boundary topography, has received much recent attention. In part, this attention stems from a proposal by *Hide* [1986] for calculating the torque from observations of the magnetic field and core-mantle boundary topography. *Bloxham and Kuang* [1993] have suggested that the method proposed by *Hide* [1986] is flawed. In a recent paper, *Hide* [1995] has sought to refute this suggestion.

Hide's method is based on using the tangentially geostrophic part of the fluid flow at the core-mantle boundary, which is determined from the geomagnetic secular variation, to calculate the horizontal pressure gradient at the core-mantle boundary. Then, using a map of core-mantle boundary topography, the torque is calculated by simply integrating this pressure force acting on the topography over the core-mantle boundary. The pressure gradient is calculated from the geostrophic part of the flow using the geostrophic approximation. However, this part of the pressure gradient does not result in a net torque since it is balanced only by terms that do not represent a transfer of angular momentum and so do not give rise to a net torque. In order to calculate the topographic torque a higher-order theory is required. This can also be seen by noting that the topographic torque depends only upon non-axisymmetric parts of the flow and that the angular momentum is carried only by axisymmetric parts of the flow, yet in the geostrophic approximation there is no coupling of axisymmetric and non-axisymmetric parts of the flow. The coupling arises at higher order.

Paper number 95GL03677
0094-8534/95/95GL-03677$03.00

Hide [1995] seeks to refute this assertion, claiming that it fails to recognize the diagnostic nature of the geostrophic relationship. Here we suggest that the reverse is true and that arguments put forward by *Hide* [1995] are based on an expression for the topographic torque which inadequately accounts for the diagnostic nature of the geostrophic relationship.

The geostrophic momentum equation is diagnostic in the sense that given the pressure field (customarily the case in meteorology), the geostrophic part of the flow can be deduced. The reverse process, finding the pressure from the flow, is not so straightforward. Hide defines the geostrophic part of the pressure gradient by

$$\nabla' p^{(G)} \equiv -2\rho(r,t)\Omega(t) \times u(r,t) \qquad \text{(Hide - 1.1)}$$

where $u(r,t)$ is the Eulerian flow velocity (necessarily not precisely geostrophic), $\Omega = \Omega\hat{z}$ is the rotation and ρ the density. Notwithstanding the undefined operator ∇' on the left-hand side of this equation, it is important to note that the right-hand side includes both an irrotational term (the gradient of a scalar) and, unless the flow is precisely geostrophic, a solenoidal term (the curl of a vector).

Hide, in turn, uses this definition to define the geostrophic part of the axial topographic torque

$$\Gamma_S^{(G)} \equiv -2\Omega \iiint_{S-C} r \times (\hat{z} \times U) d\tau \qquad \text{(Hide - 3.11)}$$

where $U = \rho u$. The integral is taken over a volume bounded by the core-mantle boundary (S) and a spherical control surface (C) in the quasi-geostrophic part of the core. For details see *Hide* [1995]. With this definition, $\Gamma_S^{(G)}$ includes two terms, one of which could represent a pressure torque plus a term due to the solenoidal part of $\hat{z} \times U$ which does not represent a pressure torque.

Thus the arguments put forward by *Hide* [1995] are based on an incorrect use of the geostrophic approximation. The reader might wonder why we are concerned with the theoretical foundations of Hide's method when it is well-known that even if the method were theoretically sound it is nonetheless of little or no value for calculating the actual torque. Hide's method is extremely sensitive to the models of the boundary topography [*Jault and LeMouël*, 1990] and the core flow [*Kuang and Bloxham*, 1993] that

are used; in fact, each would need to be determined to several orders of magnitude better accuracy than is feasible with existing observations for the method to yield statistically meaningful results. It is solely because of the uncertainty in existing models of the core flow and core-mantle boundary topography that application of Hide's method [*Hide et al.*, 1993] yields large topographical torques.

However, the method, if valid, would still place constraints on the amplitude of core-mantle boundary topography and on the process of angular momentum exchange within the core, even though it is of no deterministic value. This last point is particularly important since Hide's method implies that the magnitude of topographical coupling is $O(\delta)$ where $\delta \equiv h/c$, and h is the mean amplitude of the topography and c is the mean radius of the core-mantle boundary. In a more complete study of this problem [*Kuang and Bloxham*, ms. in preparation] we show that the leading order topographical coupling terms are $O(\delta^2)$ and $O(\delta R_o)$, where R_o is the Rossby number; in all likelihood, $\delta \gg R_o$, so the leading order term is $O(\delta^2)$. This has profound implications for the amplitude of core-mantle boundary topography.

Finally, we wish to emphasize that none of this discussion casts any doubt on Hide's original suggestion that topographical core-mantle coupling is an important mechanism of angular momentum exchange at the core-mantle boundary. These arguments only concern the method proposed subsequently by Hide for calculating the torque.

Acknowledgments. JB is supported by an NSF Presidential Young Investigator Award (EAR-9158298), and by the Packard Foundation.

References

Bloxham, J., and W. Kuang, Topographical core-mantle coupling, *EOS Trans. AGU. supp. (April)*, *74*(16), 51, 1993.

Hide, R., Interaction between the Earth's liquid core and solid mantle, *Nature*, *222*, 1055–1056, 1969.

Hide, R., The Earth's differential rotation, *Quart. J. Roy. Astron. Soc.*, *278*, 3–14, 1986.

Hide, R., The topographic torque on a bounding surface of a rotating gravitating fluid and the excitation by core motions of decadal fluctuations in the Earth's rotation, *Geophys. Res. Lett.*, *22*, 961–964, 1995.

Hide, R., R. W. Clayton, B. H. Hager, M. A. Spieth, and C. V. Voorhies, Topographic core-mantle coupling and fluctuations in the Earth's rotation, in *Relating geophysical structure and processes, The Jeffreys volume*, edited by K. Aki, and R. Dmowska, vol. 76 of *Geophys. Monog. Am. geophys. Un.*, pp. 107–120. 1993.

Jault, D., and J.-L. LeMouël, Core-mantle boundary shape: Constraints inferred from the pressure torque acting between core and mantle, *Geophys. J. Int.*, *101*, 233–241, 1990.

Kuang, W., and J. Bloxham, On the effect of boundary topography on flow in the Earth's core, *Geophys. and Astrophys. Fluid Dyn.*, *72*, 161–195, 1993.

Jeremy Bloxham and Weijia Kuang, Department of Earth and Planetary Sciences, Harvard University, Cambridge, MA 02138. (email: bloxham@geophysics.harvard.edu)

(received May 19, 1995; revised August 17, 1995; accepted August 19, 1995.)

GEOPHYSICAL RESEARCH LETTERS, VOL. 22, NO. 24, PAGES 3563-3565, DECEMBER 15, 1995

Reply

Raymond Hide[1]

Space Geodetic Science and Applications Group, Jet Propulsion Laboratory, California Institute of Technology, 4800 Oak Grove Drive, MS 238-332, Pasadena, California 91109

The findings of my recent paper (Hide [1995, cited as 95H] include *inter alia* a complete refutation of an oft-repeated naive claim by Professors Bloxham and Kuang (BK) that there is a serious flaw in the theoretical basis of my method for investigating the topography of the Earth's core-mantle boundary (CMB) using Earth-rotation and other geophysical data, and that geophysical conclusions based on applications of the method are therefore unacceptable. Stripped of rhetoric and semantic complications (including the inconsistent use of the term "geostrophic," which has no agreed definition out of context amongst geophysical fluid dynamicists (see e.g. *Greenspan* [1968], *Pedlosky* [1979], *Gill* [1982]) but which is precisely defined and used in the context of 95H), the "Comment" (CBK) by BK on 95H contains little more than an unsupported refusal by its authors to accept the clear and unambiguous evidence given in 95H against their unsubstantiated and demonstrably-erroneous claim. So far as I am aware, physical and mathematical arguments underlying their claim have yet to be divulged by BK in a scientific paper, the article "Bloxham and Kuang 1993" cited in CBK being the first of several unrefereed abstracts they have published on the same theme in the programs of various AGU and other major scientific meetings. As shown in 95H, their claim is unacceptable on the grounds that it is incompatible with the laws of fluid dynamics and the theoretical basis of my method—which in essence is the same as one put forward and applied independently by Professor J-L Le Mouël and his colleagues, see 95H—is upheld. It is hoped that this reply to CBK will be found helpful by those involved in the international SEDI (Study of the Earth's Deep Interior) program of research on the structure and dynamics of the Earth's core and lower mantle, where good ideas are needed for exploiting a wide range of geophysical data.

Consider a fluid bounded by a closed, rigid, impermeable and irregularly-shaped surface S which rotates with angular velocity $\Omega(t)\hat{z}$ relative to an inertial frame. Suppose that the density of the fluid at a general point P (with coordinates $r = x\hat{x} + y\hat{y} + z\hat{z}$ in a frame fixed in S with its origin O at the center of mass of the system) is $\rho(r,t)$, where t denotes time, and (x, y, z) are Cartesian coordinates, $\hat{z}$ being a unit vector in the axial direction and $(\hat{x}, \hat{y})$ unit vectors in the equatorial plane, and that $p(r,t)$ and $u(r,t)$ are, respectively, the pressure and the Eulerian flow velocity at P. The *instantaneous* "topographic torque" $\Gamma_S(t)$ due to the action of normal pressure forces on S is given by

$$\Gamma_S(t) = \iint_S p(r,t) r \times dS \qquad (1)$$

(see H3.1, i.e. equation (3.1) of 95H), where the integral is taken over the whole of S, the vector element of which is dS directed generally away from O. The vector $\Gamma_S(t)$ fluctuates about a time-average equal and opposite to that of other fluctuating torques (electromagnetic, viscous, gravitational) exerted by the fluid on S (for the time-average of the net torque must be zero).

Given the shape of S and determinations of $p(r,t)$ on S, the vector $\Gamma_S(t)$ could be calculated directly using (1). However, as in the case of the Earth's core and in other situations where $p(r,t)$ is *not* known from direct measurements but other information *is* available, such as $u(r,t)$ and $\rho(r,t)$ in the vicinity of S, it is still possible to investigate $\Gamma_S(t)$, by using the equations of fluid dynamics to relate the local pressure gradient ∇p to "observable" quantities. It is readily shown that

$$\Gamma_S(t) = \iiint_{S-C} r \times \nabla p(r,t) d\tau \qquad (2)$$

(see H3.3) where C is any spherical surface concentric with the origin, upon which r is therefore constant, that lies everywhere within the fluid and $d\tau$ is an element of the volume of fluid lying between S and C, over the whole of which the integral is taken. The magnetohydrodynamic equation of motion is conveniently expressed as follows:

$$\nabla p = \nabla' p^{(V)} + \nabla' p^{(G)} + \nabla' p^{(A)} \qquad (3)$$

(see H1.1 and H3.5). The three vectors $\nabla' p^{(V)}$, $\nabla' p^{(G)}$ and $\nabla' p^{(A)}$ define unambiguously the respective contributions to the instantaneous pressure gradient $\nabla p(r,t)$ at P that can be associated with (a) the buoyancy force (per unit volume), (b) the Coriolis force $2\Omega(t) \times U(r,t)$ (where $U(r,t) \equiv \rho(r,t)u(r,t)$) and (c) all the remaining ("ageostrophic") terms in the full momentum equation, notably those representing relative acceleration, viscous friction, Lorentz forces and etc. In general, none of the three vectors on the right hand side of (3) is irrotational (even though their sum has this property); hence the notation involving the use of the prime (see (9) below). The quantity

$$\Gamma_S^{(G)}(t;C) \equiv -2\Omega \iiint_{S-C} r \times (\hat{z} \times U) d\tau \qquad (4)$$

(see H3.11) expresses unambiguously the contribution made to $\Gamma_S(t)$ by Coriolis forces acting on the fluid occupying the volume "S–C".

There are corresponding unambiguously-defined expressions (see H3.10 and H3.9) for the respective contributions associated with $\nabla' p^{(V)}$ and $\nabla' p^{(A)}$. The first of these contributions depends on the non-radial component of the acceleration due to gravity plus centripetal effects. There can be circumstances in which the spherical surfaces C can be chosen such that this and the "ageostrophic" contribution are both negligible in comparison with $\Gamma_S^{(G)}(t;C)$, in which case (4) provides a good first approximation to $\Gamma_S(t)$. This is the basis of the abovementioned method for investigating topographic torques at the CMB. It is important however to emphasize here that (4) is a *diagnostic* relationship, from which $\Gamma_S^{(G)}(t;C)$ can be determined when $U(r,t)$ is already known from measurement or theory. In the determination of U from first principles, by obtaining

[1]Raymond Hide, 65 Charlbury Road, Oxford OX2 6UX, England, U.K.; Department of Physics, Clarendon Laboratory, University of Oxford, Parks Road, Oxford OX1 3PU, England, U.K.

Paper number 95GL03678

0094-8534/95/95GL-03678$03.00

simultaneous solutions of the governing equations (now used *prognostically* rather than diagnostically), ageostrophic terms *always* play a crucial role and can never be completely neglected!

Equation (4) leads directly to the following expression for the vector $\Gamma_S^{(G)}(t;C)$:

$$\Gamma_S^{(G)}(t;C) = 2\Omega(t)\iiint_{S-C} z\left[U_x(t)\hat{x} + U_y(t)\hat{y} + U_z(t)\hat{z}\right]d\tau \qquad (5)$$

(see H4.1). This equation (contrary to the views expressed in CBK) is mathematically correct, physically meaningful and geophysically useful! When, as in the case of the Earth's CMB, the surface S is almost spherical, (5) applied to that region "*S–C*" of the outer core lying below the very thin viscous boundary layer on S and above the spherical surface C that just touches the lowest point in S, (5) reduces to an expression for the "geostrophic" (or "Coriolis" or "gyroscopic") contribution to the vector $\Gamma_S(t)$ derived previously by another method (*Hide* [1989, 1986]), see 95H. It is also noteworthy, as Professor Le Mouël has kindly pointed out to me recently, that the z-component of (5) leads to an expression for the axial component of $\Gamma_S(t)$ which is essentially equivalent to one derived by *Jault and Le Mouël* [1989], in a detailed study of the transfer of axial angular momentum between different parts of the Earth's liquid core and between the core and mantle.

It follows from (5) and the impermeability condition on S that (inasmuch as very weak suction due to the thin viscous Ekman-Hartmann boundary layer on S can be neglected)

$$\Gamma_S^{(G)}(t;C)\cdot\hat{z} = -\Omega\iint_C z^2 U\cdot dS \qquad (6)$$

(see H4.4; cf. H4.2 and H4.3), remembering that dS, by definition, is directed generally *away* from the origin of coordinates O. *Of particular importance in connection with the controversy started by BK is the implication of this equation that*—in virtue of the implication of the equation of mass conservation $\nabla\cdot U = 0$ (see H3.4) that

$$\iint_C U\cdot dS = 0 \qquad (7)$$

—the axial component of $\Gamma_S^{(G)}(t;C)$ *is not in general identically equal to zero, i.e.*

$$\Gamma_S^{(G)}(t;C)\cdot\hat{z} \not\equiv 0. \qquad (8)$$

As shown in 95H, (8) suffices to refute the unsupported claim that BK have repeatedly made, in CBK and elsewhere, concerning the validity of my method. I was unable to discover the basis of their claim until November 1994, when I received a referee's report by the senior author of CBK recommending the rejection of my first attempt to publish a response to BK's pronouncements. The basis of that proposed rejection was a certain expression (in the terminology of the present paper) for $\Gamma_S^{(G)}(t;C)\cdot\hat{z}$. Had BK carried out the mathematical analysis leading to that expression correctly they would have found results equivalent to (6) and (8). In the event, owing to an unfortunate mathematical slip they obtained an erroneous expression, equivalent to (6) with r^2 in the place of z^2, which, crucially, does *not* satisfy (8)! Apparently believing this inaccurate result that $\Gamma_S^{(G)}(t;S)\cdot\hat{z} \equiv 0$, and also in their consistent but fallacious physical interpretation of the result, BK drew incorrect conclusions about the theoretical basis of my work and that of others on topographic core-mantle coupling and gave them wide publicity (see (2.2) of 95H), presumably for the intended benefit of the SEDI community! It is possible that BK have been influenced in their confused thinking by a well-known but often misunderstood result in the theory of rotating fluids (which follows directly from (6)), namely that in the very special (and hypothetical, see 95H) case when ageostrophic effects are negligible *everywhere*, the axial component of the topographic torque exerted by the fluid on its boundaries is equal to zero (see *Greenspan* [1968], *Pedlosky* [1979], *Roberts* [1988]; cf. *Hide* [1989]).

Having brought these mistakes to the attention of BK in December 1994 (when I made a further attempt to resolve the controversy Professor Bloxham had started nearly two years earlier), I was astonished to discover in May 1995, on being invited by the Editor of GRL to reply to CBK, that they continue to hold the view that the axial component of $\Gamma_S^{(G)}(t;C)$ must be identically equal to zero, notwithstanding evidence to the contrary presented clearly in 95H (see equations (6) to (8) above). In their new attempt to justify this belief, they make in CBK the remarkable and inaccurate (see below) assertion that my expression H3.11 (see (4) above) must be meaningless! In support of this assertion, BK give an "argument" which invokes an "equation" labeled "Hide (1.1)", apparently without realizing that there is a crucial difference between that "equation" and equation (1.1) of 95H. In 95H, the hydrodynamical equation of motion is expressed for convenience in the form given by (3) above (see also H1.1, 3.5), the corresponding vorticity equation being

$$\nabla\times\left[\nabla' p^{(V)} + \nabla' p^{(G)} + \nabla' p^{(A)}\right] = 0, \qquad (9)$$

since $\nabla\times\nabla p \equiv 0$. The authors of CBK apparently failed to notice that the term $\nabla' p^{(G)}$ is *not* the same as $\nabla p^{(G)}$, *so the question of "single valuedness" does not arise*. The vector $\nabla' p^{(G)}$ *is* uniquely defined by H1.1 (see (3) above) and there is no ambiguity whatsoever in the expression H3.11 for the vector $\Gamma_S^{(G)}(t;C)$ with which $\nabla' p^{(G)}$ is directly associated (see (4) to (8) above).

Before concluding, it is necessary to comment on the vague statements made in CBK concerning the magnitude of $\Gamma_S(t)\cdot\hat{z}$, which presumably refer to theoretical (including numerical) models of core motions. In realistic models, all the dependent variables $p(r,t)$, $u(r,t)$, $\rho(r,t)$ etc. would be determined simultaneously from the full equations of magnetohydrodynamics, solved under appropriate boundary conditions. Acceptable solutions obtained in this way would satisfy H3.11 and H4.1 to H4.5 (see (4) to (6) above) automatically; indeed, these equations could prove useful in diagnostic studies needed to validate such models. In none of these solutions would ageostrophic effects be negligible *everywhere*, for such solutions are impossible on general mathematical and physical grounds (see 95H and discussion following (4) above). How $\Gamma_S(t)$ depends on the various dimensionless parameters required to characterize the model is of course a matter of great interest in the study of core motions. But the statements made in CBK on this matter are largely irrelevant to the simple point at issue here, which they serve to obscure rather than illuminate.

The time-wasting controversy provoked by Professor Bloxham started with widely-publicized pronouncements offered as a (presumably) serious contribution to the geophysical discussions taking place within the SEDI community, at meetings I was unable to attend. The future interest of that community as it develops strategies for research on the Earth's deep interior will be served if BK can now acknowledge that their pronouncements were wrong and misguided. They should revise their opinions in

the light of 95H, where the simple but important scientific issue at the heart of the controversy is clearly identified and fully resolved.

Acknowledgment. It is a pleasure to acknowledge the scientific hospitality and helpful discussions with members of the Space Geodetic Science and Applications Group of Jet Propulsion Laboratory during a visit when this paper was written. The research described in the paper was supported by the Jet Propulsion Laboratory, California Institute of Technology, under a contract with the National Aeronautics and Space Administration.

References

Gill, A. E., *Atmosphere-ocean dynamics*, New York: Academic Press, 1982.

Greenspan, H. P., *The theory of rotating fluids*, Cambridge University Press, 1968.

Hide, R., Presidential address: The Earth's differential rotation, *Quart. J. Roy. Astron. Soc.*, *27*, 3-14, 1986.

Hide, R., Fluctuations in the Earth's rotation and the topography of the core-mantle interface, *Phil. Trans. Roy. Soc. London A 328*, 351-363, 1989.

Hide, R., The topographic torque on a bounding surface of a rotating gravitating fluid and the excitation by core motions of decadal fluctuations in the Earth's rotation, *Geophys. Res. Lett.*, 22, 961-964, 1995; cited as "95H".

Jault, D. and Le Mouël, J-L., The topographic torque associated with tangentially geostrophic motion at the core surface and inferences on the flow inside the core, *Geophys. Astrophys. Fluid Dyn.*, *48*, 273-296, 1989.

Pedlosky, J., *Geophysical fluid dynamics*, New York: Springer Verlag, 1979.

Roberts, P. H., On topographic core-mantle coupling, *Geophys. Astrophys. Fluid Dyn.*, *44*, 181-187, 1988.

(Received: June 1, 1995; Revised: July 28, 1995; Accepted: August 19, 1995)